Sapphire fiber optic sensors for nuclear applications: Technical overview

Chris Petrie

Oak Ridge National Laboratory

5/30/2022

Contributions from:
Brandon Wilson, Tony Birri, Tom Blue

Sapphire vs. traditional fused silica glass fibers

Singe-crystal sapphire (α-Al_2O_3)

- Maximum temperature : 1700–1800°C demonstrated, close to ~2000°C melting point
- Cost: ~$1k per meter
- Diameter: 75–500 μm
- Cladding: None (active R&D)
- Maximum continuous length: ~meters
- Typical intrinsic attenuation: ~dB/m
  - Dominated by scattering losses due to lack of cladding
- Must be single-crystalline to avoid scattering losses at grain boundaries
- High loss and short lengths generally require non-trivial splicing to a-SiO_2 leads

Fused silica glass (a-SiO_2)

- Maximum temperature: 1000°C (long-term devitrification)
- Cost: As low as ~$0.20 per meter
- Core diameter: ~8–10 μm (singlemode)
- Cladding: Routinely accomplished via chemical dopants in a-SiO_2
- Maximum continuous length: >kilometers
- Typical intrinsic attenuation: ~dB/km

Possible nuclear applications

Sheathed sapphire optical fiber bundle

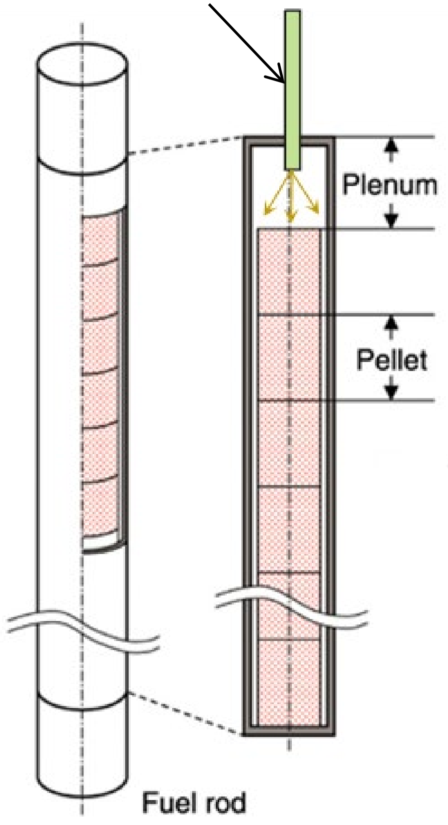

NIR borescope - Visualize fuel dimensional changes, cracking, relocation

Sapphire optical fiber

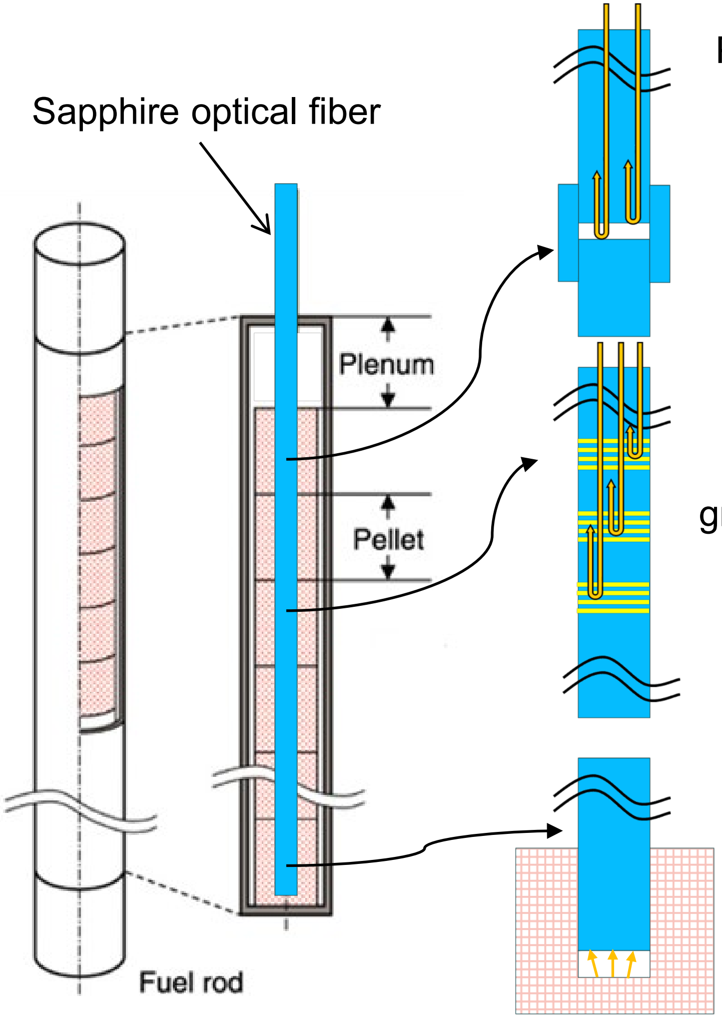

Option 1: Fabry-Perot cavity formed by Al_2O_3 capillary tube (single point)

Option 2: Bragg gratings in sapphire fiber (distributed measurement)

Option 3: Pyrometer (single point)

Single-point or distributed measurement of fuel centerline temperature

Prismatic graphite fuel block

Bonded sapphire optical fiber

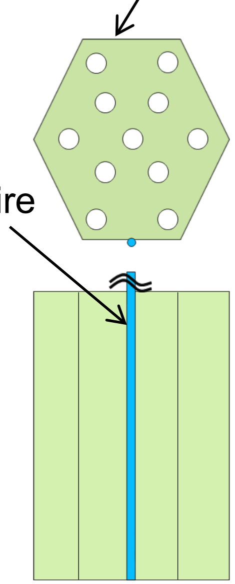

Single-point or distributed measurement of strain in fuel or structural materials

Option 1: Fabry-Perot cavity formed by Al_2O_3 capillary tube (single point)

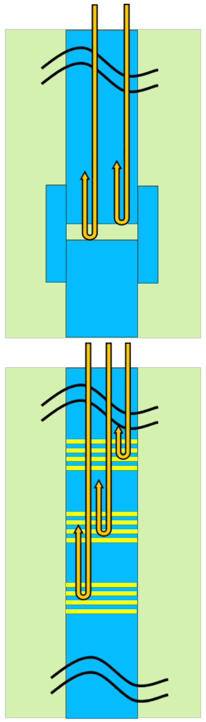

Option 2: Bragg gratings in sapphire fiber (distributed measurement)

Fuel rod images adapted from http://jolisfukyu.tokai-sc.jaea.go.jp/fukyu/mirai-en/2010/img/honbun/6-4.jpg

High-temperature operation

- Large increases in attenuation in air at ~1400°C
  - Formation of surface bubbles, likely aluminum hydroxide $Al(OH)_3$
- Attenuation and bubbles not observed in an inert environment
  - Promising for nuclear applications that can locate sapphire sensors in a metal sheath or fuel cladding backfilled with an inert gas

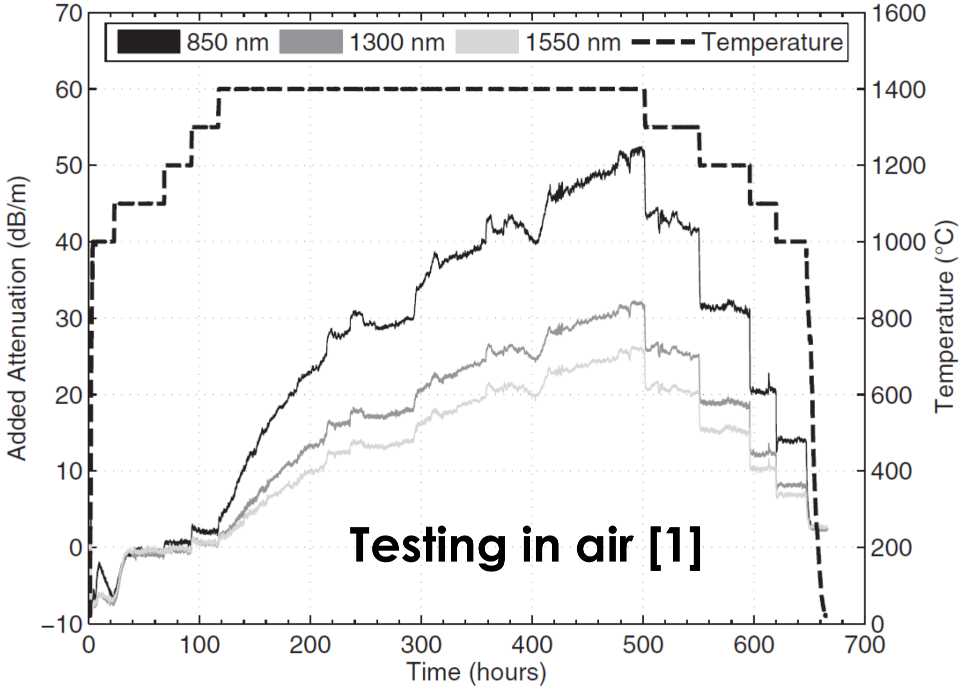

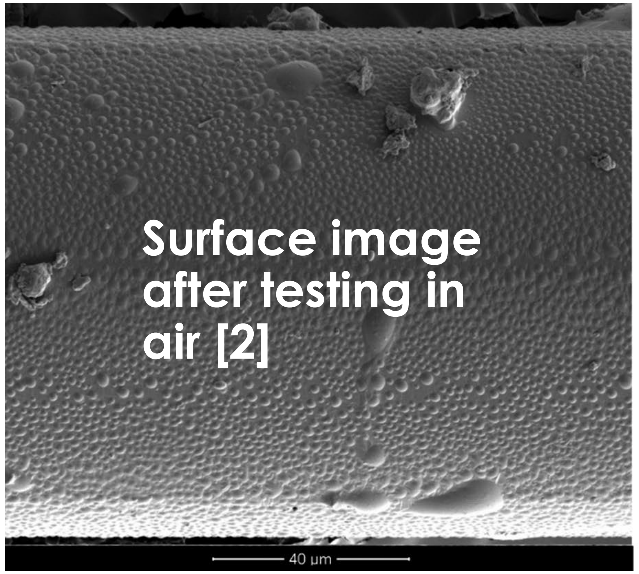

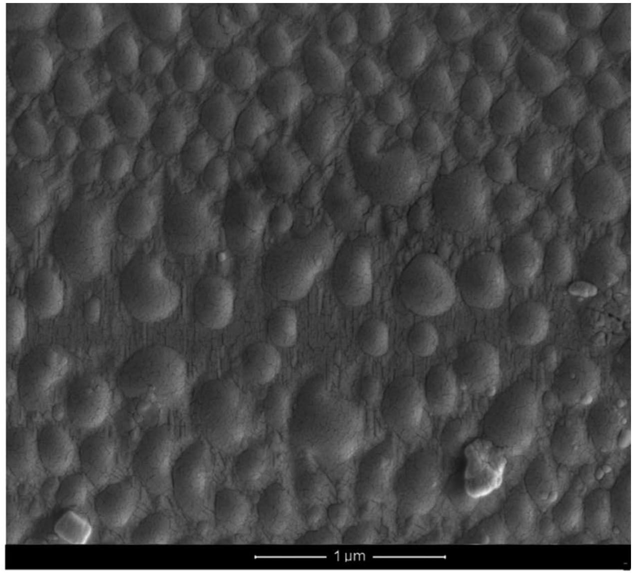

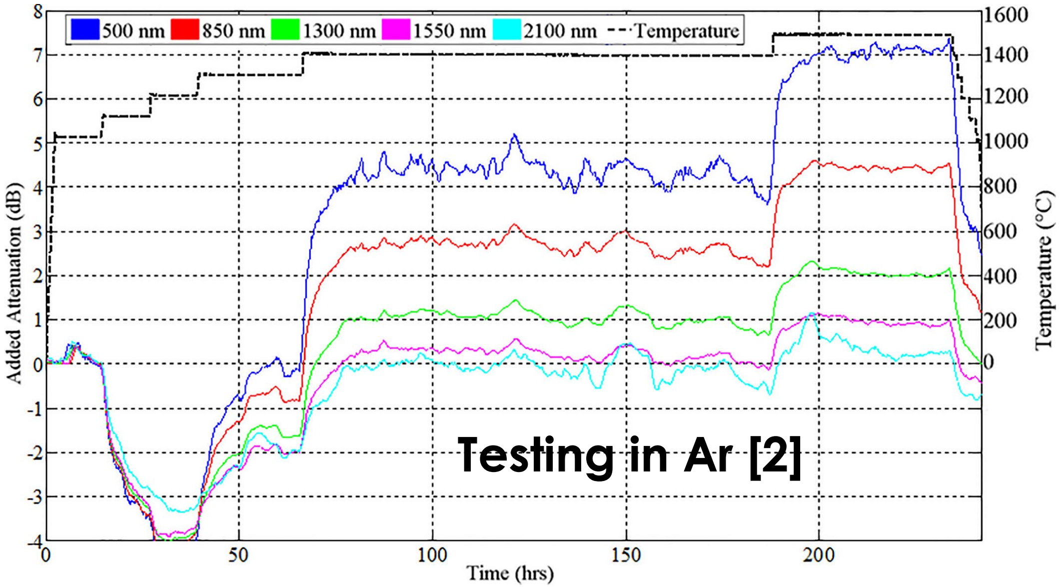

[1] C.M. Petrie and T.E. Blue, "In-situ Thermally Induced Attenuation in Sapphire Optical Fibers Heated to 1400°C," *Journal of the American Ceramic Society* **98** (2014) 483-489.
[2] B.A. Wilson et al., "High Temperature Effects on the Light Transmission through Sapphire Optical Fiber," *Journal of the American Ceramic Society* **101** (2018) 3452-3459.

Radiation effects

- In general, sapphire would be expected to have lower radiation tolerance compared to silica because it is an ordered single crystalline structure with no grain boundaries to serve as sinks for point defects vs. the amorphous nature of fused silica
  - Point defects create trapping states within the band gap, causing increased optical absorption at energies corresponding to band transitions
  - Aggregation of point defects can result in microstructural and dimensional changes that cause drift of Bragg gratings or other sensors that rely on changes in refractive index or thermal expansion
  - All optical fibers see increased noise due to radiation-induced emissions

Ordered crystal structure of α-Al_2O_3

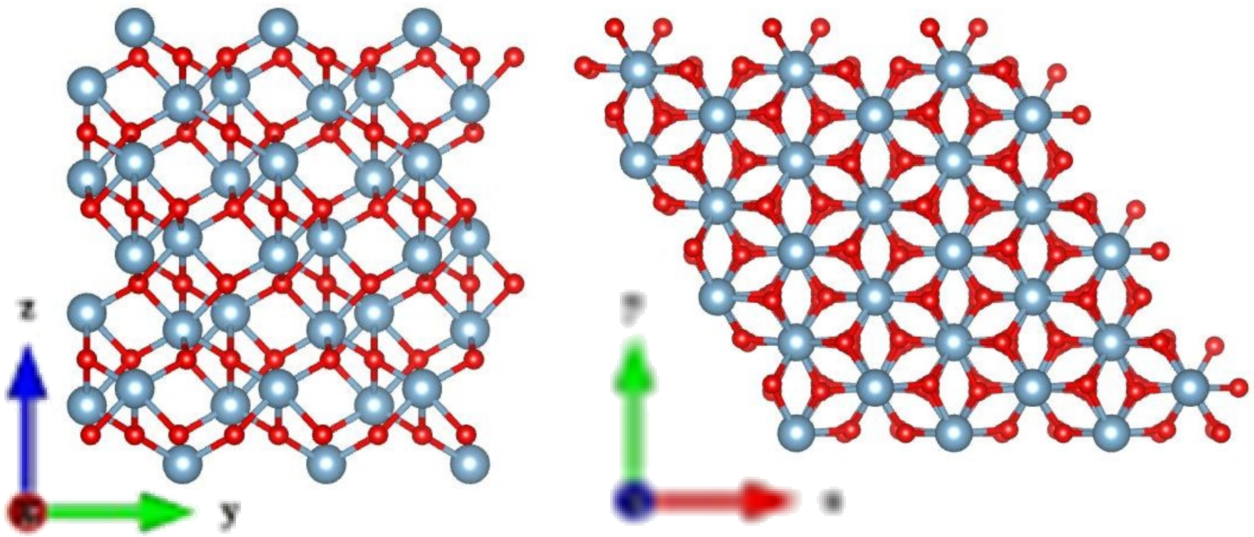

Amorphous structure of a-SiO_2

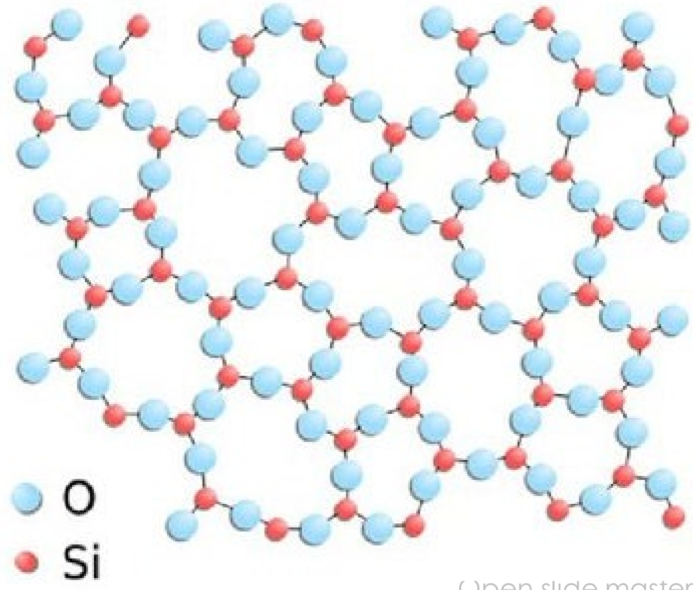

Dimensional stability

Sapphire swells >4% under neutron irradiation [1]

- No evidence of saturation up to ~2.3×10^{22} n/cm^2
- Swelling higher at higher temperatures

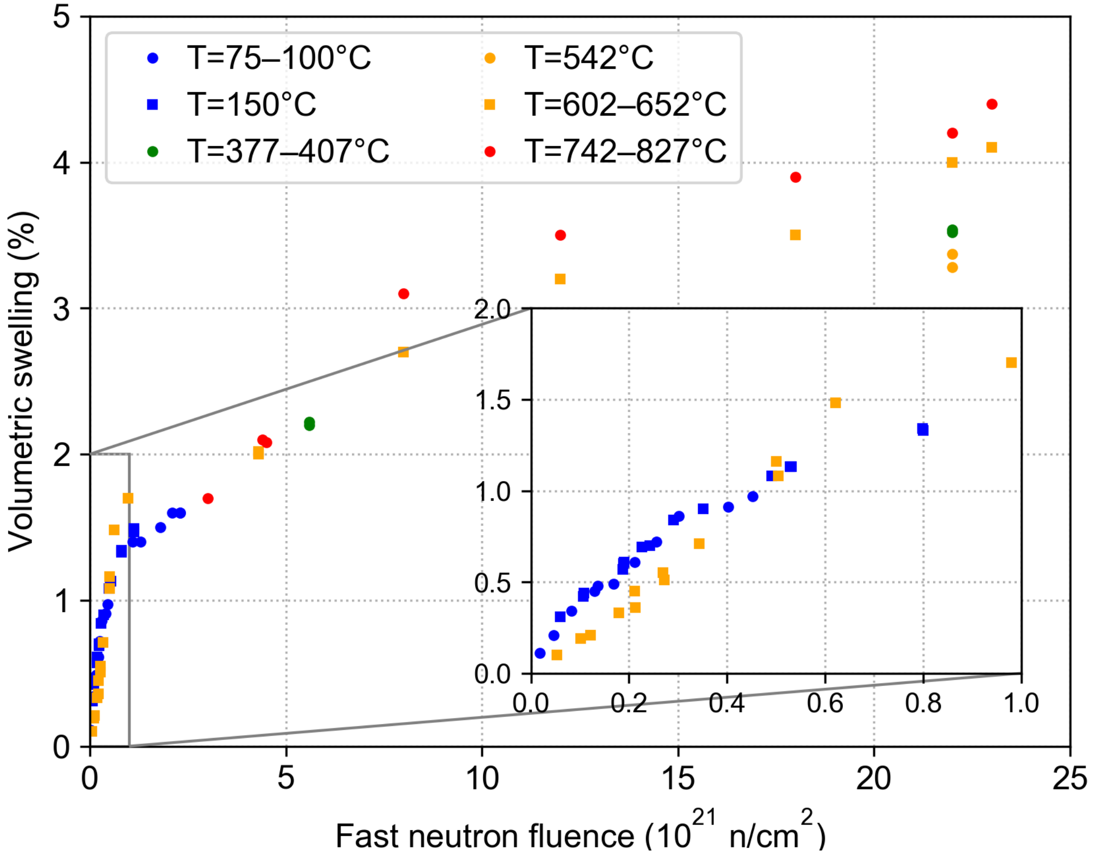

Fused silica compacts ~2% under neutron irradiation [2]

- Saturates after ~10^{20} n/cm^2
- Equilibrium compaction lower at higher temperatures

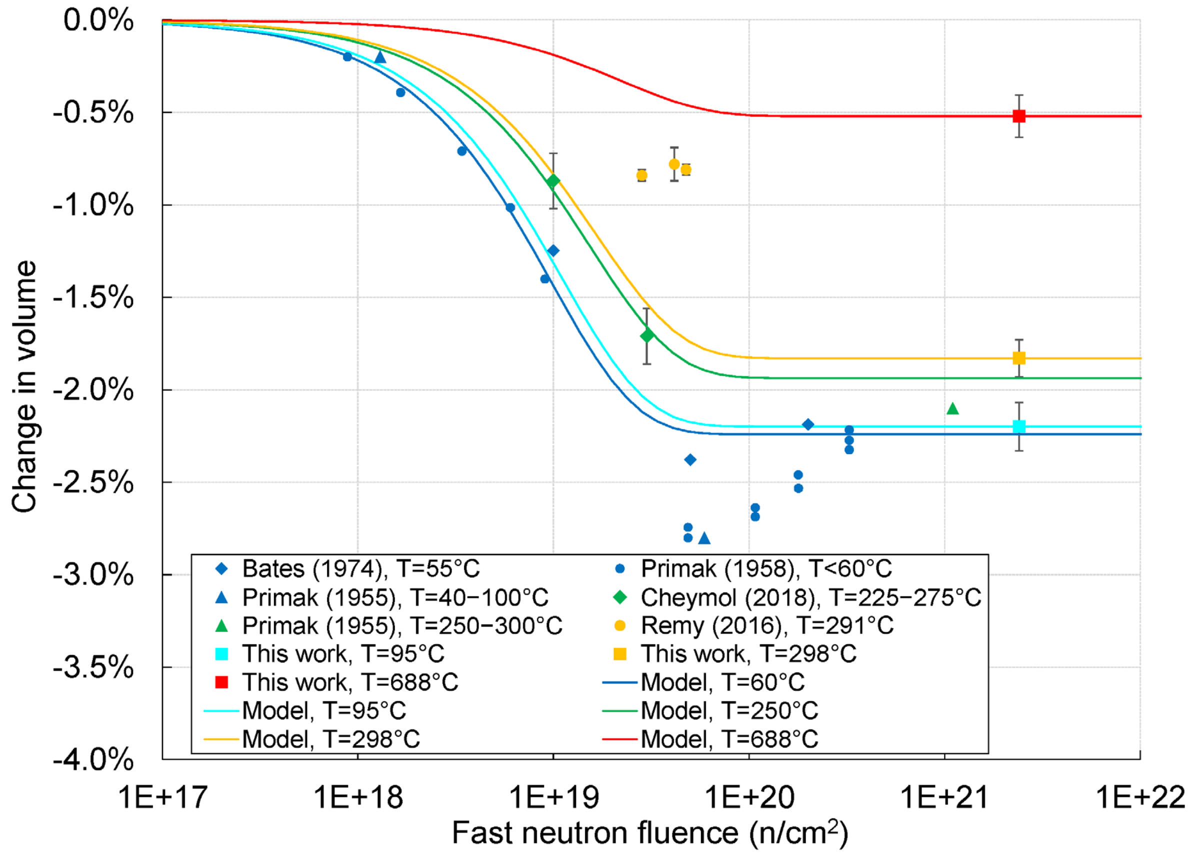

[1] C.M. Petrie et al., "Optical transmission and dimensional stability of single-crystal sapphire after high-dose neutron irradiation at various temperatures up to 688°C," *Journal of Nuclear Materials* **559** (2022) 153432.

[2] C.M. Petrie et al., "High-Dose Temperature-Dependent Neutron Irradiation Effects on the Optical Transmission and Dimensional Stability of Amorphous Fused Silica," *Journal of Non-Crystalline Solids* **525** (2019) 119668.

High neutron fluence (2.4×10^{21} n_{fast}/cm^2) measurements

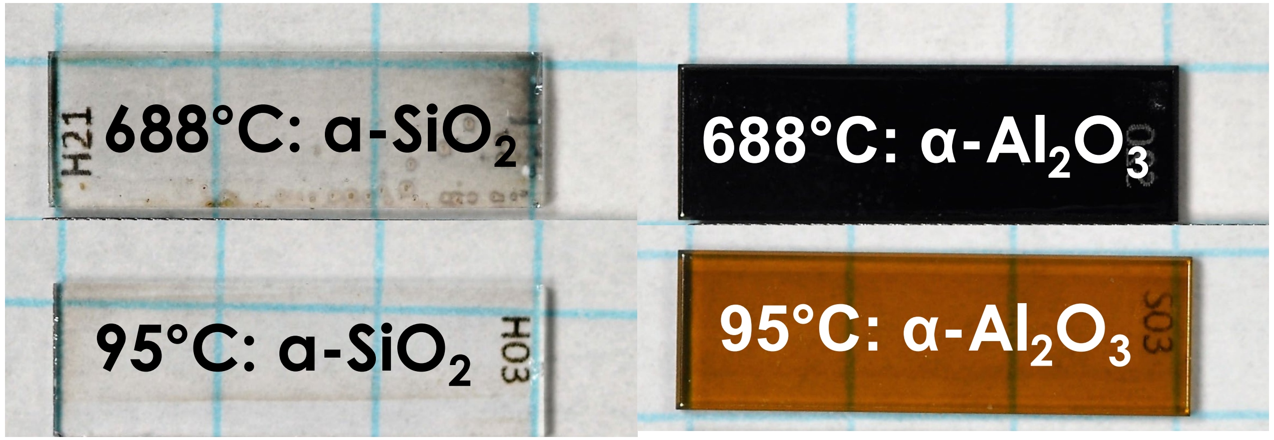

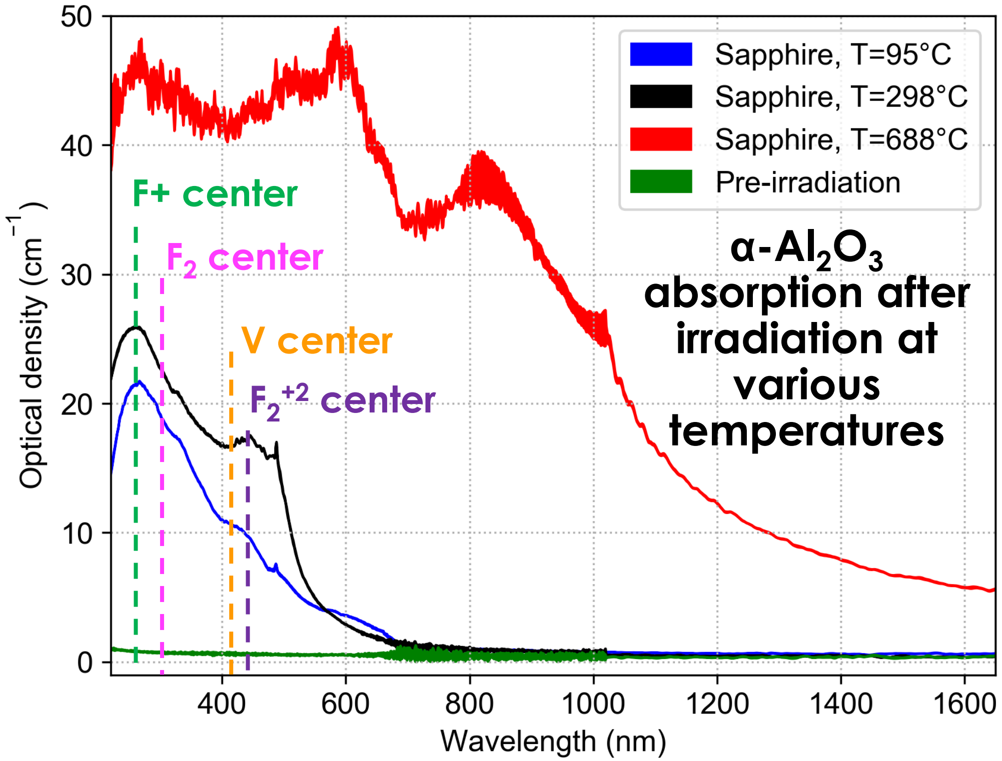

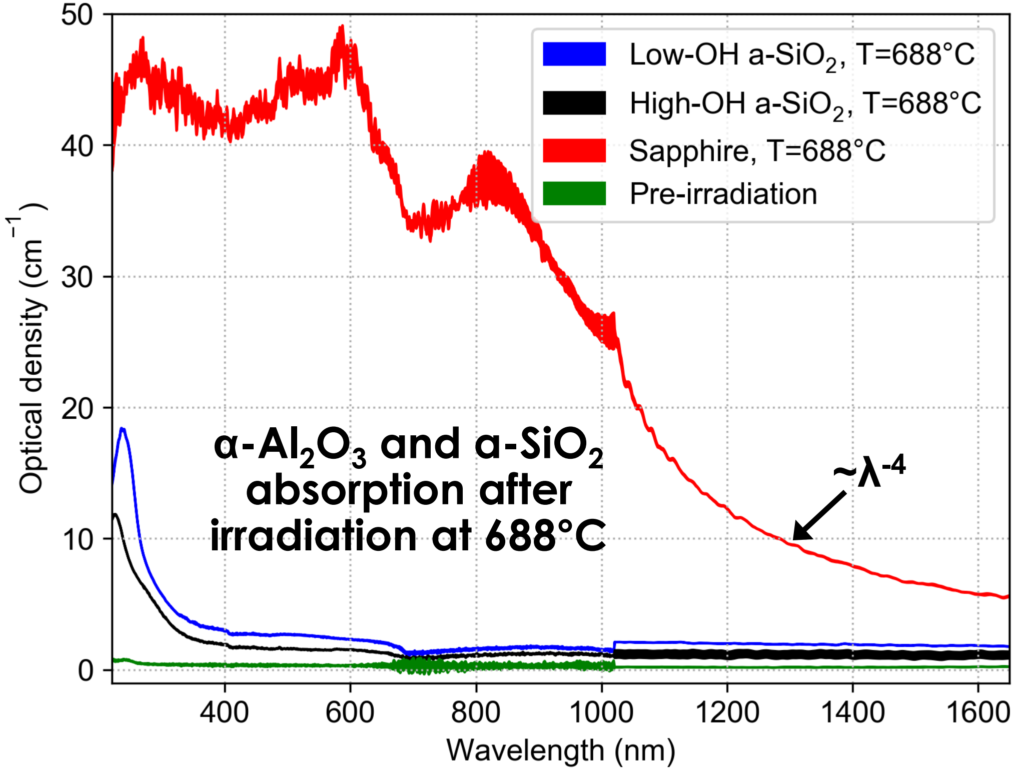

[1] C.M. Petrie et al., "Optical transmission and dimensional stability of single-crystal sapphire after high-dose neutron irradiation at various temperatures up to 688°C," *Journal of Nuclear Materials* **559** (2022) 153432.
[2] C.M. Petrie et al., "High-Dose Temperature-Dependent Neutron Irradiation Effects on the Optical Transmission and Dimensional Stability of Amorphous Fused Silica," *Journal of Non-Crystalline Solids* **525** (2019) 119668.

Comparison to previous low neutron fluence in situ measurements

- High neutron fluence testing [1]
  - Post-irradiation attenuation (or optical density, OD) measurement
  - OD at 650 nm normalized to value measured after irradiation at 95°C
  - 1.1×10^{15} n/cm^2/s fast flux
  - 2.4×10^{21} n/cm^2 fast fluence
- Previous low neutron fluence testing [2]
  - In situ measurement
  - Attenuation rates ($\dot{A}$) at 650 nm normalized to value during irradiation at 56°C
  - 6.3×10^{10} n/cm^2/s fast flux
  - 6.9×10^{15} n/cm^2 fast fluence
- Clearly very different temperature trends, suggesting different phenomena at low vs. high neutron fluence

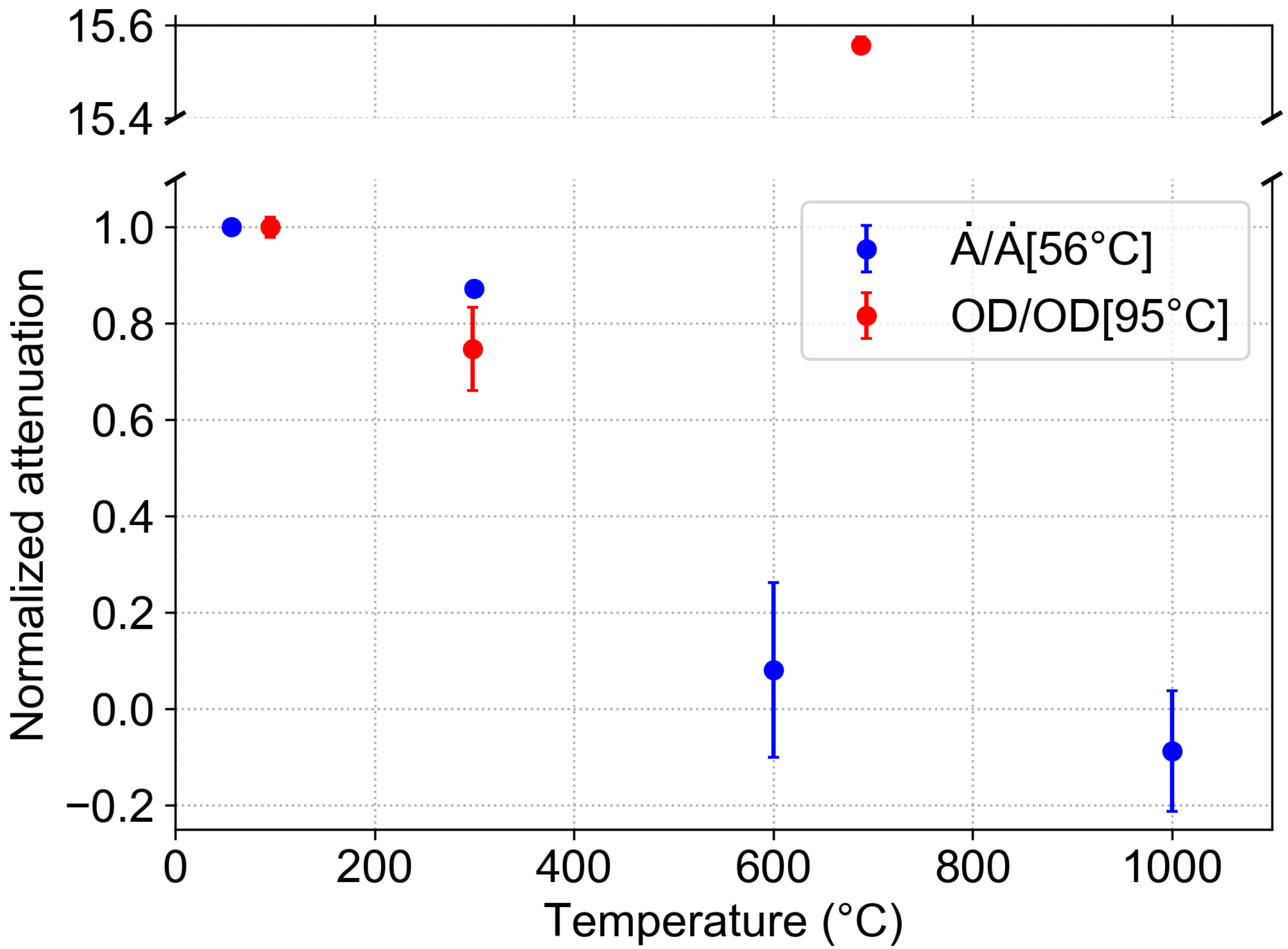

[1] C.M. Petrie et al., "Optical transmission and dimensional stability of single-crystal sapphire after high-dose neutron irradiation at various temperatures up to 688°C," *Journal of Nuclear Materials* **559** (2022) 153432.
[2] C.M. Petrie and T.E. Blue, "In-situ reactor radiation-induced attenuation in sapphire optical fibers heated up to 1000°C," *Nuclear Instruments and Methods in Physics Research B: Beam Interactions with Materials and Atoms* **342** (2015) 91-97.

Current theory: Rayleigh scattering losses from radiation-induced voids that occur at high dose and temperature

298°C: Dislocation loops, no voids

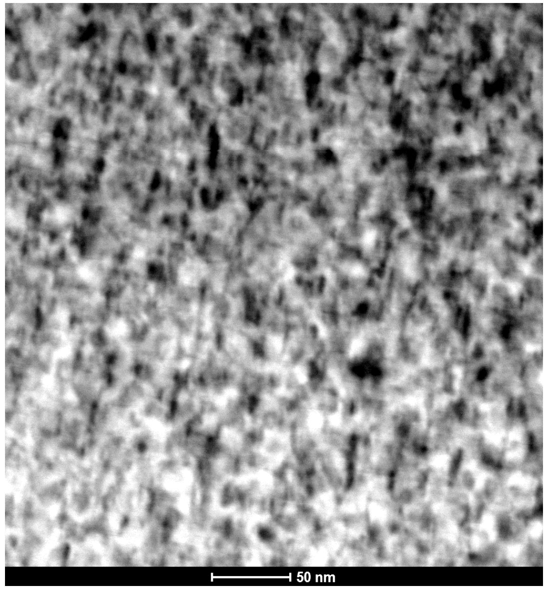

688°C: Voids aligned along c-axis

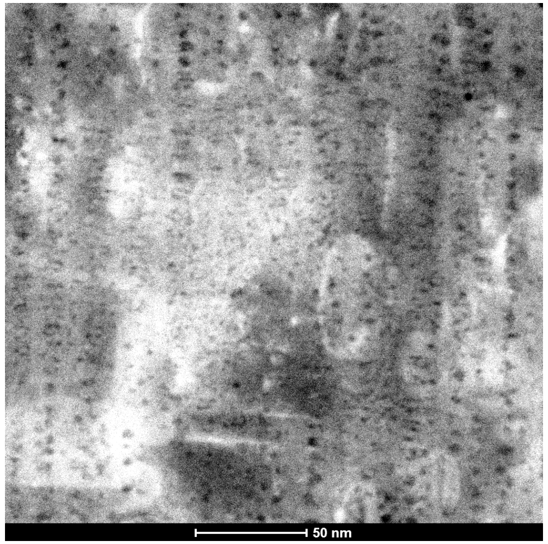

- Observations of voids oriented along c-axis consistent with previous literature
  - Requires temperatures >500°C for fluence tested in HFIR
- Void diameter (~3 nm) << λ (~1 μm), $n_{void} \approx 1$
- Observed λ^{-4} attenuation dependence consistent with theory

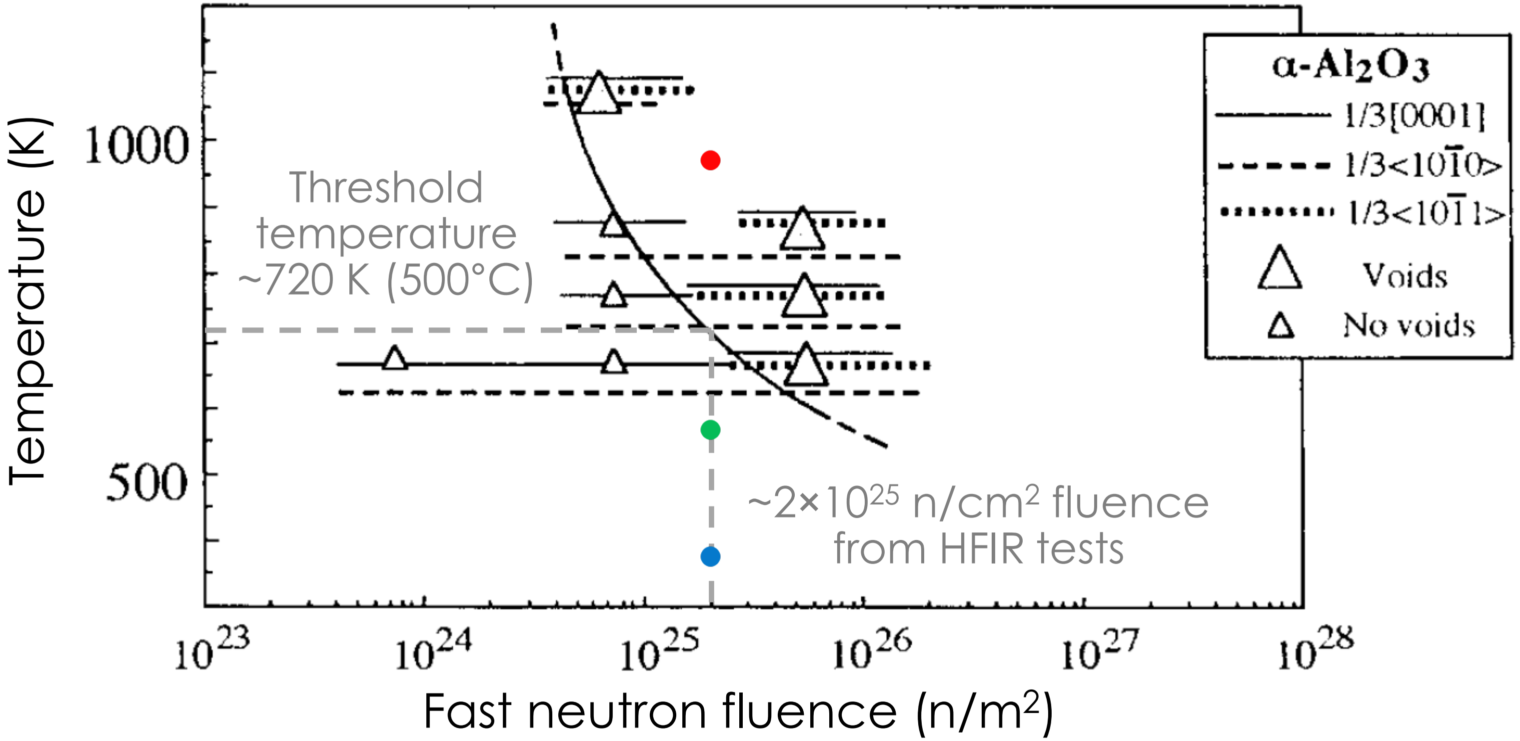

[1] C. Kinoshita and S.J. Zinkle, "Potential and limitations of ceramics in terms of structural and electrical integrity in fusion environments," *Journal of Nuclear Materials* **233–237** (1996) 100–110.

OAK RIDGE National Laboratory

Ongoing R&D efforts

- Efforts to reduce modal volume: cladding (Blue–OSU, Rountree–LUNA, Buric–NETL) vs. reduced core diameter (Pickrell–VTU)
  - Cladding must have $\mathrm{n_{cladding}} < \mathrm{n_{core}}$, similar thermal expansion coefficient, and be thermodynamically compatible at extreme temperatures
  - Efforts include coatings ($MgAl_2O_4$, ZrO_2, polycrystalline Al_2O_3, metals, etc.), chemical dopants, ion implantation, or other means of introducing porosity or micro-structured architectures
- MITR irradiations of FBGs inscribed in sapphire using OSU's cladding technique (Daw, McCary–INL)
  - Will provide another data point regarding high temperature, high neutron fluence effects on fiber transmission, grating reflectivity, and potential drift

Summary

- Sapphire's main benefit is a much higher operational temperature vs. fused silica
  - Significant loss when heated beyond 1300°C in air but can be mitigated with an inert environment
  - Potential nuclear applications primarily targeting ceramic fuel centerline temperatures or potentially very high-temperature gas-cooled reactor structural materials
- Sapphire has several challenges, including high cost, limitations on fiber diameter and continuous length, and the lack of a cladding that results in large intrinsic attenuation and a high modal volume
  - **Focused R&D efforts to develop sapphire cladding are a priority (several ongoing)**
- However, sapphire is a single crystal with no grain boundaries to serve as a sink for radiation-induced defects, making it more susceptible to radiation damage than amorphous fused silica
- **High neutron fluence testing shows prohibitively high attenuation after irradiation at the highest temperature (688°C), very different from observations during low neutron fluence testing**
  - Theory is that the prohibitively large RIA results from increased Rayleigh scattering losses from voids that form at high temperature and high fluence
  - Consistent with spectral dependence of RIA, previous literature, and recent TEM images of irradiated samples
  - **Upcoming MITR irradiations will hopefully provide more insight into whether unfavorable results observed after high neutron fluence testing of bulk materials are indeed a major concern**

Questions?
Chris Petrie, petriecm@ornl.gov

Oak Ridge National Laboratory

U.S. DEPARTMENT OF ENERGY | Office of NUCLEAR ENERGY

ASI Advanced Sensors and Instrumentation

High Fluence Active Irradiation and Combined Effects Testing of Sapphire Optical Fiber Distributed Temperature Sensors

Kelly McCary, Josh Daw

NSUF Nuclear Science User Facilities

Project Overview

- Goals and Objectives

Investigate the in-pile performance of sapphire optical fiber temperature sensors and to develop clad sapphire optical fibers for in-pile instrumentation. Evaluate the distributed sensing performance of the sensors through optical backscatter reflectometry under combined radiation and temperature effects, and high fluence.

- Objective 1: Fabricate sapphire optical fiber sensors.
- Objective 2: Evaluate the clad sapphire fiber to verify single-mode behavior and determine and characterize light modes supported by optical fibers.
- Objective 3: Characterize in-pile temperature sensing of sapphire optical fiber and combined temperature and irradiation effects.
- Objective 4: Evaluate the lifetime and sensing performance of the sensor under irradiation to high neutron fluence.

- Participants (2022)
  - Idaho National Laboratory: Lead organization
    - Dr. Joshua Daw, Kelly McCary
  - The Ohio State University
    - Dr. Thomas Blue, Josh Jones, NRL
  - The Massachusetts Institute of Technology
    - NRL
  - National Energy Technology Laboratory
    - Dr. Michael Buric
  - Oak Ridge National Laboratory
    - Dr. Christian Petrie

FY2020		Status	Scheduled	Actual	Notes
Task 1	Clad Sapphire Optical fiber	Complete	January 2020	March 2021	Delayed due to procurement of sapphire fibers
Task 2	Characterize Sapphire Fiber	Complete	June 2020	April 2021	Delayed -covid travel restrictions
Task 3	OSURR Irradiation	Complete	October 2020	April 2021	Delayed -covid travel restrictions
	Deliverable 1: Sapphire Fibers	Complete	September 2020	March 2020	
	Deliverable 2: FY20 Annual Report	Complete	September 2020	September 2020	
FY2021					
Task 2	Characterize Sapphire Fiber	Complete	June 2020	April 2021	Delayed -covid travel restrictions
Task 3	OSURR Irradiation	Complete	October 2020	April 2021	Delayed -covid travel restrictions
Task 4	Data Analysis: OSURR Data	On-going	May 2022		
Task 5	MITR Irradiation	Delayed	July 2022	TBD	Pushed by Facility
	Deliverable 1: Experimental Data	Complete	September 2021	April 2021	
	Deliverable 2: FY21 Annual Report	Complete	September 2021	September 2021	
FY2022					
Task 4	Data Analysis: MITR	Planned	September 2022		
Task 5	MITR Irradiation	Delayed	July 2022		Pushed by Facility
	Deliverable 1: Journal Paper	Planned	September 2022		
	Deliverable 2: Final Report	Planned	September 2022		

Technology Impact

- This work is advancing nuclear technology by characterizing and demonstrating a new sensor technology with the potential to make measurements with high spatial and temperature resolution at higher temperatures than prior optical sensors. This technology can also be applied to measurements other than temperature.
- This research will deliver modern optical fiber sensing techniques usable in multiple extreme environment applications. In the area of nuclear fuel/material testing, these fibers will enable access to operational data with excellent time and space resolution during irradiation testing.
- Commercialization is underway by Luna Innovations. This research represents the opportunity to close technology gaps and demonstrate the potential of sapphire optical fibers.

Accomplishments

- Sapphire fiber preparation:
  - Fiber procurement
  - FBG inscription
  - Fiber cladding irradiations
  - Annealing
  - Mode-stripping treatment
- Out of pile furnace testing
- Heated irradiation at OSURR
- MIT Irradiation Ready for insertion

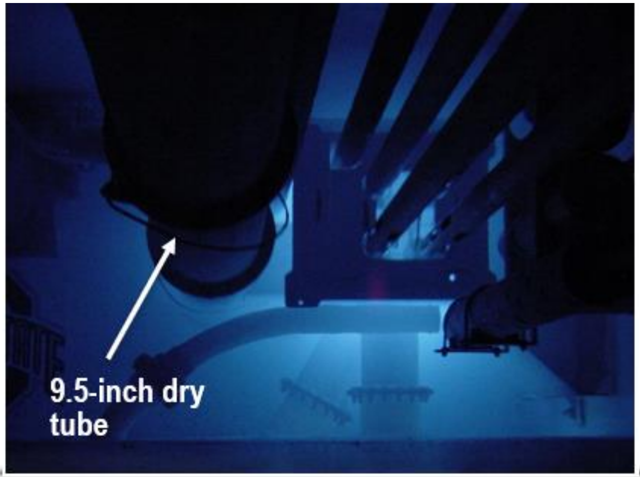

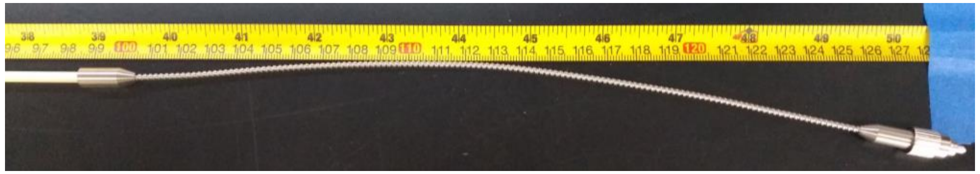

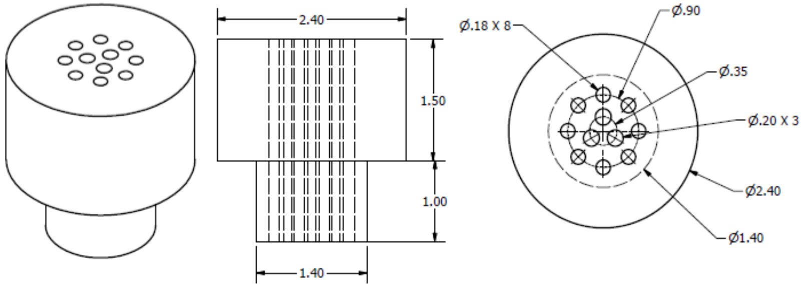

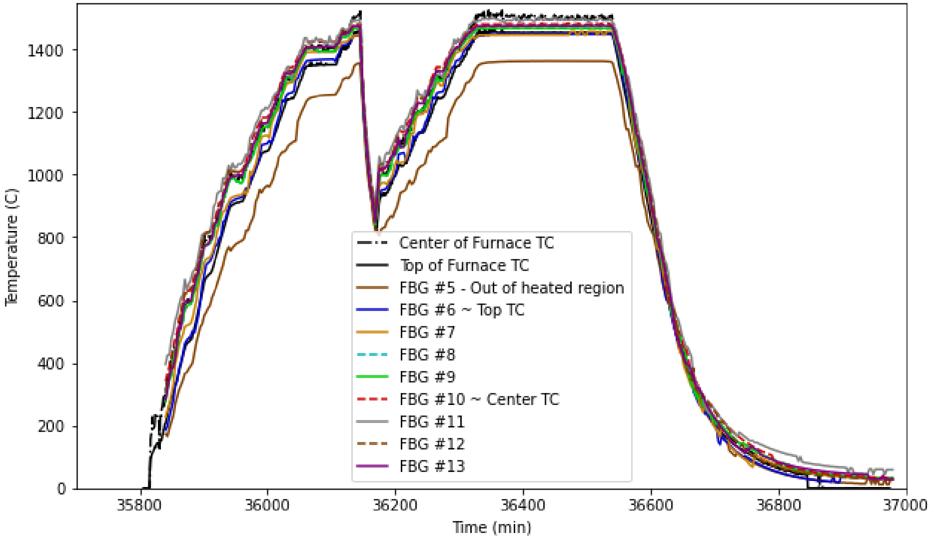

Accomplishments: Sapphire Preparation

Sapphire fiber cladding:

- Four one-day irradiations were completed with the purpose of cladding sapphire fiber
  - Cladding Irradiation #1: Completed January 24, 2019
    - 2 fibers, 100 um OD, with 2 FBGs inscribed by UPitt
    - 1 fiber, 100 um OD, without FBGs
    - 1 fiber, 75 um OD, with 13 FBGs inscribed by FemtoFiberTec
  - Cladding Irradiation #2: Completed March 13, 2020
    - 4 fibers, 100 um OD, each with 1 FBG inscribed by UPitt
  - Cladding Irradiation #3: Completed March 12, 2021
    - 2 fibers, 125 um OD, each with 4 FBGs inscribed by FemtoFiberTec
  - Clad Irradiation #4: Completed March 19, 2021
    - 4 fibers, 125 um OD, each with 4 FBGs inscribed by FemtoFiberTec

Post-Processing:

- Thermal annealing, polishing and splicing

Challenges: Annealing, Splicing

Accomplishments: MITR Ready for Insertion

- 8 Sensors prepared and provided to MITR in preparation for irradiation
  - 5 Sapphire sensors
    - 125, 100, and 75 um diameter fibers with inscribed FBGS
    - Clad, and annealed
    - Placed in silica microcapillary tubes to prevent any material interaction
  - 3 Silica Sensors
    - Pure silica core single mode fiber – baseline
    - iXblue and Technica type-II FBGs
    - Active Compensation sensor

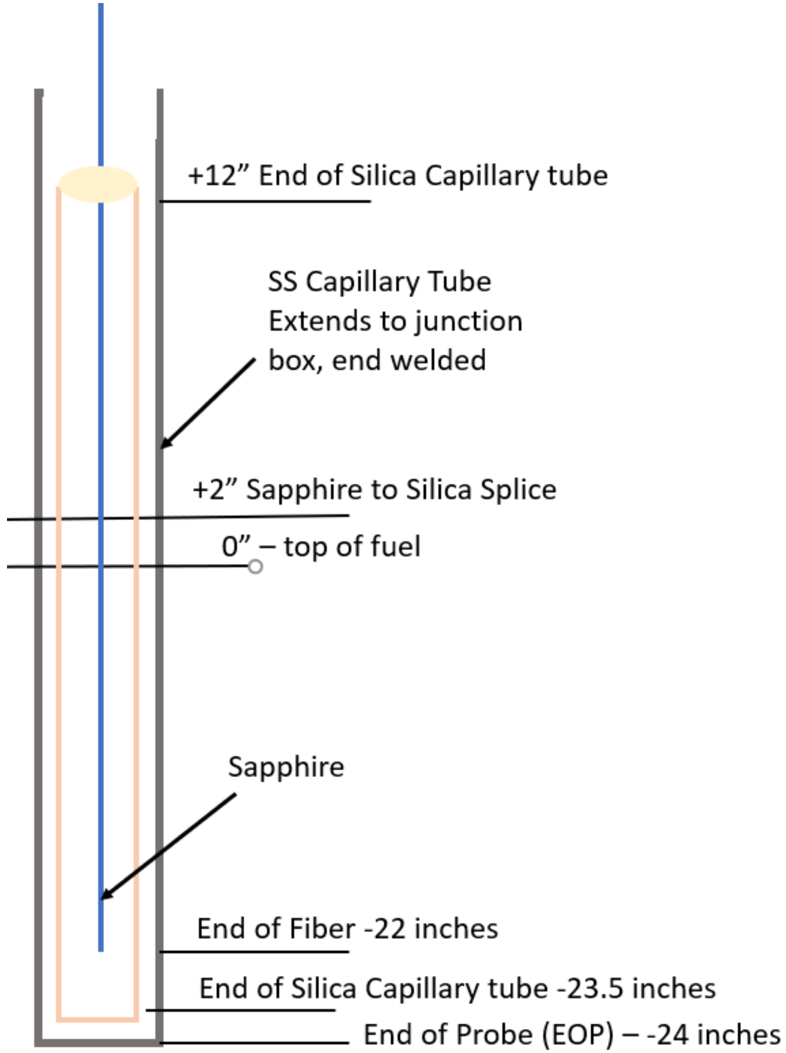

Results: Out of Pile Testing

Sapphire optical fiber sensors were tested in a box furnace at up to 1500ºC prior to deployment in OSURR

- 8 in. heated region
- Interrogated with a Luna Innovations OBR 4600
- All the fibers were placed in alumina tubes that were closed on the heated end, then spliced to silica lead-out fibers
- When the furnace was heated past 1100ºC, the sensing mechanism failed
  - Attenuation and exceeded range of OBR

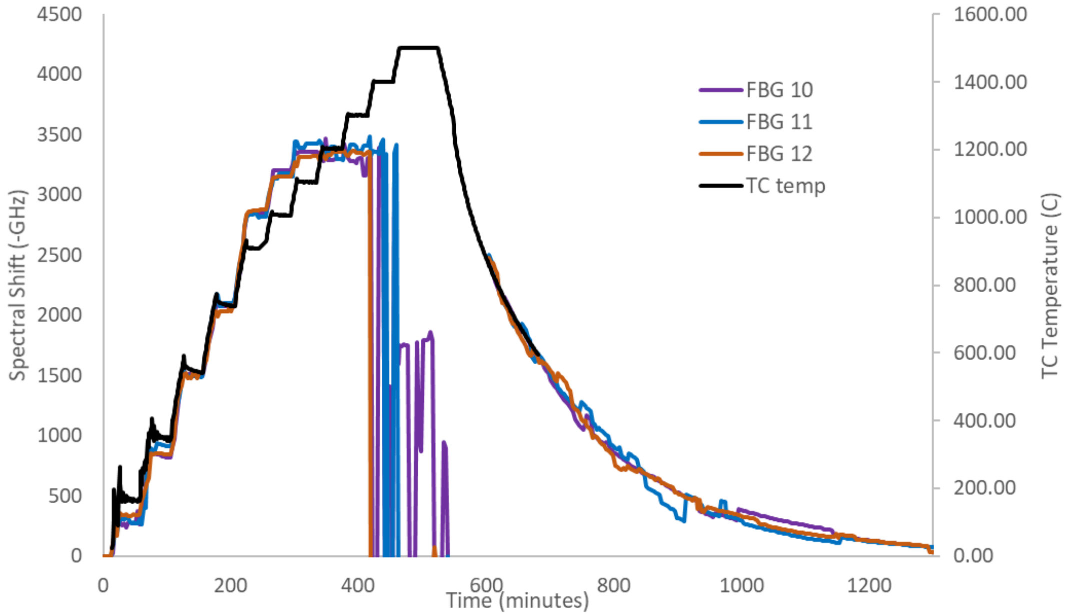

Sensor 1: 75 um diameter – 13 FBGs inscribed by FemtoFiberTec

Results: Heated Irradiation

Sensor 1: 75 um diameter – 13 FBGs inscribed by FemtoFiberTec
- Annealed to 1500˚C in air, 23.5 in. long

Sensor 2: 100 um diameter – 2 FBGs inscribed by UPitt
- Annealed to 1500˚C in air, 13 in. long

Sensor 3: 100 um diameter – 1 FBG inscribed by Upitt
- Annealed to 1200˚C in air, 15.25 in. long

Sensor 4: 100 um diameter – No FBGs
- Annealed to 1500˚C in air, 9.25 in. long

Sensor 5: 100 um diameter – 1 FBG inscribed by Upitt
- Annealed to 1500˚C in air, 16.25 in. long

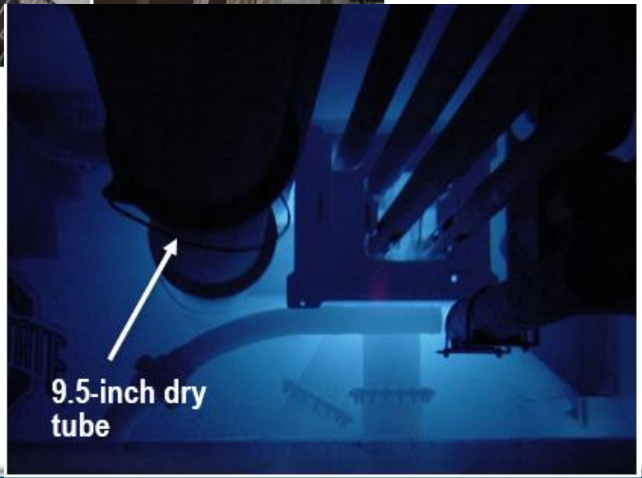

Results: Heated Irradiation

The heated irradiation was designed to test the fibers at various temperatures from ambient to 1600ºC

- Total fluence: 3.2×10^{17} n/cm^2
  - Thermal: 2.3×10^{17} n/cm^2

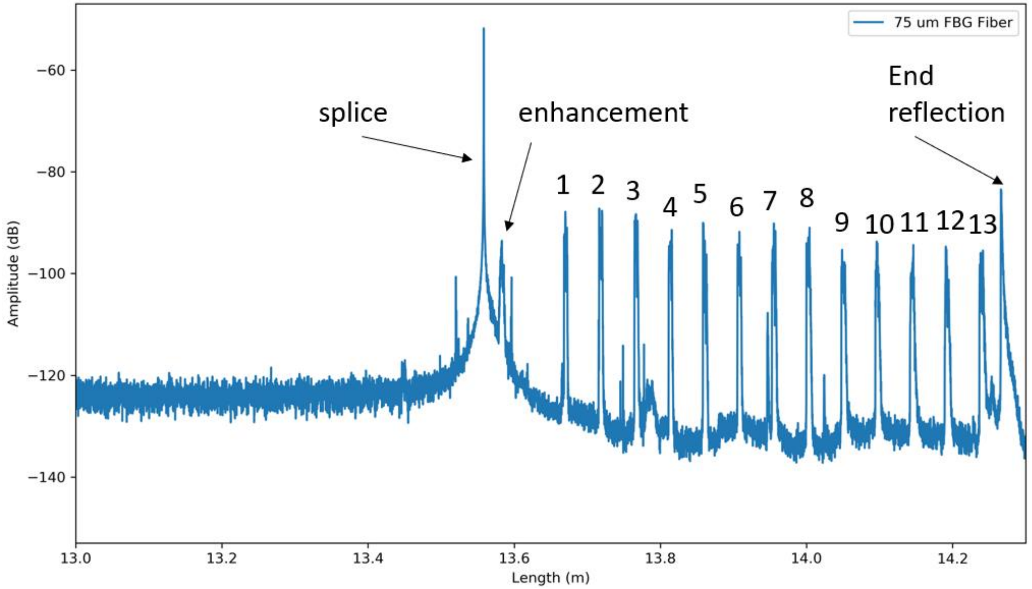

Backscatter profile of sensor #1, 75 um OD sapphire fiber featuring FBGs inscribed by FemtoFiberTec.

Day	Hours	Power (kW)	Furnace Temp. (Celsius)	Notes
1	7	450	off/200	
2	7	450	400/600	
3	7	450	800	
4	4	450	900	4 hours, some hours for another customer at 5 kw
5-1	0		1000	Fuse blow
5-2	7	450	1000	
6	7	450	1100	
7	7	450	1200	
8	7	450	1300	
9	7	450	1400	
10	7	450	1.5 hrs at 800, 2 hrs at 1000, 2 hrs at 1200	
11	7	450	1400 1 hr at 1500	Fuse blow during heating
12	6	450	1500 1 hr at 1600	

Results: Heated Irradiation

- The measurement was resolved at the locations of the FBGS
- Sensor 1 – 75 um OD – performed the best
- Sensor gets less noisy with higher temperatures

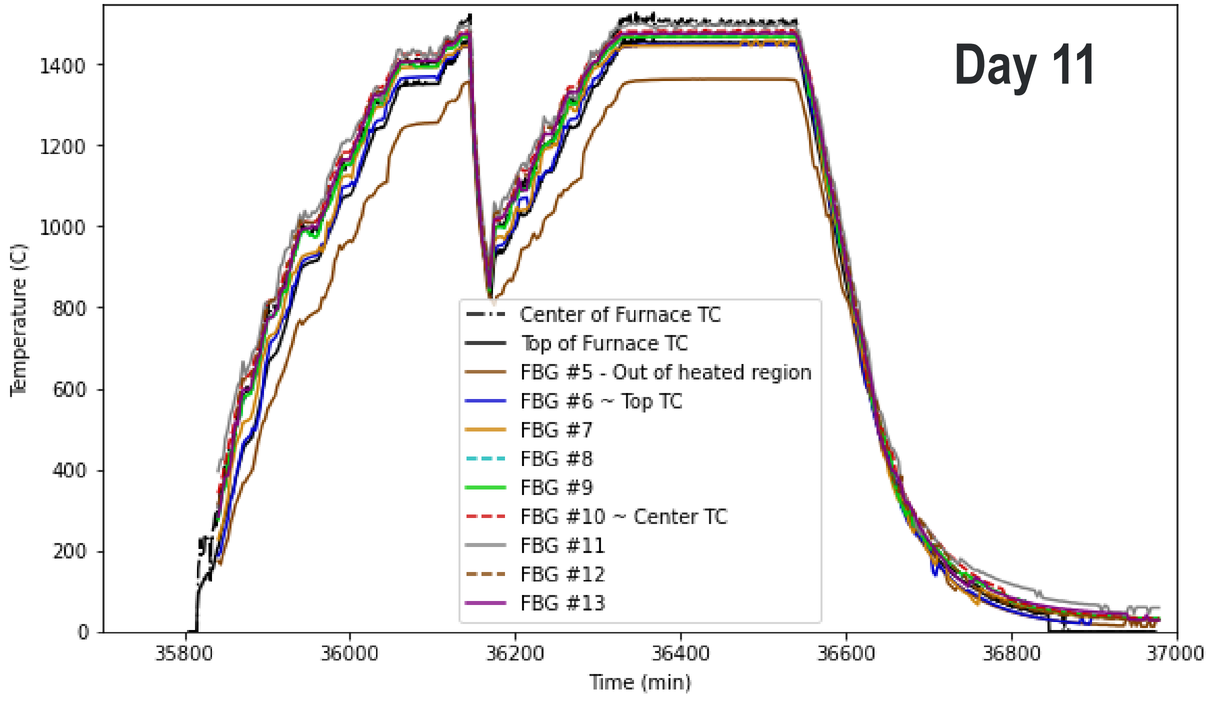

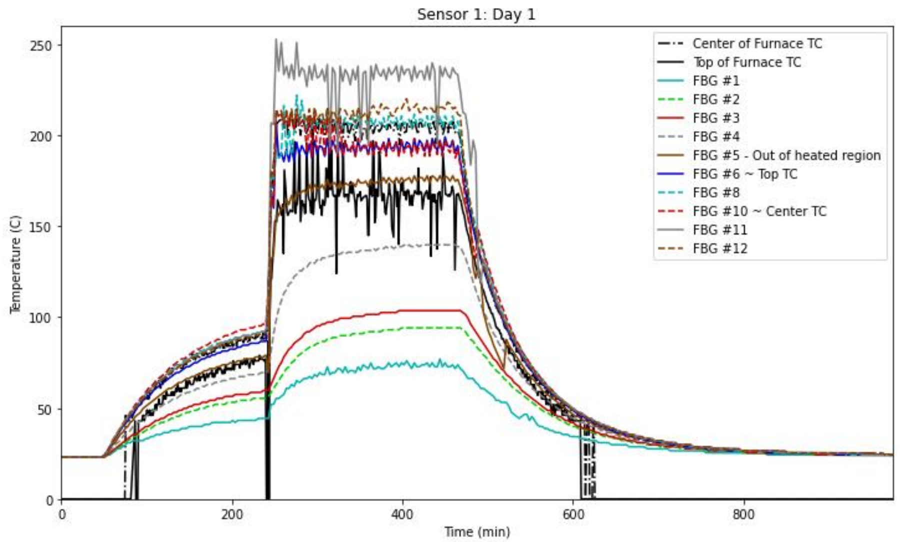

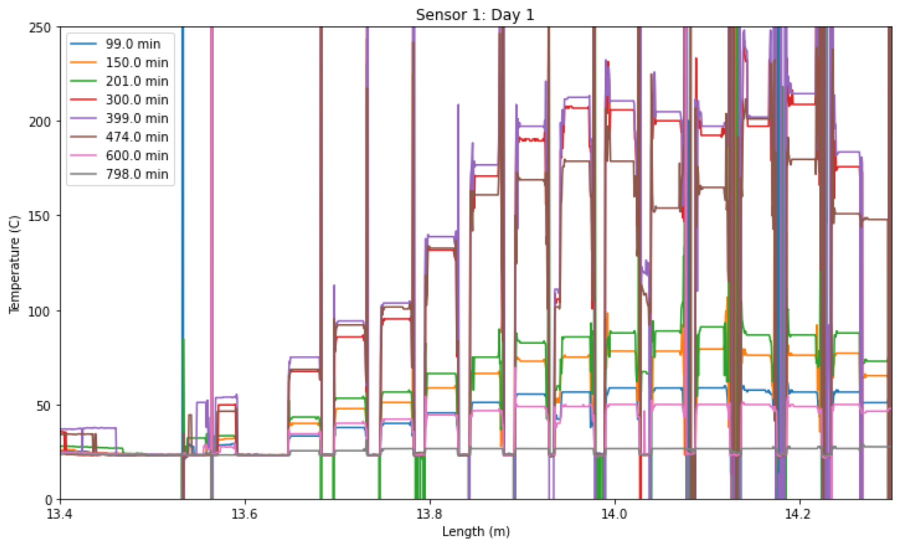

Results: Heated Irradiation

- Similar failure mechanism was observed at 1600ºC in-pile as was observed in out of pile testing.

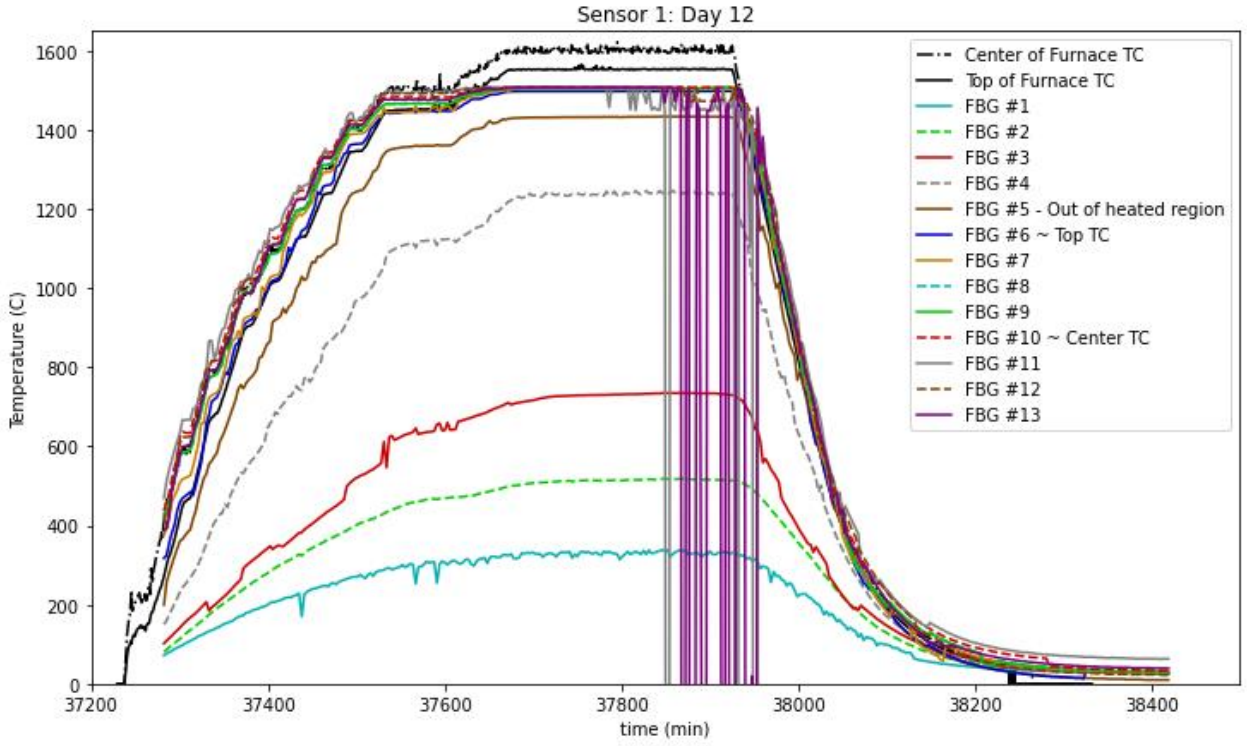

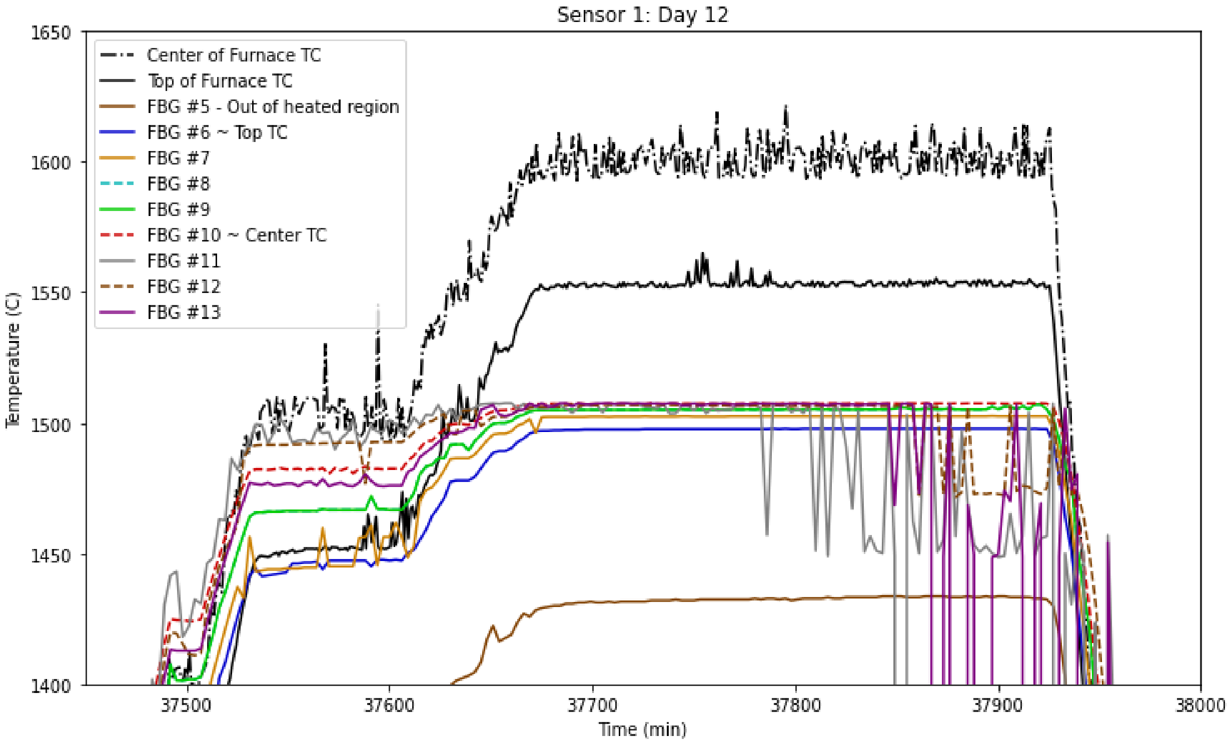

Results: Heated Irradiation

- After signal loss and amplitude reduction the FBGs recover as the fiber cools to room temperature
- Similar amplitude reduction up to 1500ºC that was seen in furnace testing

Backscatter profile and wavelength response of FBG #12 for sensor #1 for the last day of irradiation heating.

Backscatter profile and wavelength response of FBG #12 for sensor #1 for the last day of irradiation cooling.

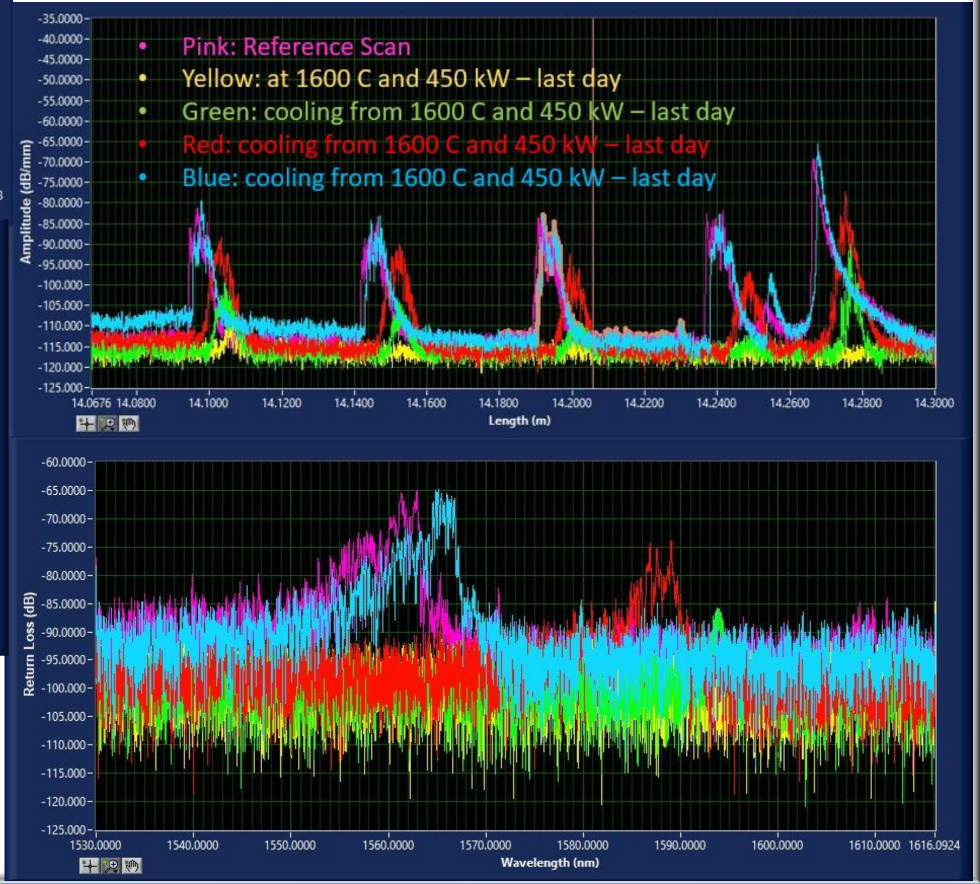

Conclusion

Challenges:

- Procurement, inscription, and processing of sapphire
  - Non-commercial supplier of sapphire fibers experienced unforeseen issues
  - Inscription of sapphire fibers is not a trivial task
  - Splicing fibers can produce variable results
- Handling tritium-implanted fibers at INL
- Navigating through travel restrictions and shutdowns

Conclusions:

- Objectives 1-3 have been completed
- Heated irradiation indicates potential for sapphire fiber-based sensors to be sued in extreme environments beyond silica fiber limits

Future Work:

- Further evaluation of un-clad sapphire fibers to determine source of attenuation in fiber
- High-fluence irradiation at MITR

Kelly McCary

PhD Candidate, OSU

Research Scientist, Radiation Measurements

Idaho National Laboratory

Kelly.Mccary@inl.gov

W (208)-526-2601

We would like to acknowledge the support of The Ohio State University Nuclear Reactor Laboratory and the assistance of the reactor staff members, Andrew Kauffman, Dr. Susan White, Kevin Herminghuysen, Matthew Van Zile, and Maria McGraw for the irradiation services provided.

Special thanks to Dr. Blue, Josh Jones, and Dr. Birri for their assistance at Ohio State.

This work was supported by the U.S. Department of Energy, Office of Nuclear Energy as part of a Nuclear Science User Facilities experiment

NSUF Nuclear Science User Facilities

U.S. DEPARTMENT OF ENERGY | Office of NUCLEAR ENERGY

U.S. DEPARTMENT OF ENERGY | Office of NUCLEAR ENERGY

ASI | Advanced Sensors and Instrumentation

Irradiation of Optical Components of In-situ Laser Spectroscopic Sensors for Advanced Nuclear Reactor Systems

Sapphire Summit
May 31, 2022

Igor Jovanovic
University of Michigan

Project overview

Goal and Objective: understand the effect of radiation damage on the performance of materials used in optical spectroscopic sensors with special emphasis on:

(1) nonlinear refractive index
(2) transient radiation-induced absorption
(3) concurrent radiation damage and thermal annealing

Schedule:

Year 1: Procure samples; develop mobile PIE system
Year 2: Evaluate neutron activation; construct and test heating setup; conduct gamma irradiation with post-heating
Year 3: Conduct neutron irradiation with post-heating
Year 4: Conduct gamma and neutron irradiation with concurrent heating

Research team and collaborations




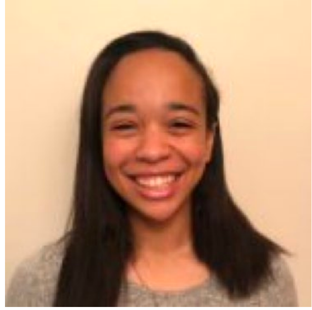

Igor Jovanovic, Bryan Morgan, Londrea Garrett, Milos Burger (UM)

Piyush Sabharwall (INL)

Paul Marotta (MicroNuclear)

Lei Cao (OSU-NRL: NSUF)

Sungyeol Choi (Seoul National University – INERI collaborator)

Christian Petrie (ORNL – collaborator)

Technology impact

- Optical instrumentation can be subjected to challenging environments: radiation, temperature, pressure, limited access
- Develop an improved understanding of radiation damage in optical materials <u>in conditions relevant for their operation in real-time optical sensors</u>
  - Rapid post-irradiation examination
  - Concurrent irradiation and annealing
  - Nonlinear refractive index
- First-ever attempt to quantify the effect of irradiation on <u>nonlinear</u> optical properties of materials
- **Cross-cutting impact: design and concept of operation for a wide range of optical instrumentation in nuclear applications**

Mobile post-irradiation examination setup

- Mobile PIE system constructed and validated (linear and nonlinear component)
- PIE system moved and operated at OSU NRL
- Soon to returned to University of Michigan
- Available for future collaborative campaigns

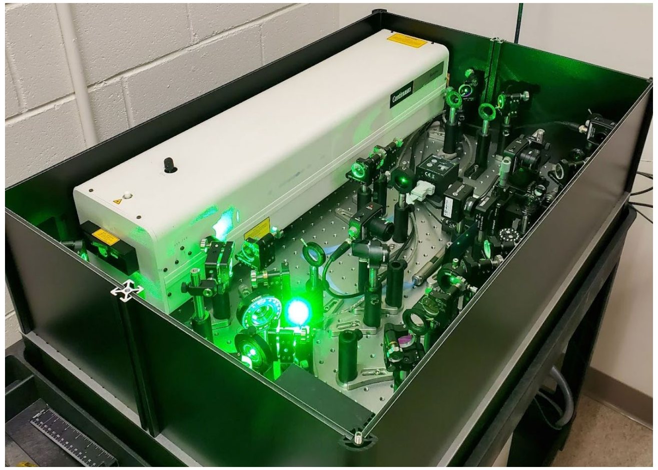

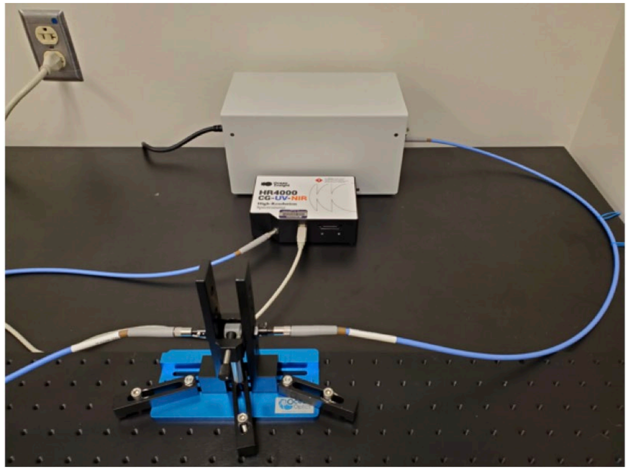

Irradiation facilities

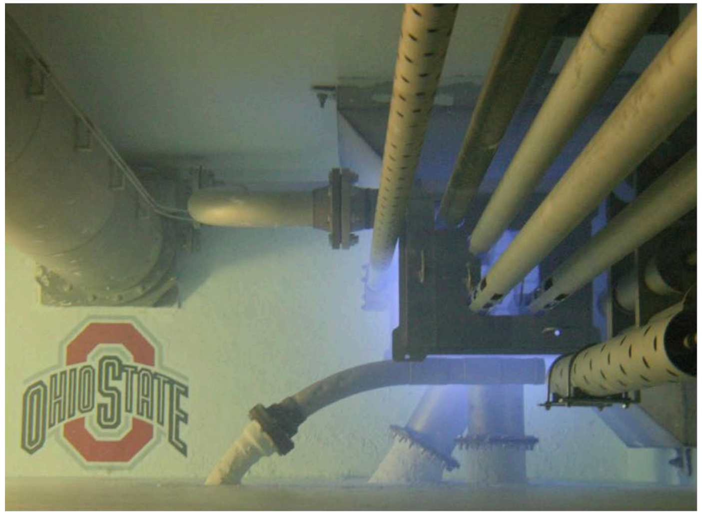

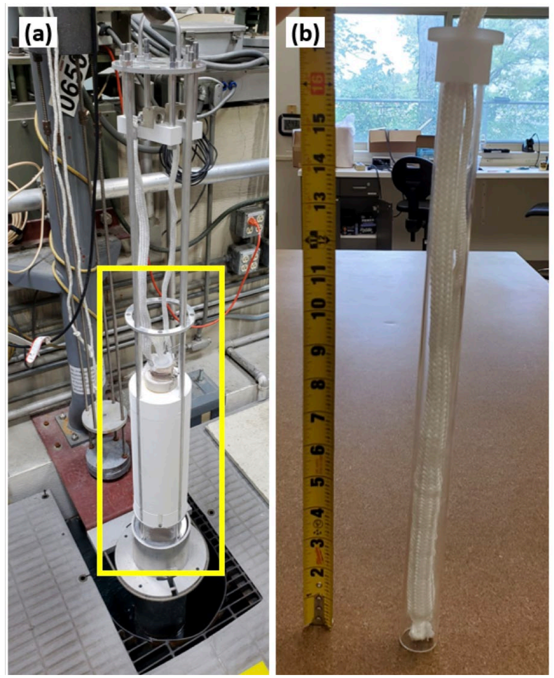

Sample irradiation and thermal annealing at the OSU Nuclear Reactor Laboratory (DOE NSUF)
Gamma irradiation at the PSU Radiation Science & Engineering Center (DTRA IIRM-URA)

Irradiation conditions and samples

Source	Dose/Fluence	Anneal Type	Temp.	Time
^{60}Co	600 krad 1.2 Mrad 3.4 Mrad	Post	200 °C 400 °C 600 °C 800 °C	30 min. 30 min. 30 min. 30 min.
^{60}Co	600 krad 1.2 Mrad 3.4 Mrad	Concurrent	800 °C	Duration
Reactor	3.4×10^{16} n · cm^{-2} (42 Mrad) 1.7×10^{17} n · cm^{-2} (211 Mrad)	Post	200 °C 400 °C 600 °C 800 °C	30 min. 30 min. 30 min. 30 min.
Reactor	3.4×10^{16} n · cm^{-2} (42 Mrad) 1.7×10^{17} n · cm^{-2} (211 Mrad)	Concurrent	800 °C	Duration

Material	Vendor	Type	OH Content
High-OH Fused Silica	Heraeus	Spectrosil 2000	$\leq$ 1300 ppm
Low-OH Fused Silica	Heraeus	Infrasil 302	$\leq$ 8 ppm
Sapphire	Guild Optical Associates	Optical Grade	

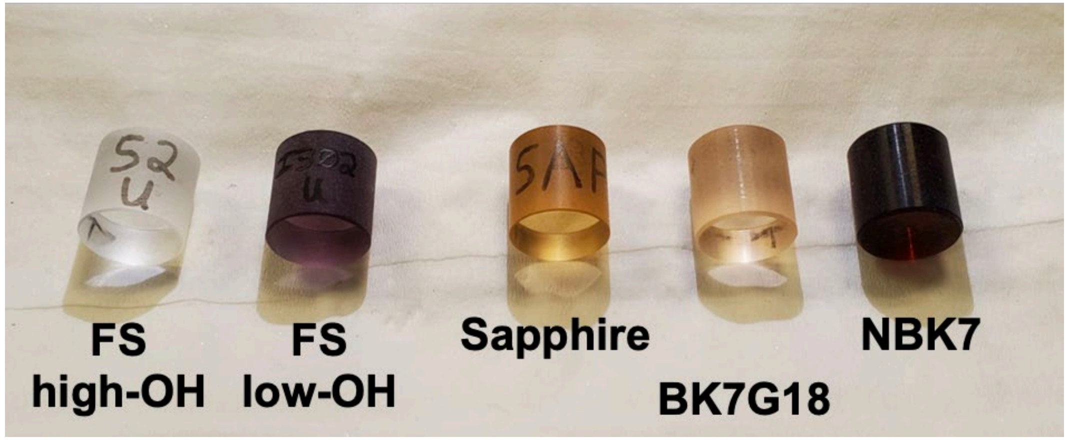

Neutron irradiation conditions

Label	Fluence/Dose	Anneal Type	Temp.	Time
n-Dose 1	$3.4 \times 10^{16}\ n \cdot cm^{-2}$ (42 Mrad)	Post	200 °C 400 °C 600 °C 800 °C	30 min. 30 min. 30 min. 30 min.
n-Dose 1	$3.4 \times 10^{16}\ n \cdot cm^{-2}$ (42 Mrad)	Concurrent	800 °C	Duration
n-Dose 2	$1.7 \times 10^{17}\ n \cdot cm^{-2}$ (211 Mrad)	Post	200 °C 400 °C 600 °C 800 °C	30 min. 30 min. 30 min. 30 min.
n-Dose 2	$1.7 \times 10^{17}\ n \cdot cm^{-2}$ (211 Mrad)	Concurrent	800 °C	Duration

Nonlinear refractive index and absorption

Materials exhibit nonlinear optical properties caused by variation of induced electronic polarization (P) with the applied electric field (E)

$$P = \epsilon_0 \chi^{(1)} E + \epsilon_0 \chi^{(2)} E^2 + \boxed{\epsilon_0 \chi^{(3)} E^3} + \dots$$

The third-order nonlinear susceptibility leads to processes such as third-harmonic generation, two-photon absorption, and the intensity-dependent refractive index.

$$n = n_0 + n_2 I \left\{ \begin{array}{l} \text{self-focusing} \\ \text{nonlinear absorption} \end{array} \right.$$

$$n_2 = \frac{12\pi^2 \chi^{(3)}}{n_0^2}$$

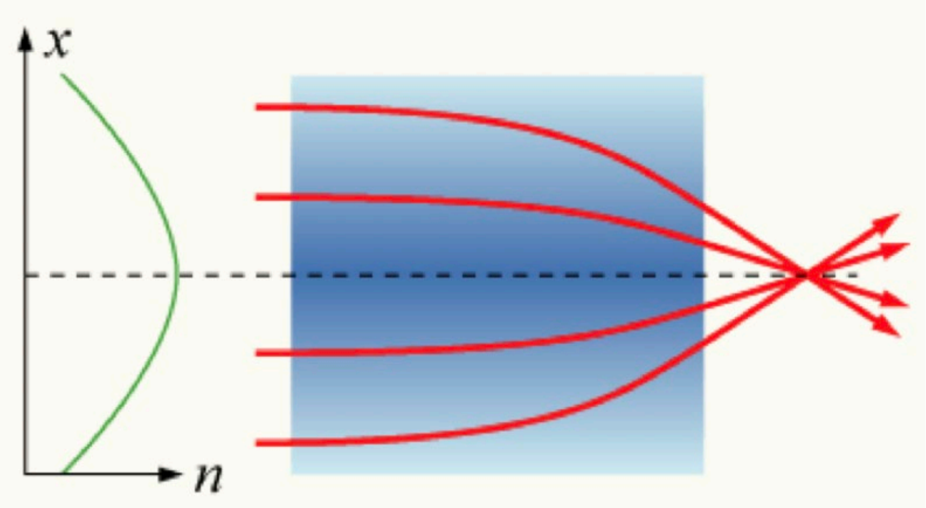

Measurement of n_2: Z-scan

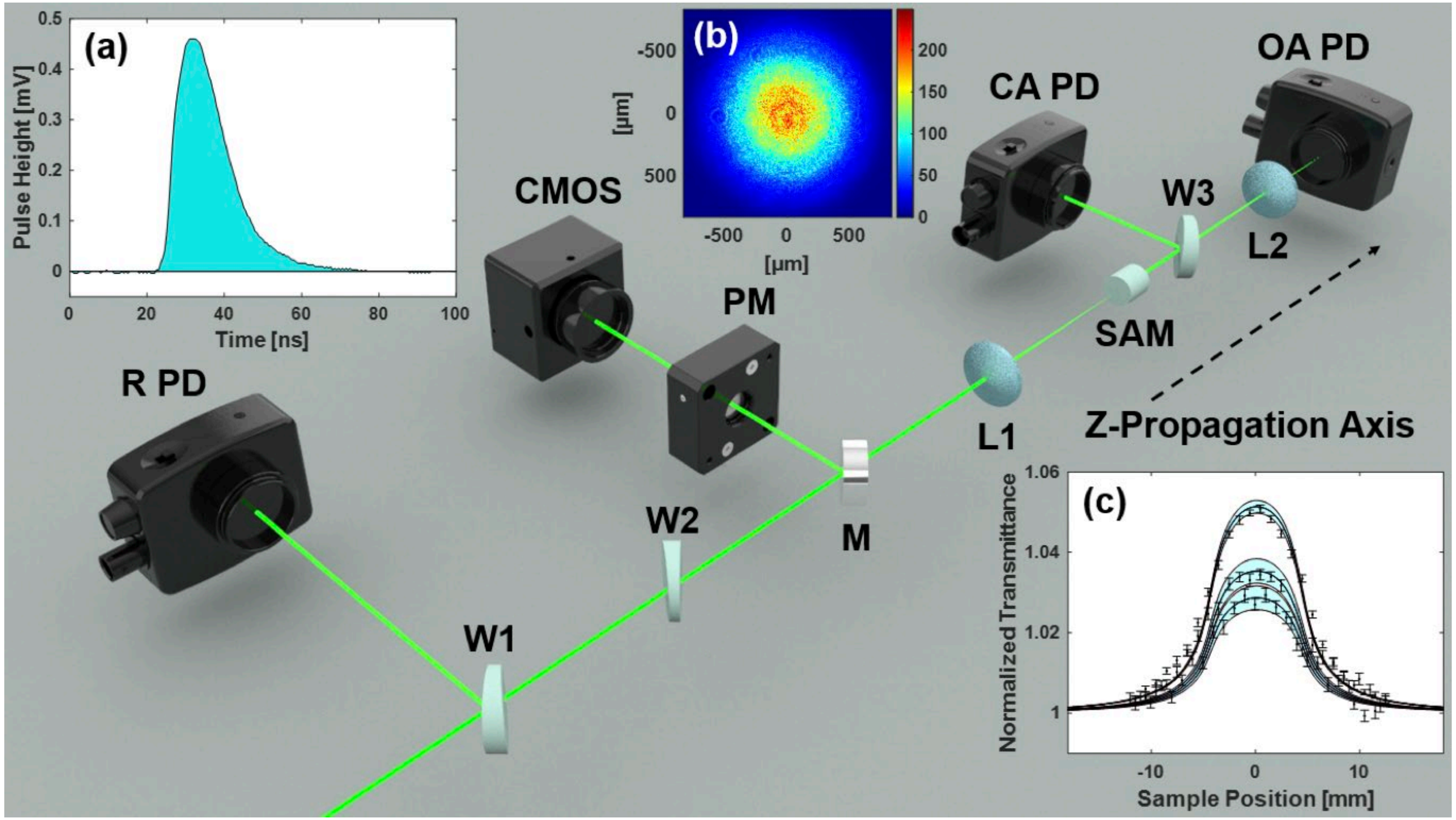

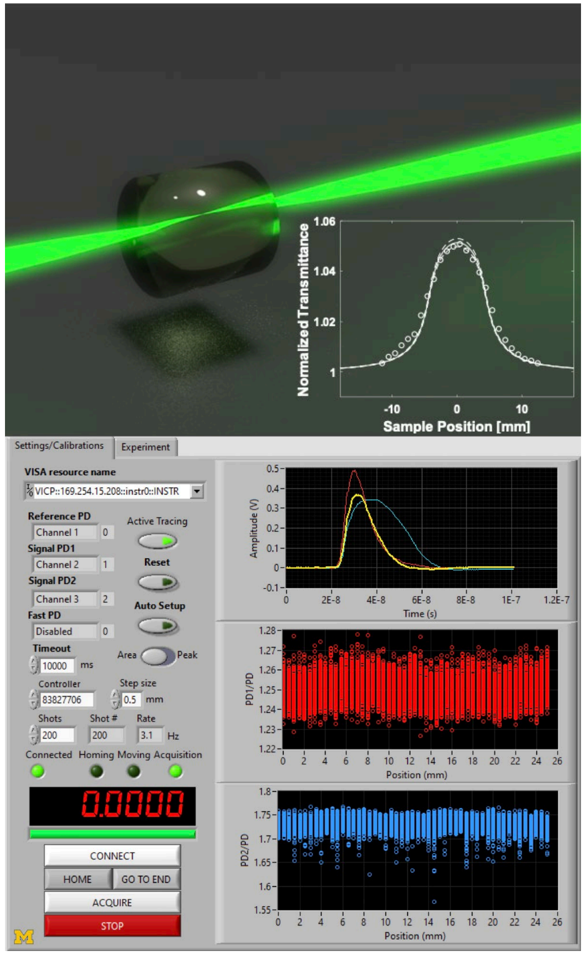

Significant findings

Linear Attenuation

Concurrent-irradiation thermal annealing did not fully anneal RIA:

Fused silica high-OH
213 nm E’ center
233 nm Trapped exciton
260 nm NBOHC

Fused silica low-OH
213 nm E’ center
233 nm Trapped exciton
246 nm ODC
260 nm NBOHC
300 nm Al-E’
387 nm ODC
550 nm Al-OHC

Sapphire
205 nm F center
260 nm F^{+} center
300 nm F_2 center
355 nm F_2^{+} center
450 nm F_2^{2+} center
572 nm Al-OHC

Nonlinear Optical Properties

Negative nonlinear absorption observed in irradiated:

Fused silica low-OH
Fused silica high-OH
Sapphire
NBK7
BK7G18

Negative nonlinear refraction observed in irradiated:
BK7G18

Photobleaching observed in irradiated:
Fused silica low-OH
Sapphire
NBK7
BK7G18

Nonlinear absorption in sapphire

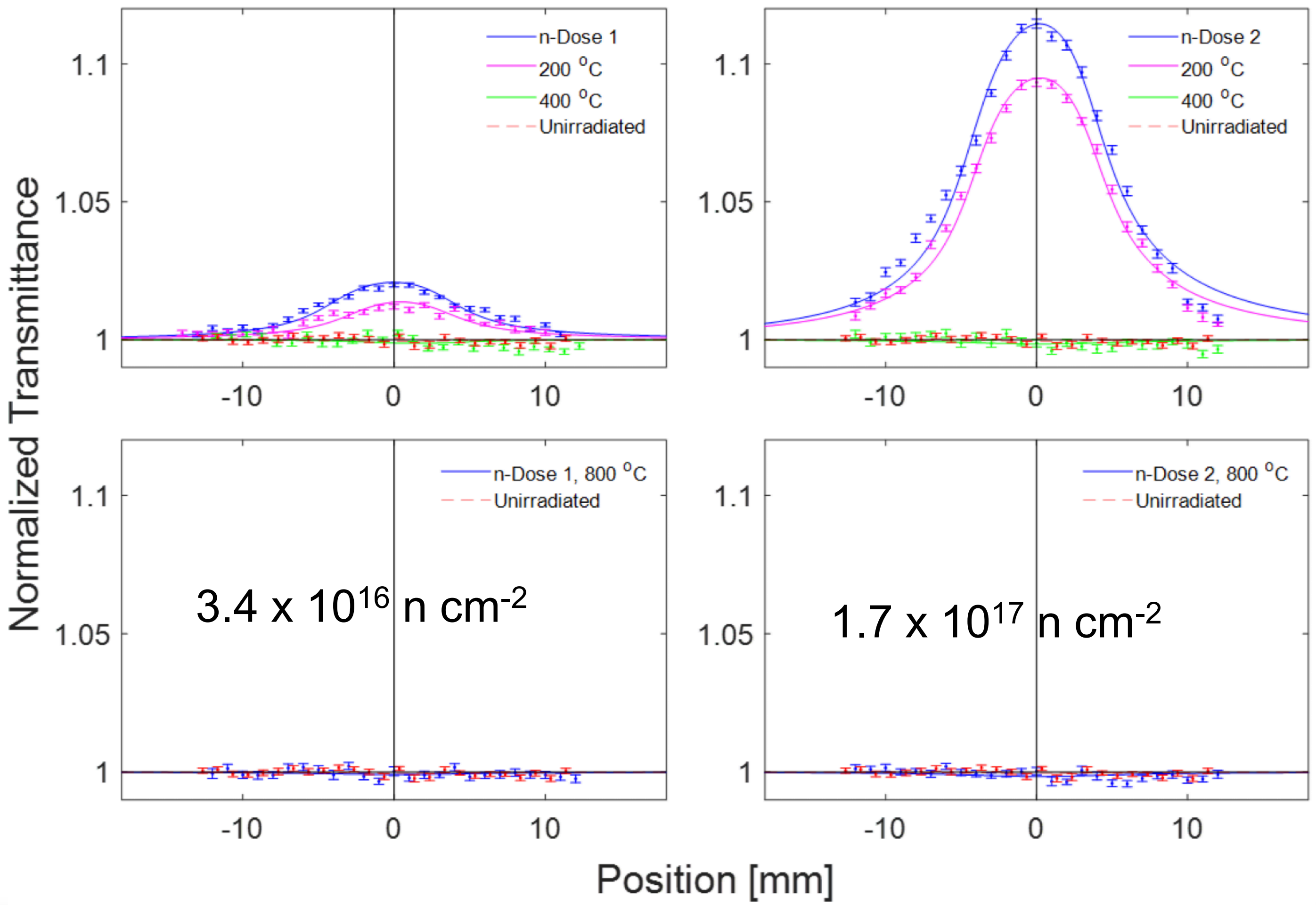

Saturable absorption may be responsible for negative nonlinearity

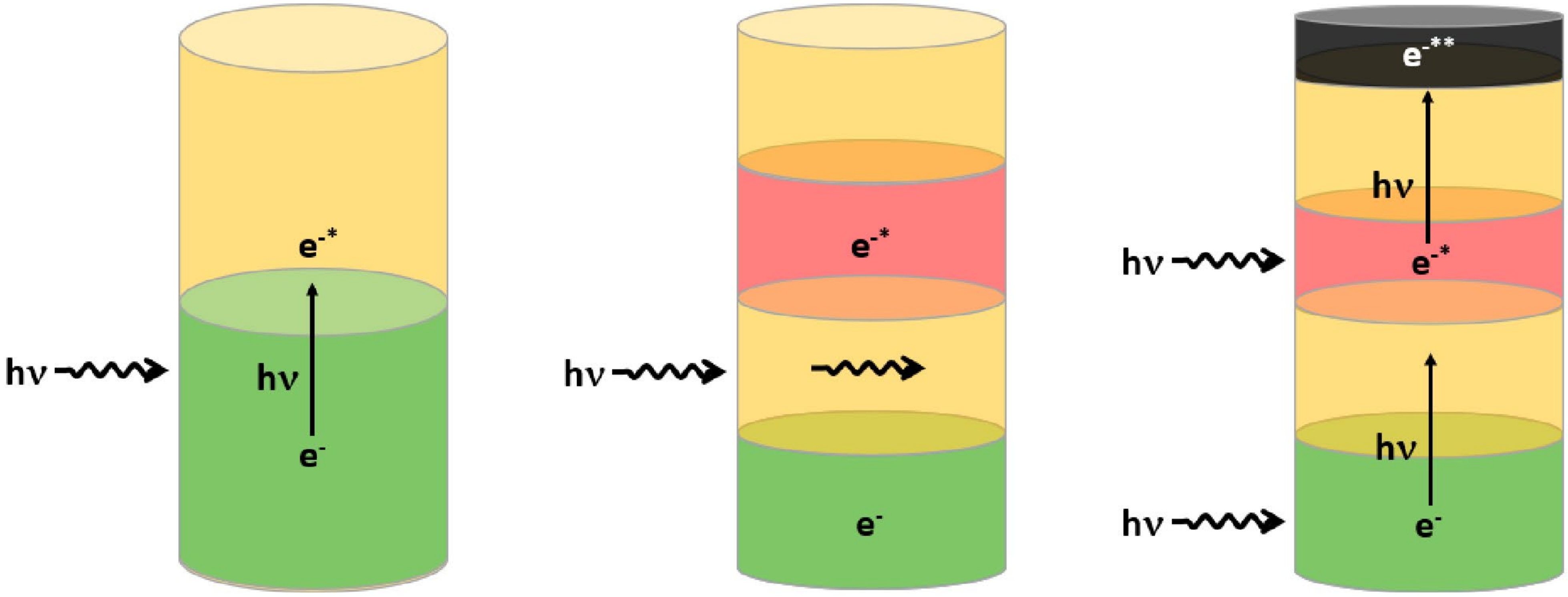

"Standard" linear absorption

Saturable absorption

Reverse saturable absorption

$$\alpha_{SA} = \frac{\alpha_0}{1 + I_0/I_S}$$

Measured Nonlinear Absorption Coefficients

Nonlinearity	n-Dose Anneal Temperature	Optical Sample				
		S2000	I302	Sapphire	NBK7	BK7G18
β $[\mathrm{m{\cdot}W^{-1}}]$	Unirradiated	$(<5)\times10^{-15}$	$(<5)\times10^{-15}$	$(<1.6)\times10^{-14}$	$(2.8)\times10^{-14}$	$(2.8)\times10^{-14}$
β $[\mathrm{m{\cdot}W^{-1}}]$ Post-irradiation Annealing	n-Dose 1	$(-1.96\pm0.31)\times10^{-14}$	$(-1.21\pm0.01)\times10^{-12}$	$(-4.04\pm0.20)\times10^{-14}$	$(-1.01\pm0.02)\times10^{-11}$	$(-1.86\pm0.27)\times10^{-14}$
	n-Dose 1 200 °C	$(-7.01\pm1.20)\times10^{-15}$	$(-7.61\pm0.07)\times10^{-13}$	$(-2.37\pm0.21)\times10^{-14}$	$(-1.67\pm0.05)\times10^{-12}$	$(1.53\pm0.32)\times10^{-14}$
	n-Dose 1 400 °C	$(2.50\pm2.31)\times10^{-15}$	$(5.16\pm4.40)\times10^{-15}$	$(2.50\pm3.86)\times10^{-15}$	$(2.91\pm0.30)\times10^{-14}$	$(2.86\pm0.25)\times10^{-14}$
	n-Dose 2	$(-2.33\pm0.32)\times10^{-14}$	$(-5.01\pm0.02)\times10^{-12}$	$(-1.74\pm0.04)\times10^{-13}$	$(-1.99\pm0.05)\times10^{-11}$	$(-5.77\pm0.27)\times10^{-14}$
	n-Dose 2 200 °C	$(-1.55\pm0.21)\times10^{-14}$	$(-4.48\pm0.02)\times10^{-12}$	$(-1.47\pm0.04)\times10^{-13}$	$(-4.41\pm0.02)\times10^{-12}$	$(-1.23\pm0.24)\times10^{-14}$
	n-Dose 2 400 °C	$(1.20\pm2.50)\times10^{-15}$	$(-9.17\pm0.55)\times10^{-14}$	$(1.99\pm2.62)\times10^{-15}$	$(2.84\pm0.31)\times10^{-14}$	$(2.66\pm0.51)\times10^{-14}$
	n-Dose 2 600 °C	-	$(2.85\pm6.33)\times10^{-15}$	-	-	-

preliminary

Photobleaching in sapphire

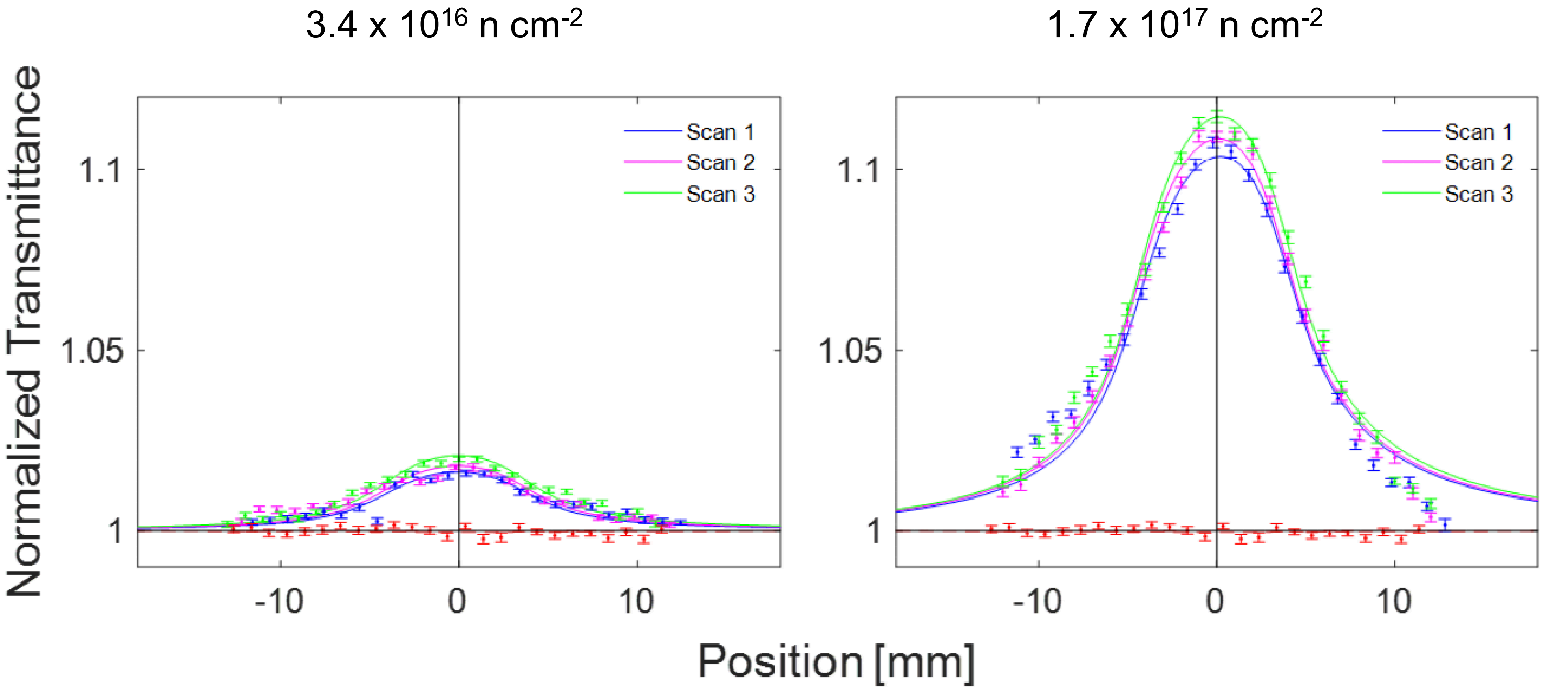

RIA in sapphire with post-annealing

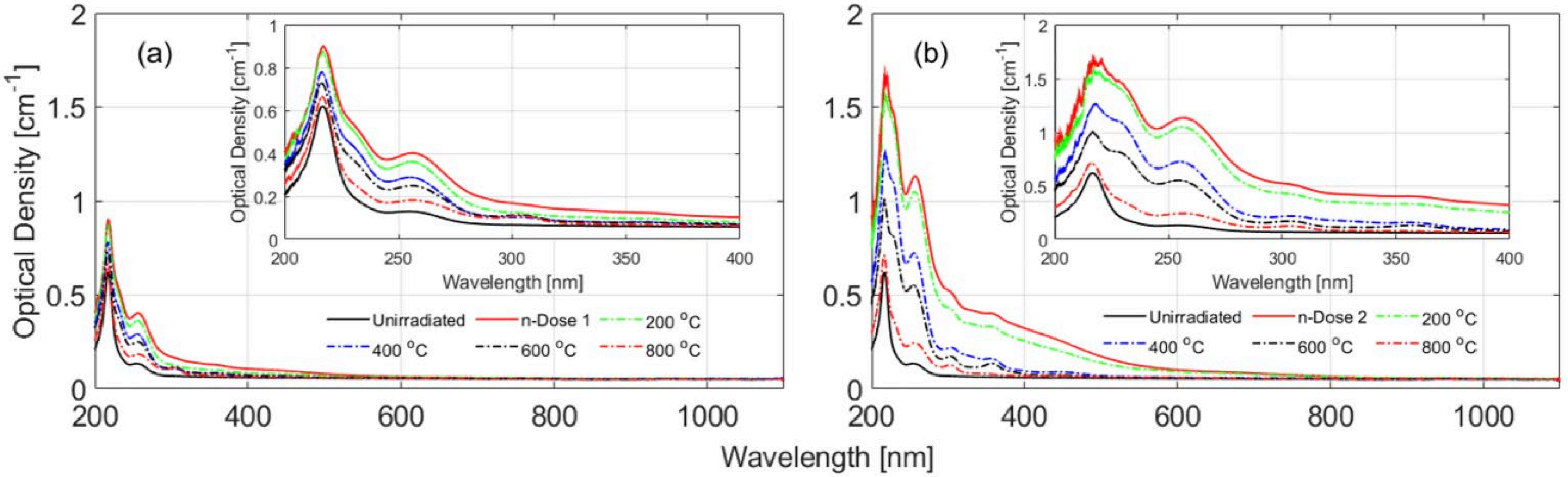

n-Dose 1: 3.4×10^{16} n · cm^{-2}
n-Dose 2: 1.7×10^{17} n · cm^{-2}

RIA in sapphire with concurrent annealing

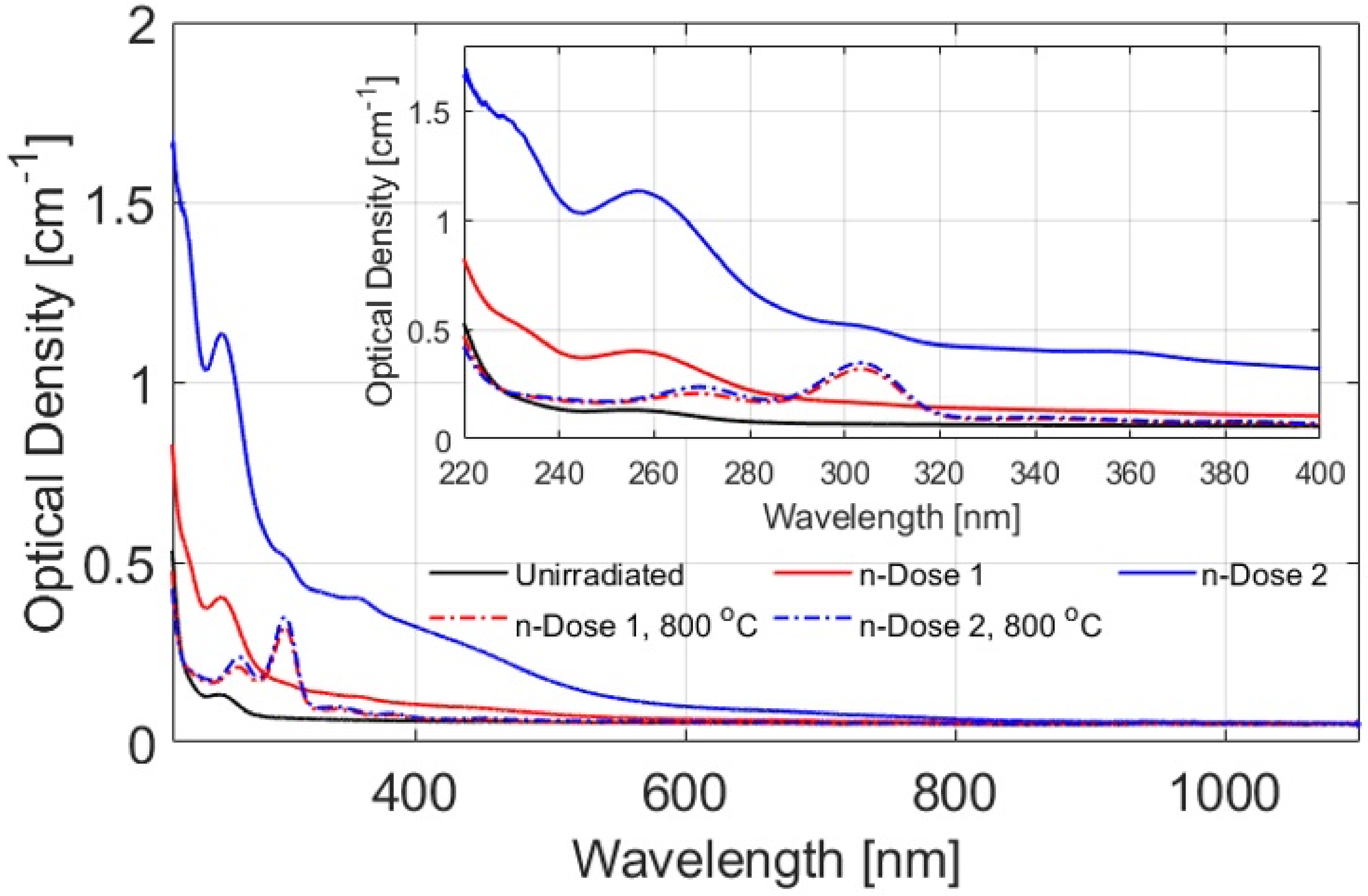

n-Dose 1: 3.4×10^{16} n · cm^{-2}
n-Dose 2: 1.7×10^{17} n · cm^{-2}

RIA in gamma-irradiated sapphire with concurrent annealing

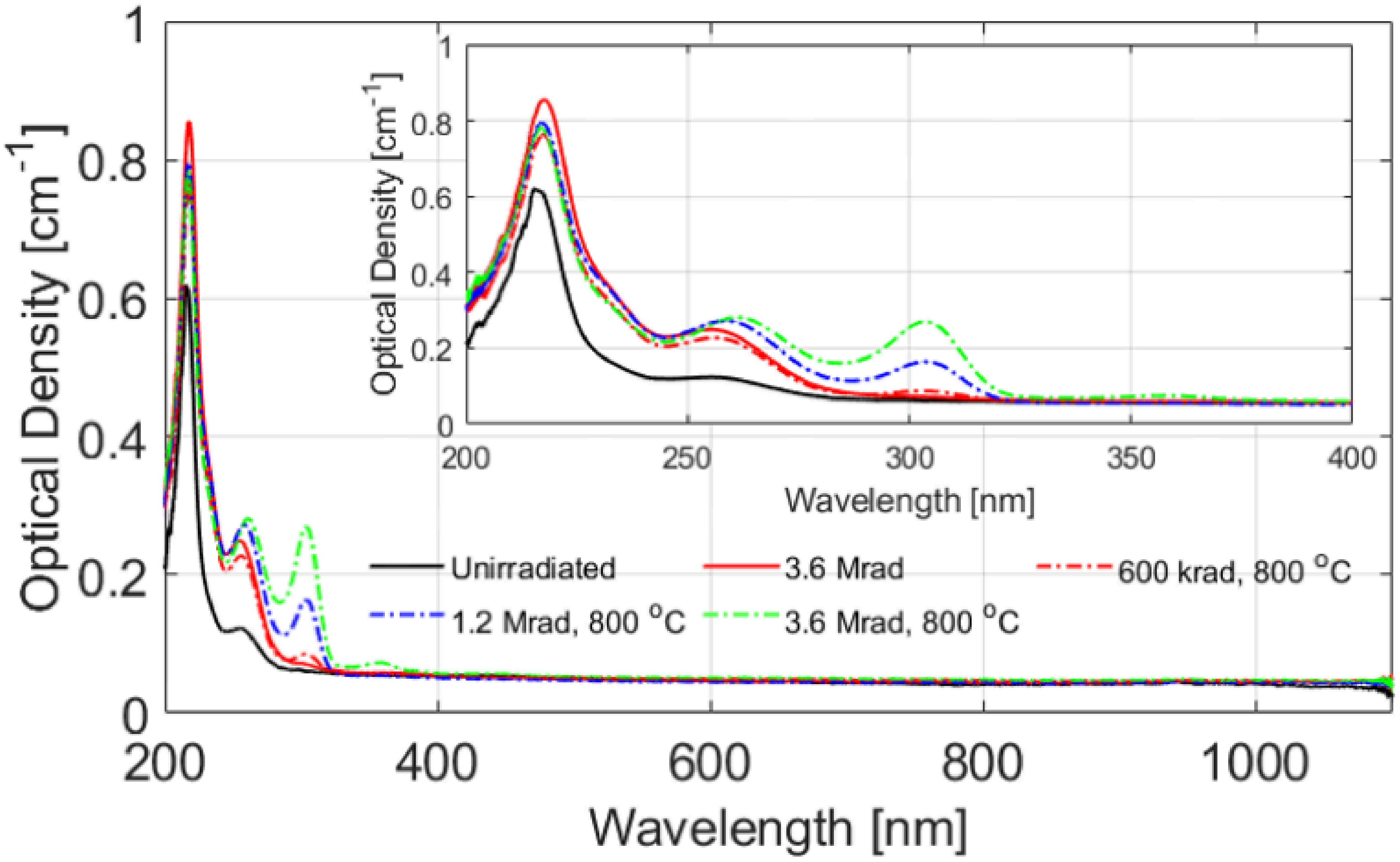

Features of radiation-induced absorption

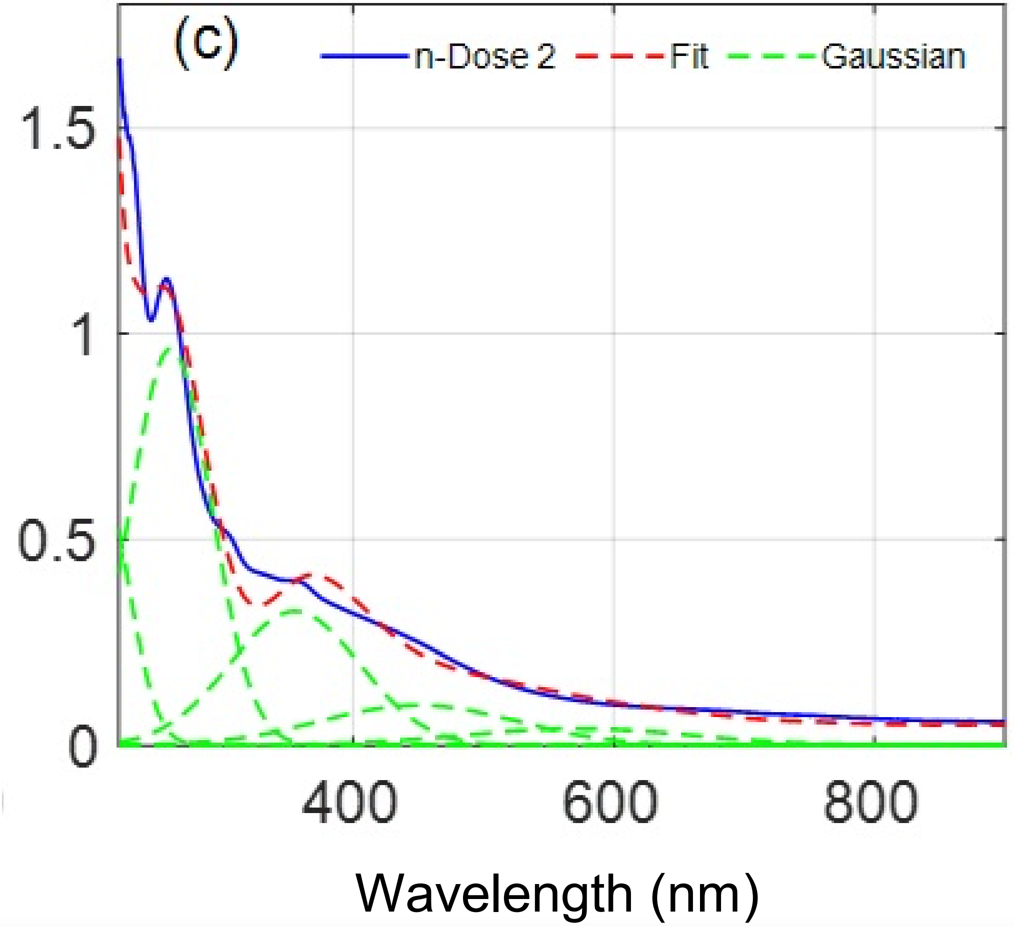

Experimental data were fit with sums of Gaussians accounting for previously reported centroids and widths.

Centroid	FWHM
205 nm	44 nm
260 nm	62 nm
300 nm	66 nm
355 nm	102 nm
450 nm	150 nm
572 nm	178 nm

205 nm F center
260 nm F+ center
300 nm F2 center
355 nm F2+ center
450 nm F22+ center
572 nm Al-OHC

Evaluating the effect of irradiation on instrumentation

Long-term irradiation of windows and fibers alters material absorbance and LIBS spectral properties.

Linear Absorbance Scaling

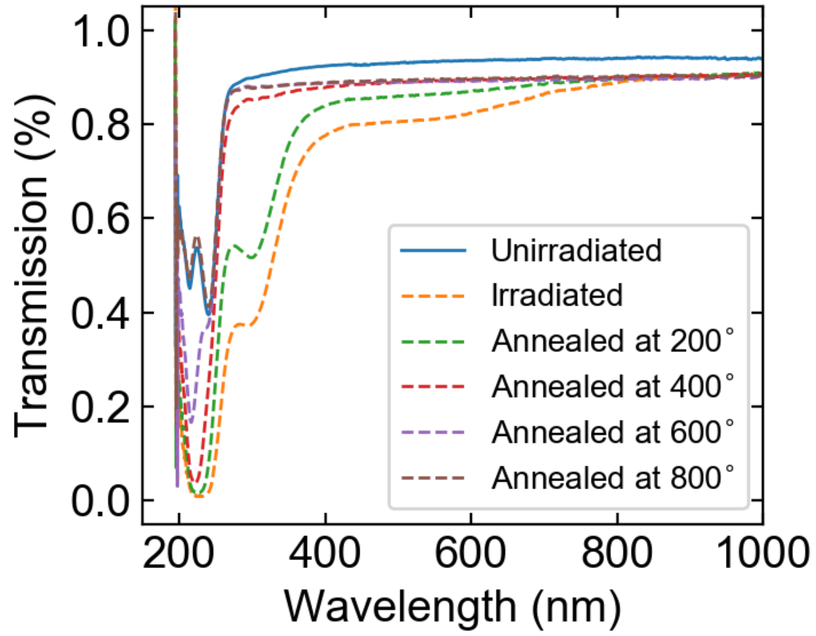

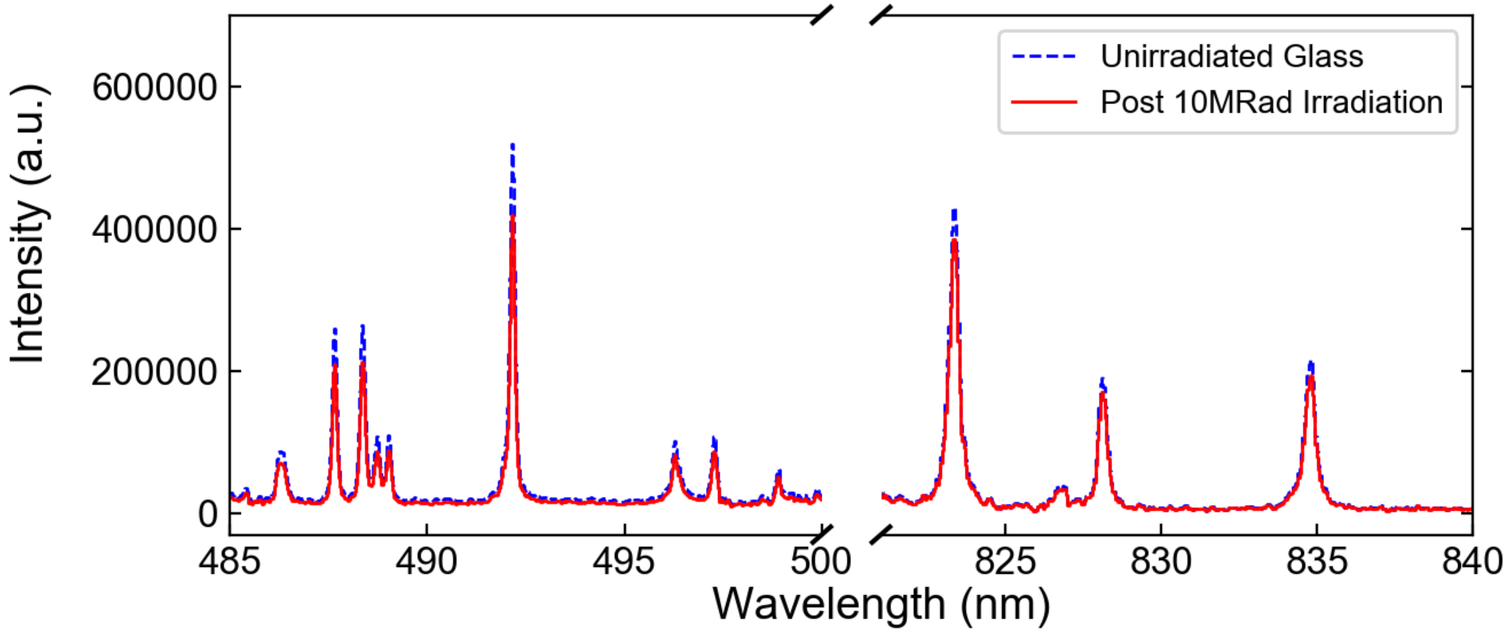

Assumptions: 1% Xe in He, 2us delay scaled by Infrasil-302, 10 MRad gamma irradiation data

Evaluating the effect of irradiation on instrumentation

Single Line Effects

For 497 Xe II emission and 10 Hz repetition rate:

Dose (Mrad)	Shots for 3σ	Detection Time (s)
0.60	1	0.10
1.20	1	0.10
3.60	2	0.20
10	2	0.20

Multi-Line Effects

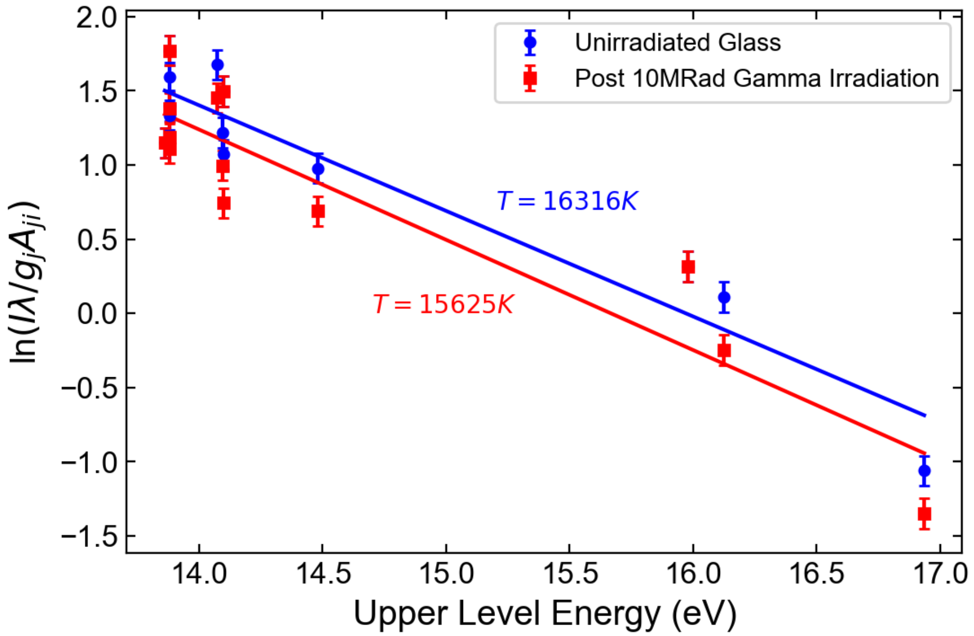

Publications

- B. W. Morgan, M. P. Van Zile, C. M. Petrie, P. Sabharwall, M. Burger, and I. Jovanovic, “Optical Absorption of Fused Silica and Sapphire Exposed to Neutron and Gamma Radiation with Simultaneous Thermal Annealing,” under review.
- Y. Lee, S. Yoon, H. Kim, N. Kim, W. Yang, D. Kang, M. Burger, I. Jovanovic, and S. Choi, “Distance-corrected Laser-induced Breakdown Spectroscopy for High-precision In-situ Measurement in High-temperature Molten Salts,” under review.
- B. W. Morgan, M. Van Zile, P. Sabharwall, M. Burger, and I. Jovanovic, “Gamma-radiation-induced negative nonlinear absorption in quartz glass,” *Optical Materials Express* 12, 1188-1197 (2022).
- B. W. Morgan, M. Van Zile, P. Sabharwall, M. Burger, and I. Jovanovic, “Post-Irradiation Examination of Optical Components for Advanced Fission Reactor Instrumentation,” *Review of Scientific Instruments* 92, 105107 (2021).
- B. Morgan, M. Burger, and I. Jovanovic, “Linear and Nonlinear Optical Properties of Fused Silica and Sapphire in Extreme Radiation and Thermal Environments,” IEEE Nuclear & Space Radiation Effects Conference, Provo, UT July 18–22, 2022.
- B. Morgan, M. Van Zile, P. Sabharwall, M. Burger, and I. Jovanovic, “Radiation-induced Negative Nonlinear Absorption in Glass and Sapphire,” Conference on Lasers and Electro-Optics, San Jose, CA, May 15-20, 2022.
- B. Morgan, M. Van Zile, P. Skrodzki, X. Xiao, P. Sabharwall, P. Marotta, M. Burger, and I. Jovanovic, “Post-Irradiation Examination of Irradiated Optical Components of In-Situ Spectroscopic Sensors for Advanced Fission Reactors,” ANS Winter Meeting, November 30–December 3, 2021.
- B. Morgan, P. Skrodzki, M. Burger, P. Sabharwall, P. Marotta, and I. Jovanovic, “Post-Irradiation Examination System Development for Irradiated Optical Components of In-Situ Spectroscopic Sensors,” ANS Winter Conference [online], November 15-19, 2020.

Journals–under review Journals–published Conferences

Thank you! Questions?

Nuclear Science User Facilities

Advanced Sensors and Instrumentation

This work has been supported by the Department of Energy, Nuclear Science User Facilities Program under award DE-NE0008906.

U.S. DEPARTMENT OF ENERGY | Office of NUCLEAR ENERGY

Molten salt-loop development acceleration with distributed single-crystal harsh-environment optical fiber-sensors

Michael Buric, NETL: presenter
With Pattrick Calderoni (INL), Ruchi Gahkar (INL), and Koroush Shirvan (MIT) (co-PI's)

May 31, 2022

Single Crystal Distributed Sensing: Team

- National Energy Technology Lab (fiber growth, sensor design, interrogator design)
  - Michael Buric (PI, fiber optics and systems)
  - Guensik Lim (LHPG, Raman DTS)
  - Gary Lander (LHPG #2)
  - Jeff Wuenschell (DTS field testing)
- Idaho National Lab (reactor expertise, system implementation and testing)
  - Pattrick Calderoni
    (in-pile instrumentation director, co-PI)
  - Joshua Daw (nuclear instrumentation)
  - Ruchi Gakkar (nuclear materials)
  - Kelly McCary (Molten Salt testing)
- MIT (material compatibility, efficacy simulations)
  - David Carpenter (Irradiation Engineering Director)
  - Koroush Shirvan (reactor design and simulation, co-PI)
  - Yeongshin Jeong (now at ANL, simulation programming)
  - Tony Zheng (radiation testing)

Single Crystal Distributed Sensing: Project Objectives

- Introducing fully-distributed sensing to Molten-Salt Reactors
- Growing new cladded single-crystal optical fibers for molten-salt environments (YAG, Sapphire, +cladding)
- Gathering thousands of data-points to map reactor coolant-path temperatures or other parameters
- Mapping in-core temperature distributions
- Next-gen sensing replaces single-point sensors like thermocouples
- Providing data to guide reactor design and improvement through thermal efficiency
- How?: Novel 2-stage LHPG, Raman distributed interrogation

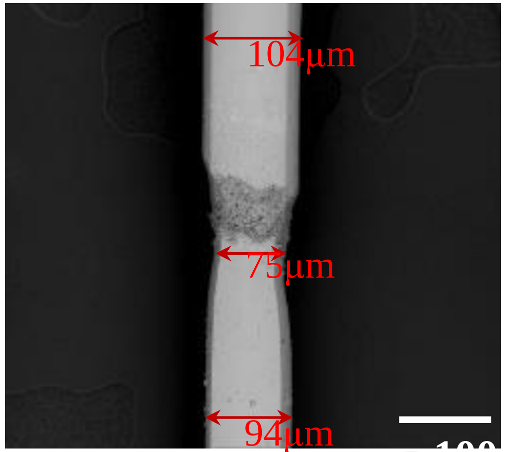

Single Crystal Distributed Sensing:

- Successful completion of materials compatibility studies
  - Reasonable fiber performance in ss 316 tubing
- Molten Salt baths measured successfully
- MITR brief reactor startup measurement
- Completion of Reactor Simulation
  - Best locations for fiber sensors determined
- Successful growth of pure feedstock materials
- World’s first 2-stage LHPG constructed
  - Pure unclad fiber to clad fiber
  - First evidence of high-temp claddings

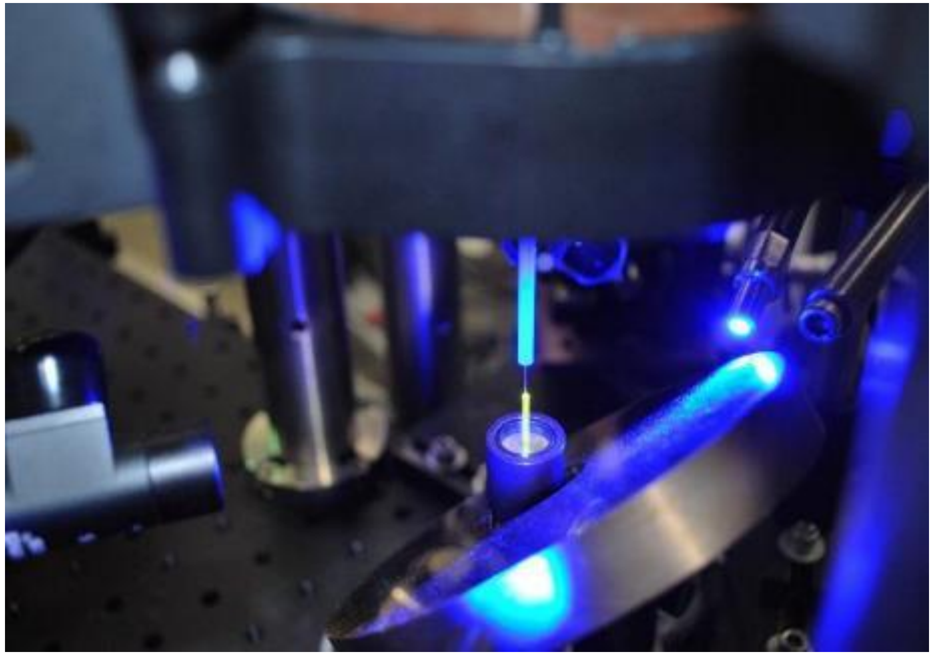

First successful growth of Cerium YAG fiber by LHPG

Crystal fiber distributed sensing

- Grow cladded fibers with 2-stage LHPG
  - Sapphire or YAG
  - Sol-gel (or other) dopant additions
- Evaluate materials compatibility in fluoride and chloride salts (bench tests)
- Evaluate radiation durability (gamma source, research reactor)

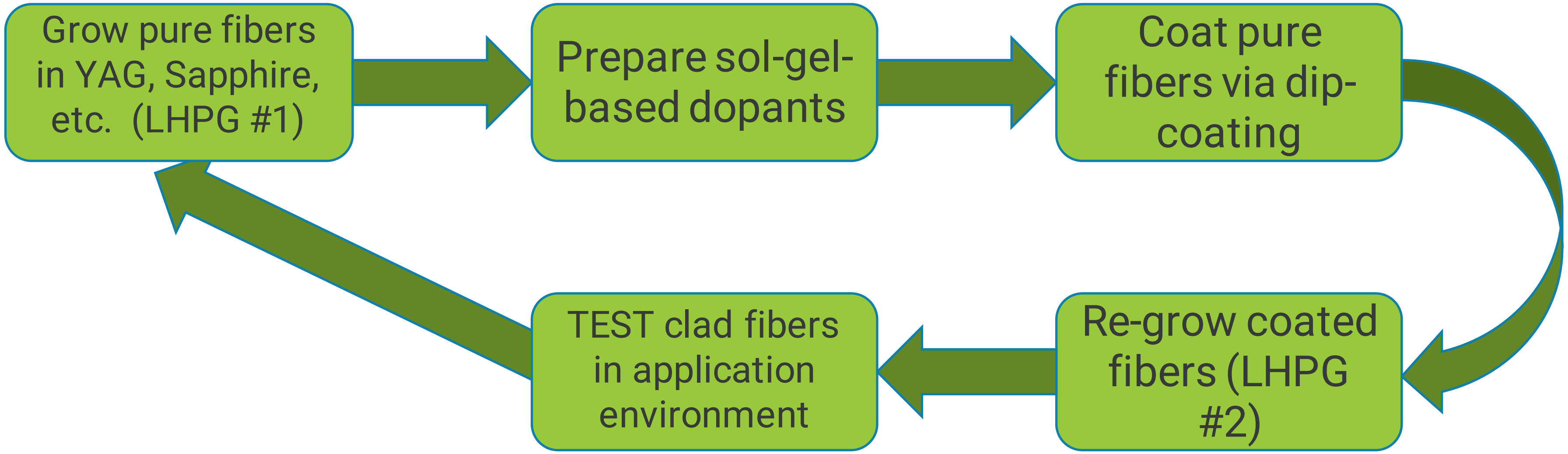

Crystal fiber distributed sensing - Claddings

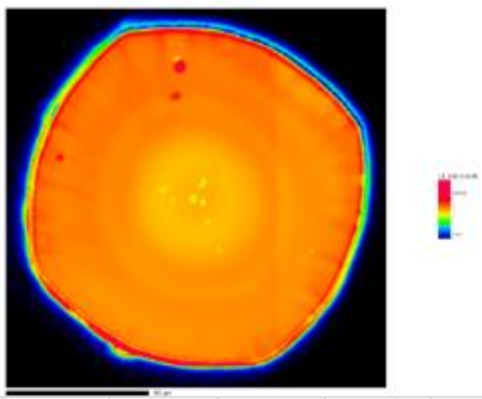

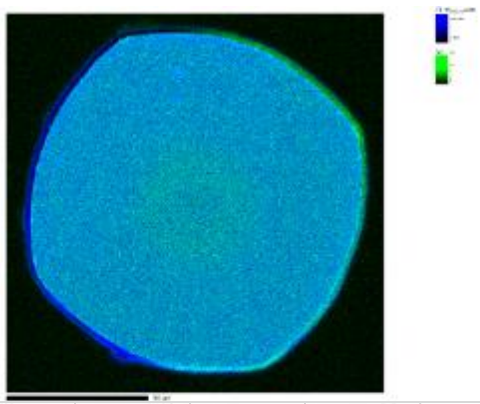

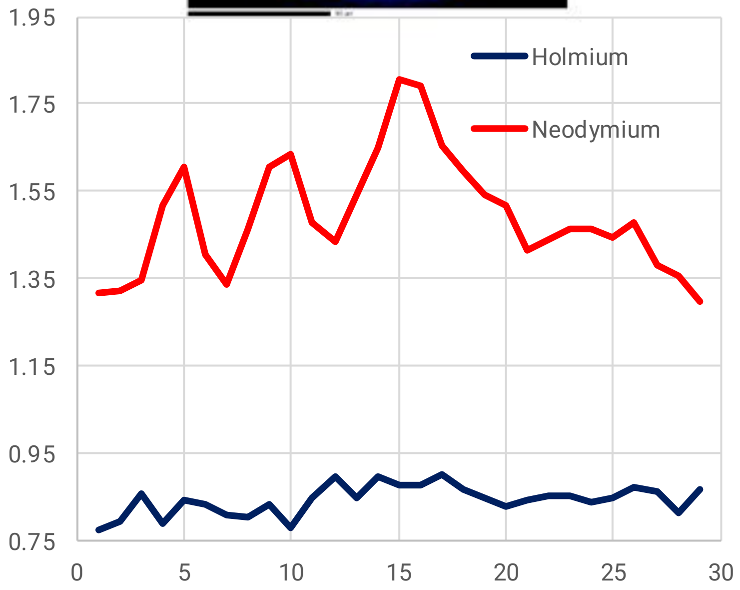

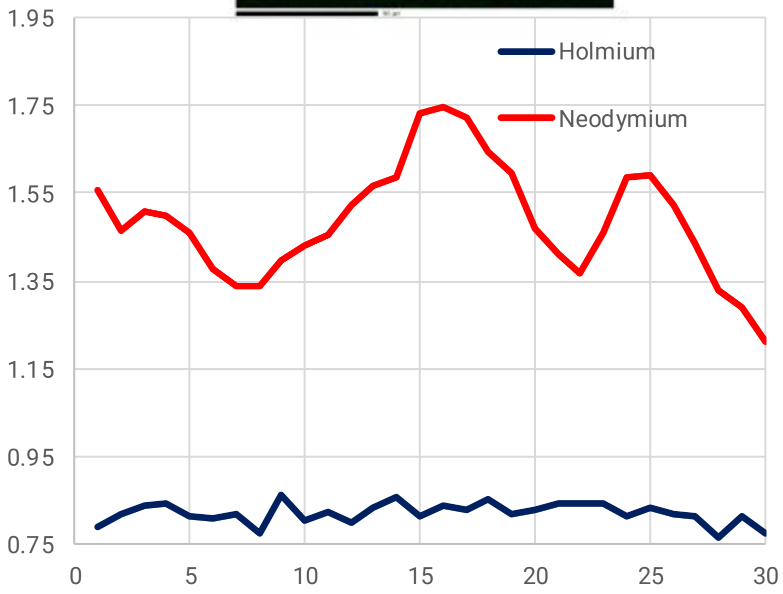

Automatic Dopant Segregation through LHPG: Top left: Visible light guiding in GRIN YAG fiber, Top right: EMPA map of Nd concentration in a GRIN YAG fiber, Bottom plots: Co-doped Nd and Ho: YAG fiber dopant concentrations in X (left) and Y (right)

arpa·e CHANGING WHAT'S POSSIBLE

Regrowth LHPG System

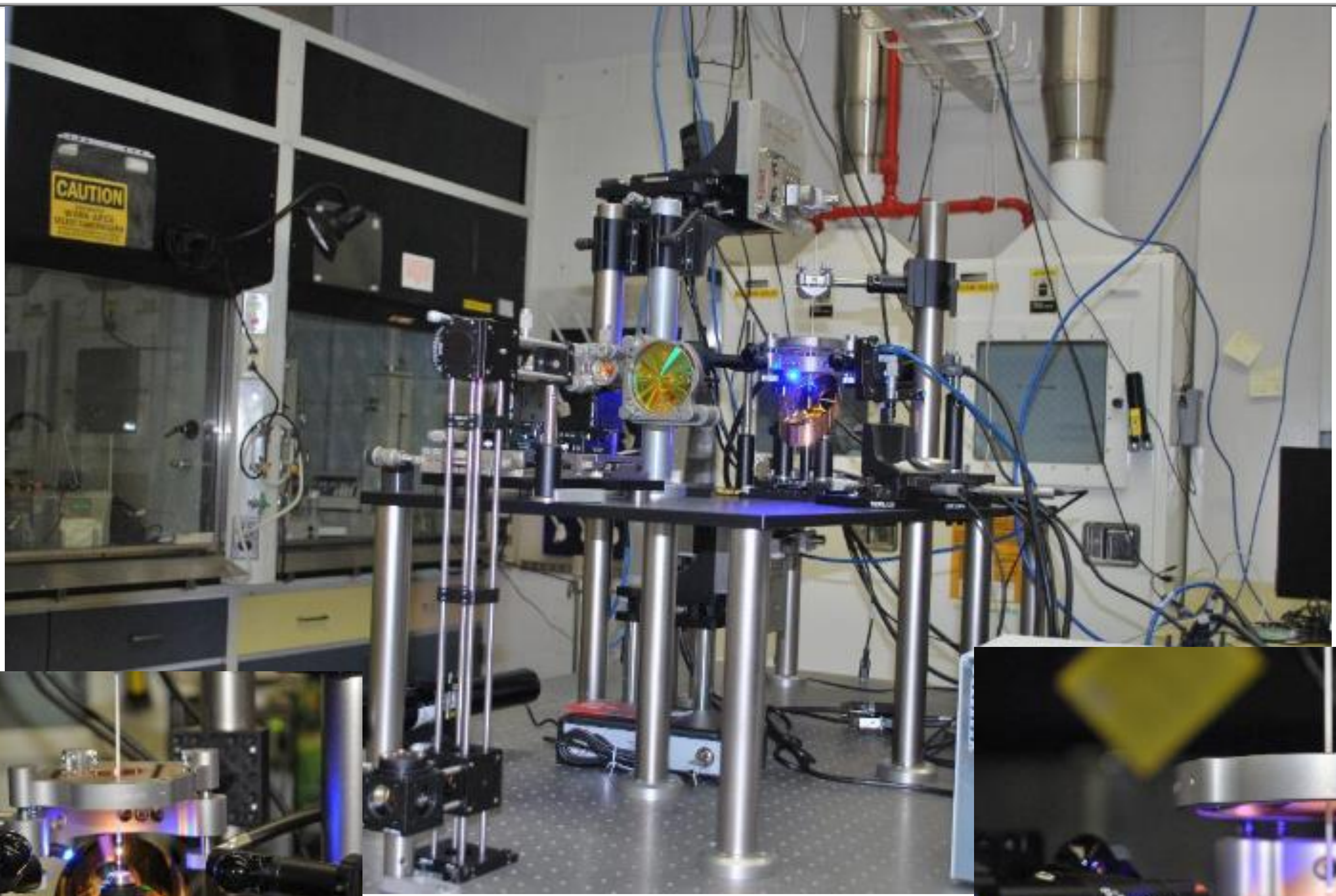

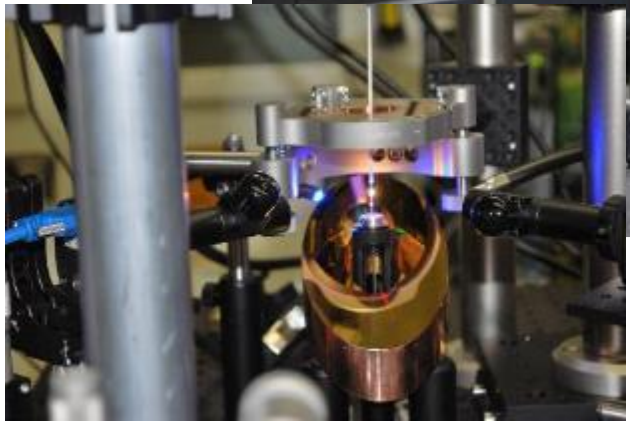

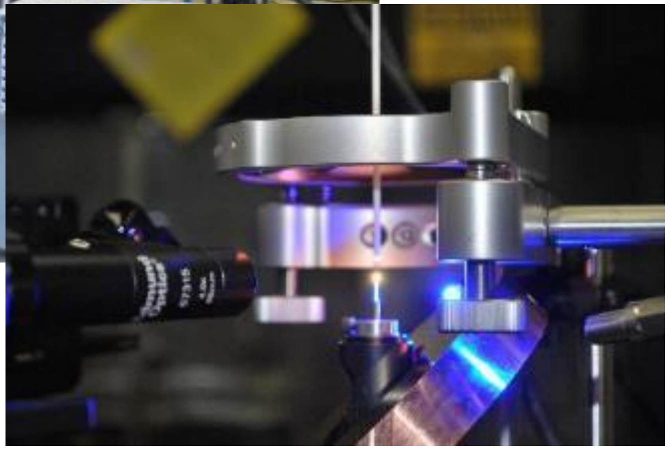

Distributed Sensing – Raman OTDR

- OTDR with Single Crystal fiber
- Useful for high-rad/ high-T
- ~5cm, ~1C resolution

Raman OTDR, Liu et al Opt. Lett., 2016

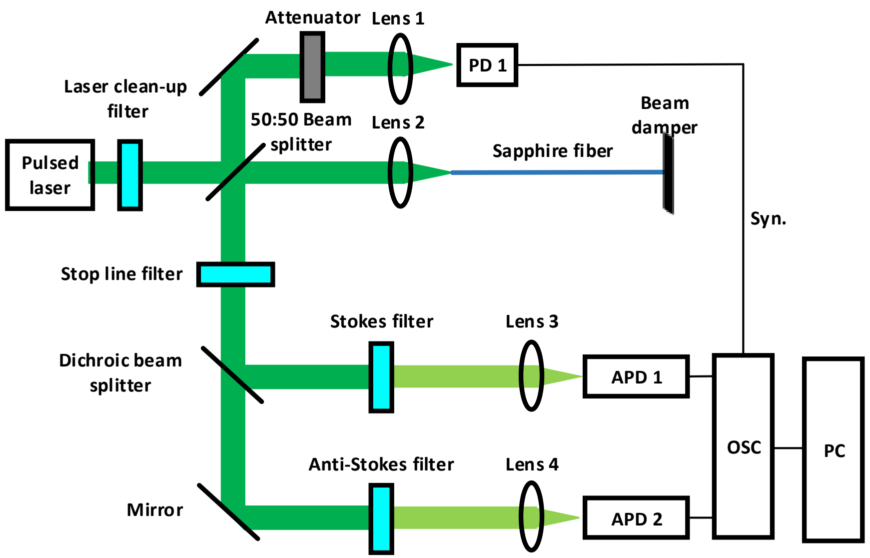

Sapphire fiber attenuation at 532nm, measured by a Raman OTDR system

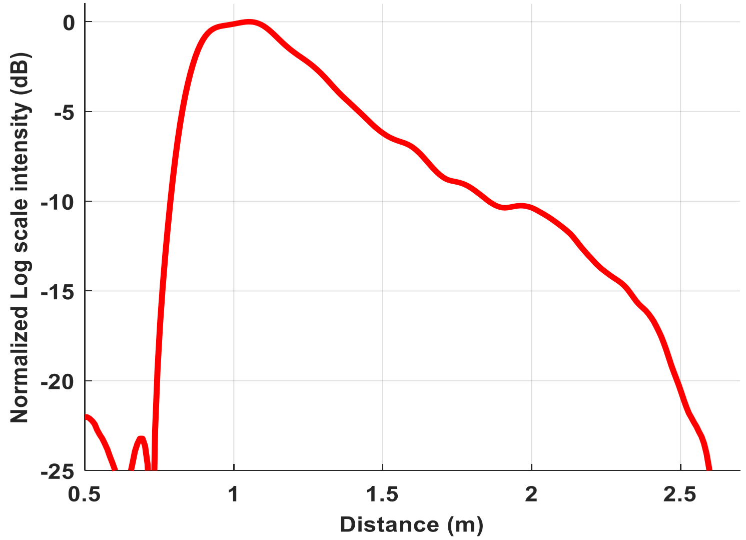

Raman DTS design and operations

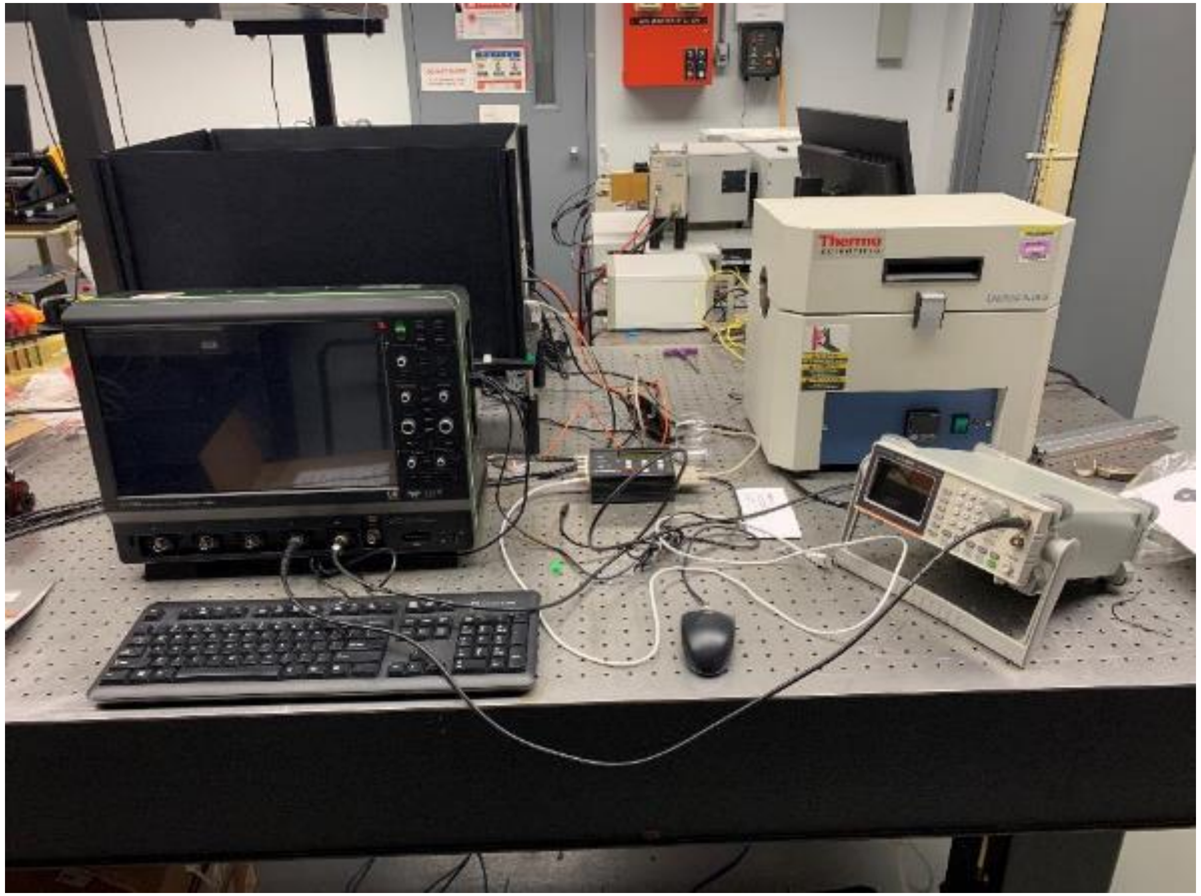

Current view of Raman DTS in the lab
with external test systems

Project accomplishments: LHPG and Raman DTS

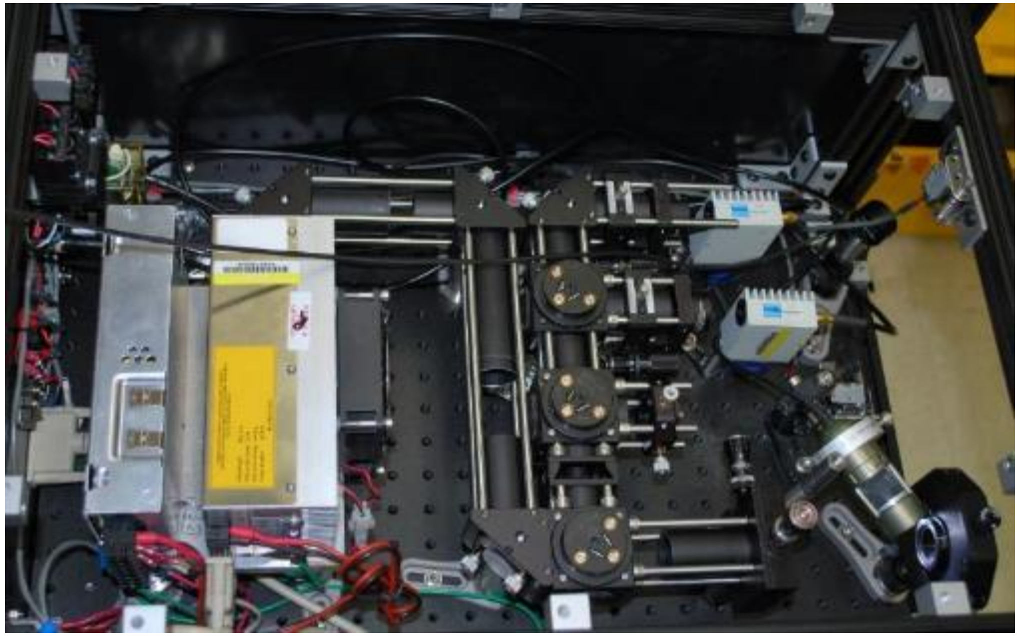

Raman DTS photo of internal components

- First DTS system for single-crystal fiber
- 5cm spatial, 2C temperature resolution
- Compatible with up to 100m of SC fiber
- Fieldable product design completed
- Long lead-in fiber + SC fiber signal processing
- Tested at MITR and INL

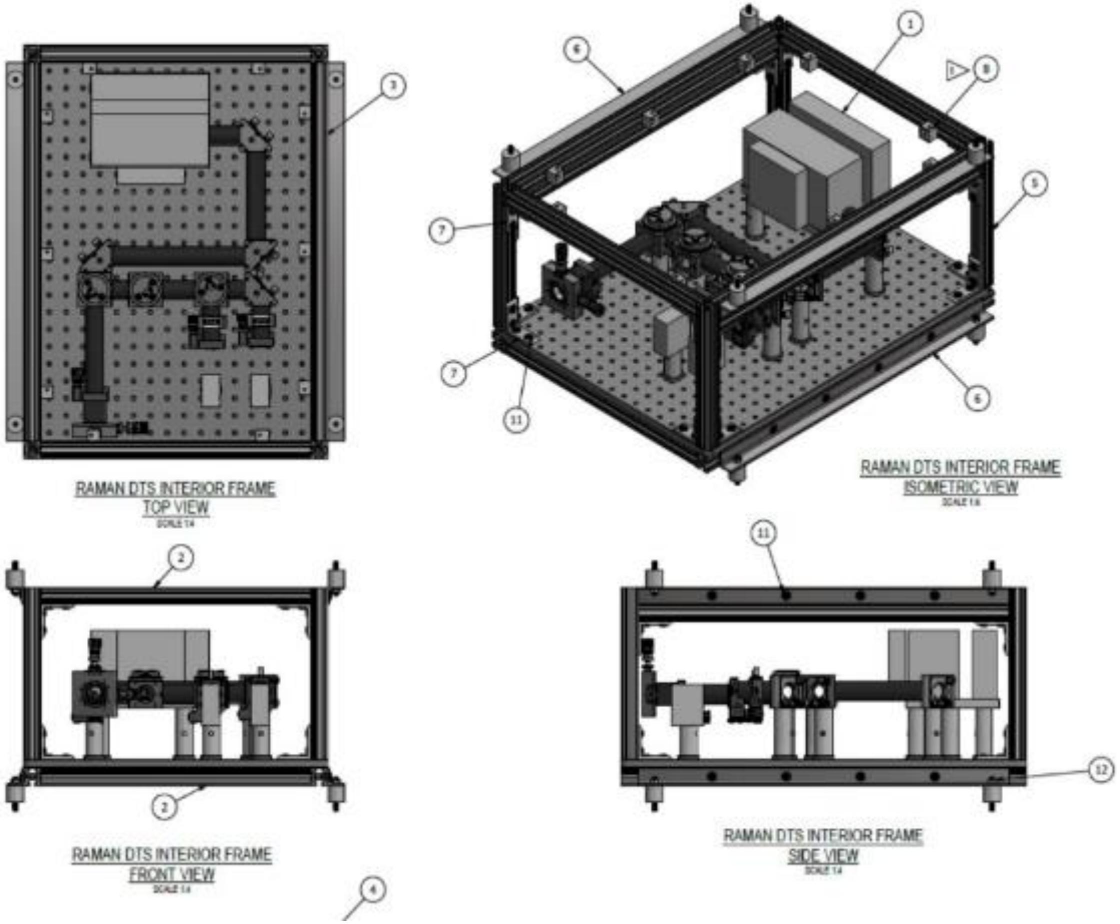

Raman DTS System drawing

Project accomplishments – materials compatibility

Recommendations for fiber protection materials

Protective coating Type	Chloride Salts	Fluoride Salts
Metallized fibers	Ni, Mo and Ta	Ni, Mo and Ta
Tubular fiber sleeves (primary choice)	SS316	Ni-200
Tubular fiber sleeves (further considerations)	Alloy 617, 800H and TZM (Titanium Zirconium Molybdenum (98-99% Mo)	Hastelloy and Haynes alloys

Project accomplishments – molten salt testing (Gahkar, McCary, Calderoni)

Experimental Setup at INL

SS316 Capillary

Thermocouple

Alumina lid

Fiber: Heat-treated Pure Silica core, f-doped cladding single mode optical fiber

Salt-mixture: NaCl-$MgCl_2$ eutectic

Crucible: Glassy carbon, dimensions H: 80mm, D: 37mm

Data recorded: 466, 500, 525, 550, 575, 600, 625 and 650ºC

Depth of thermocouple inserted in salt – below the set screw

With respect to the fiber:
Top of Lid: 358.8 cm
Bottom of Lid: 359.44 cm
Top of Salt: 360.4 cm
Bottom of crucible (inside): 367.2 cm

Glassy carbon rod dipped in molten salt – to demonstrate Depth of salt bath

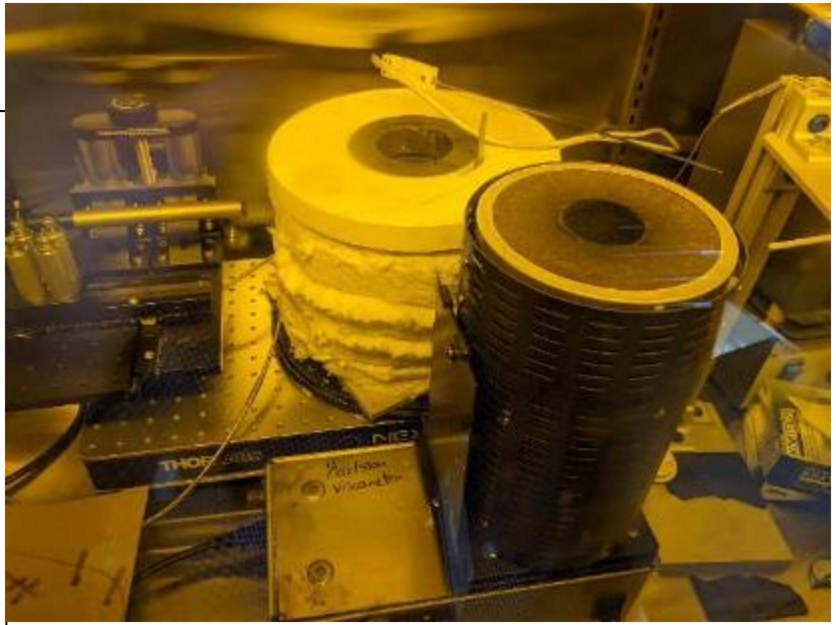

Molten Salt test results (patch cable + sapphire)

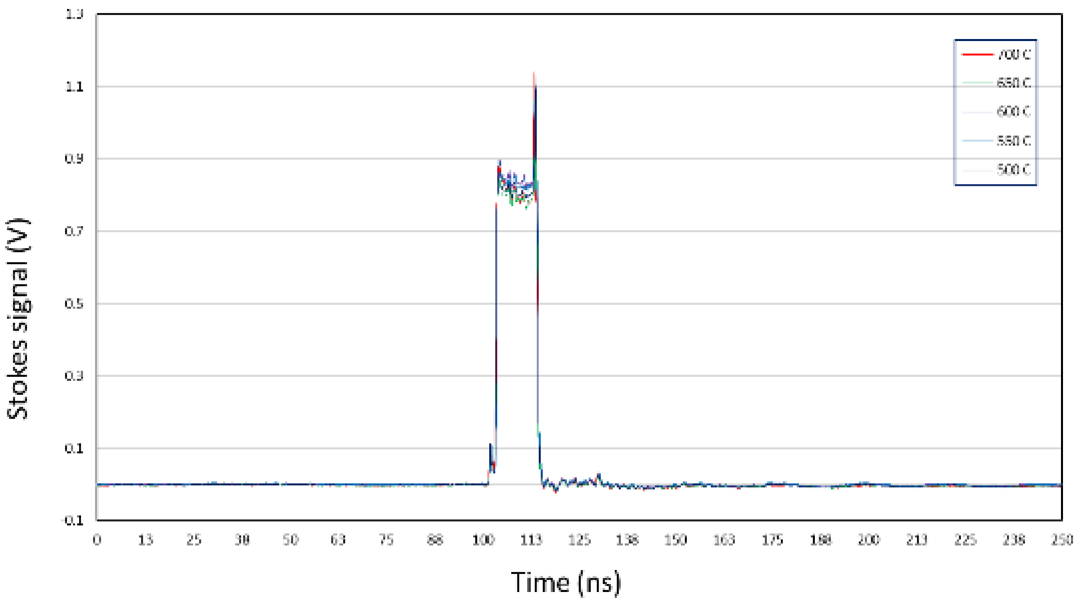

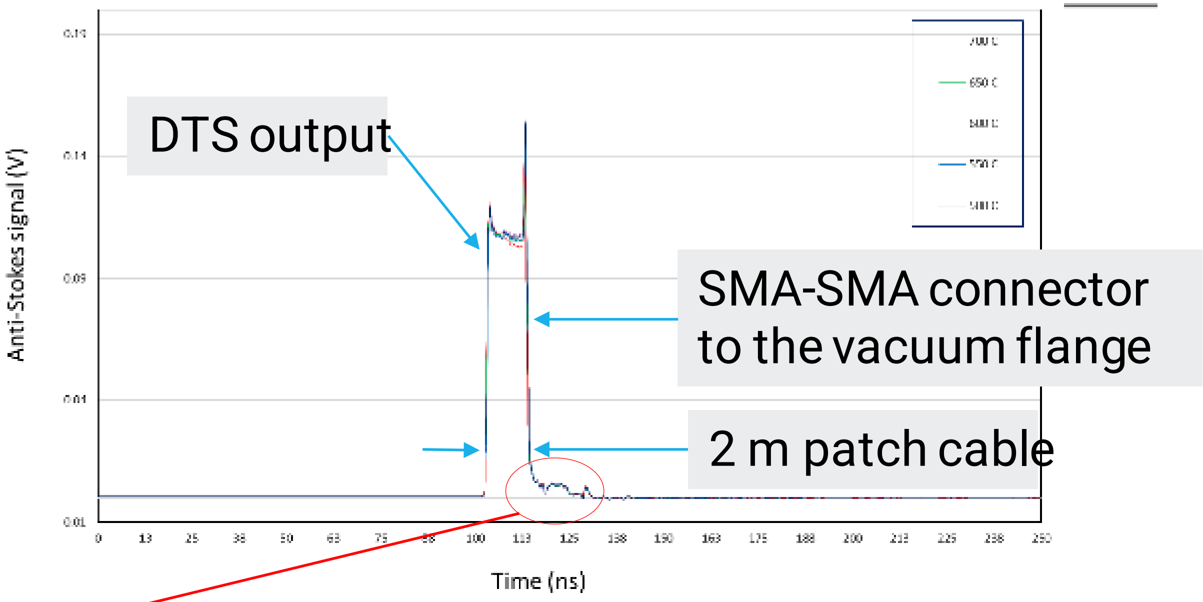

- **Furnace temperature rang:** 500 to 700°C with 50°C increments

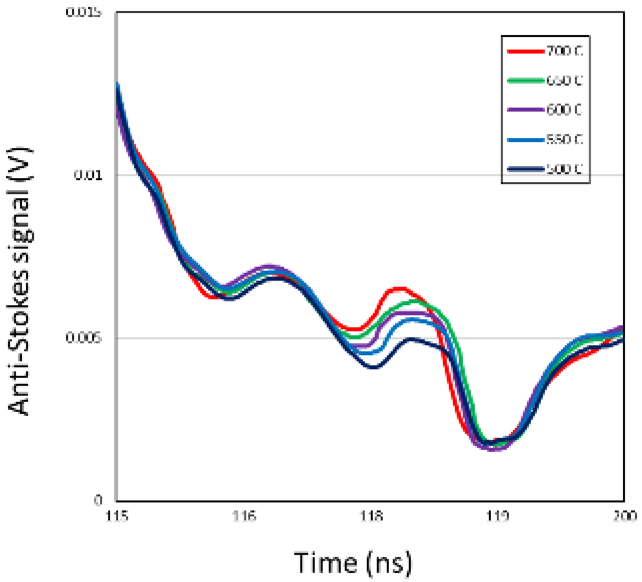

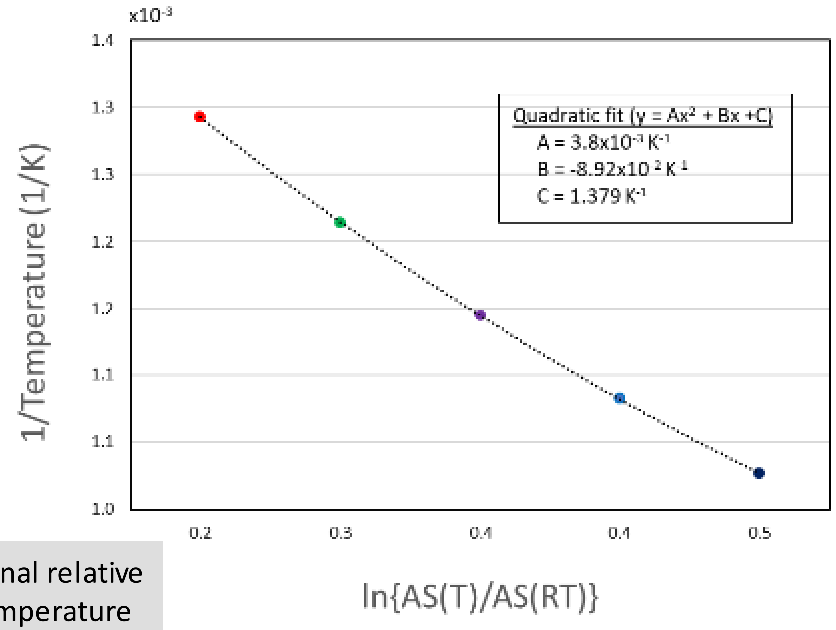

Temperature calibrated to AS signal relative to room temperature at peak temperature

Project accomplishments – Radiation testing (Shirvan, Zheng, Carpenter, Wuenschell)

Gamma Exposure testing completed at MIT

Reactor startup observed at MITR

Project accomplishments: reactor simulations (Shirvan, Jeong)

- Completed simulation of reactor transient response under normal conditions and fault scenarios

Neutronics (SERPENT)

- ✓ Generation of neutronics parameters
- ✓ 0-D/3-D, Steady state
  - ➢ Neutronics: static fuel at constant temperature

Coupled neutronics/T-H (Simplified MSR Kinetics Model)

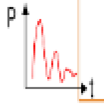

- ✓ Transient response of state variables (power, salt and structure temperature, reactivity, etc.)
- ✓ Lumped model, transient
  - ➢ Neutronics: effects of precursor transport due to flow T/H: energy balance only, constant flow rate

Thermal-Hydraulics (Star-CCM+)

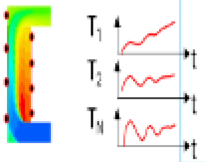

- ✓ Thermal response of MSR in time and space
- ✓ 2-D (or 3-D), transient
  - ➢ Neutronics: power changes imported from simulator
  - ➢ T/H: momentum/energy balance incl. convective and radiative heat transfer of salt

Validation

ORNL MSRE Data

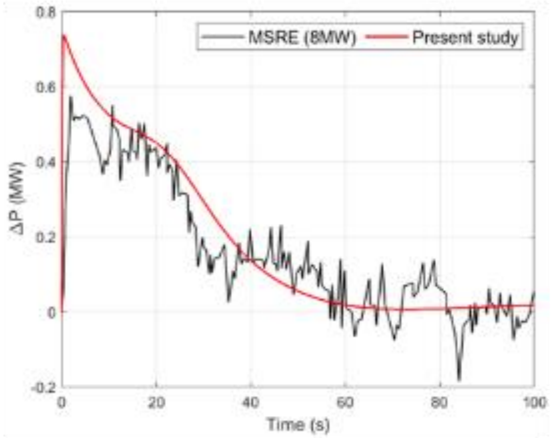

Verification

European MSR Simulator

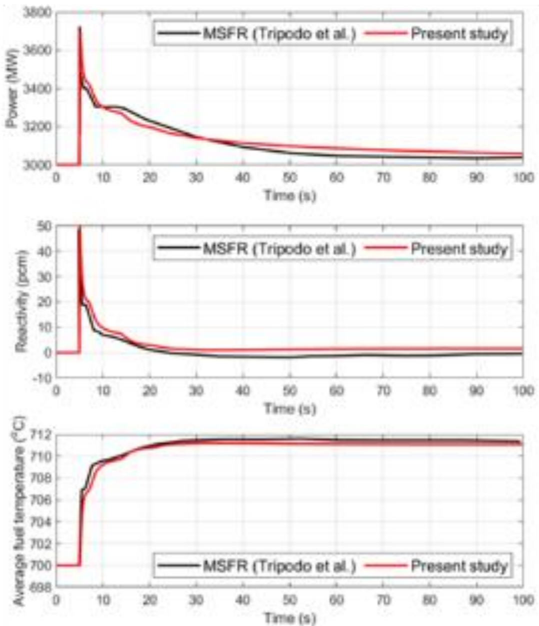

MCFR Application (Based on Available Literature on TerraPower MCFR Design)

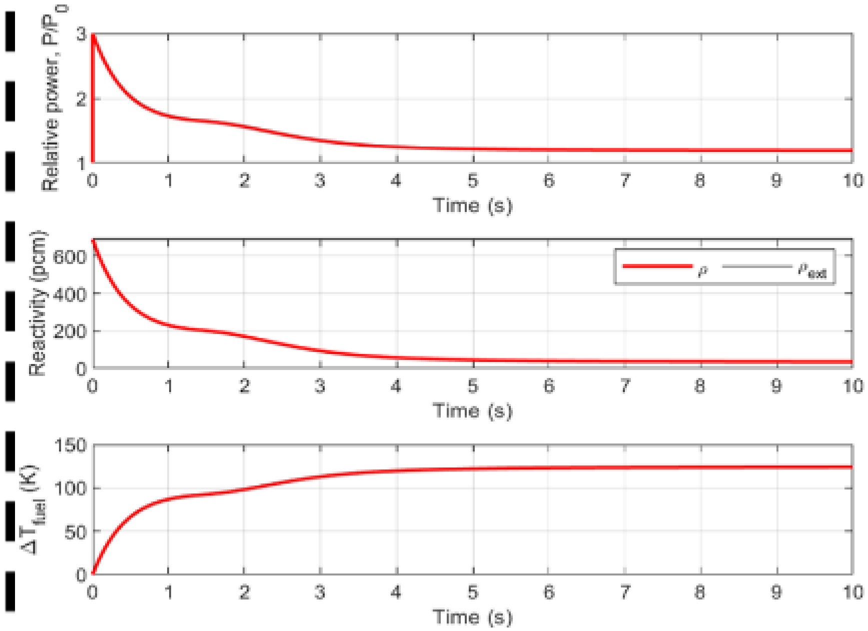

$\Delta\rho = +2\beta$

Transient response of power, reactivity, and fuel salt temperature changes (1)

TEA sim: optimal sampling rate and resolution

Technology-to-Market

- Demonstrates the Techno-Economic Value of Continuous Temperature Monitoring
  - ✓ Temperature distribution in the salt, reflector and vessel walls experience meaningful gradients and local peaks

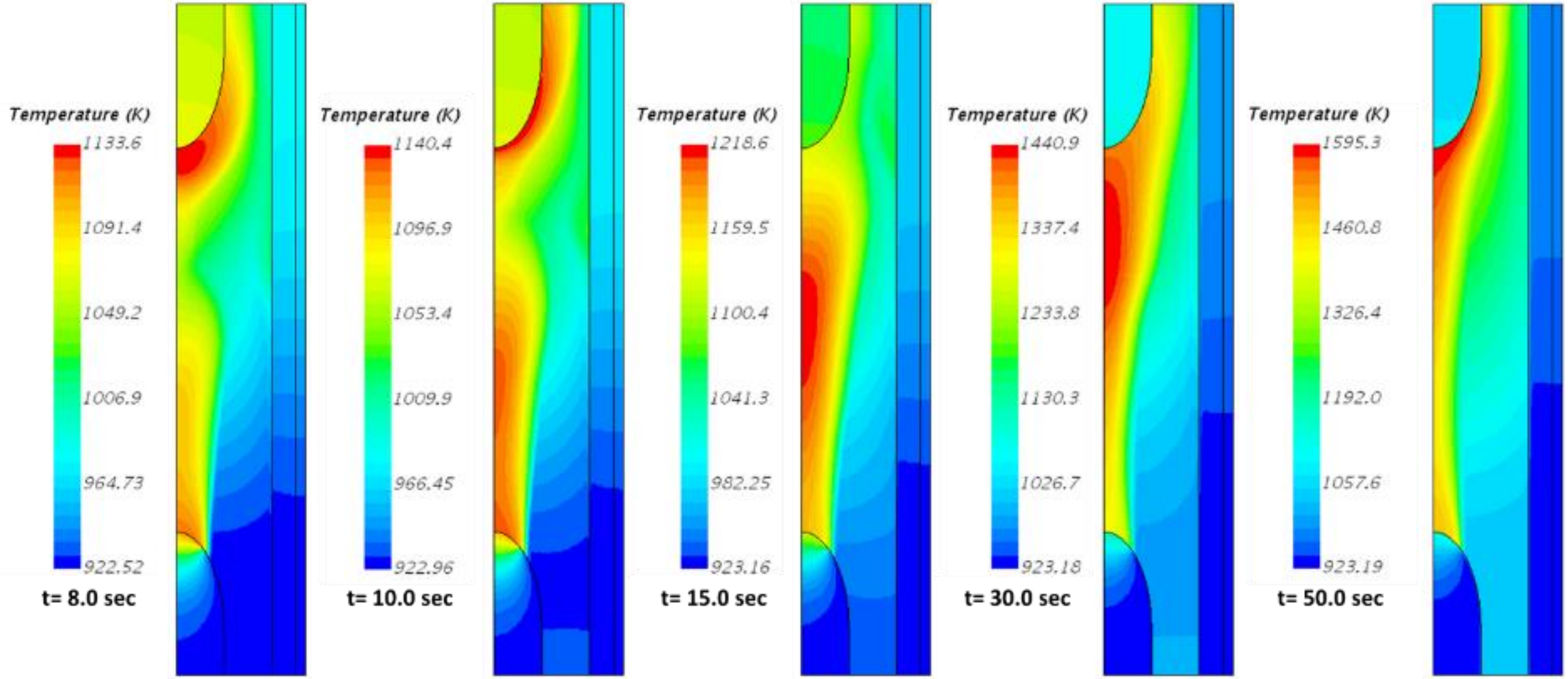

Unprotected LOF (Decrease of fuel salt flow rate to 80 % exponentially with time constant of 5 sec)

arpa·e CHANGING WHAT'S POSSIBLE

TEA Simulations: sensor placement

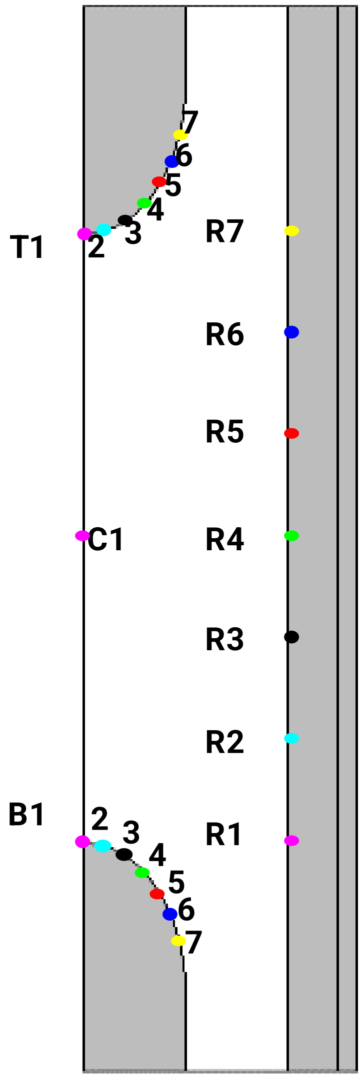

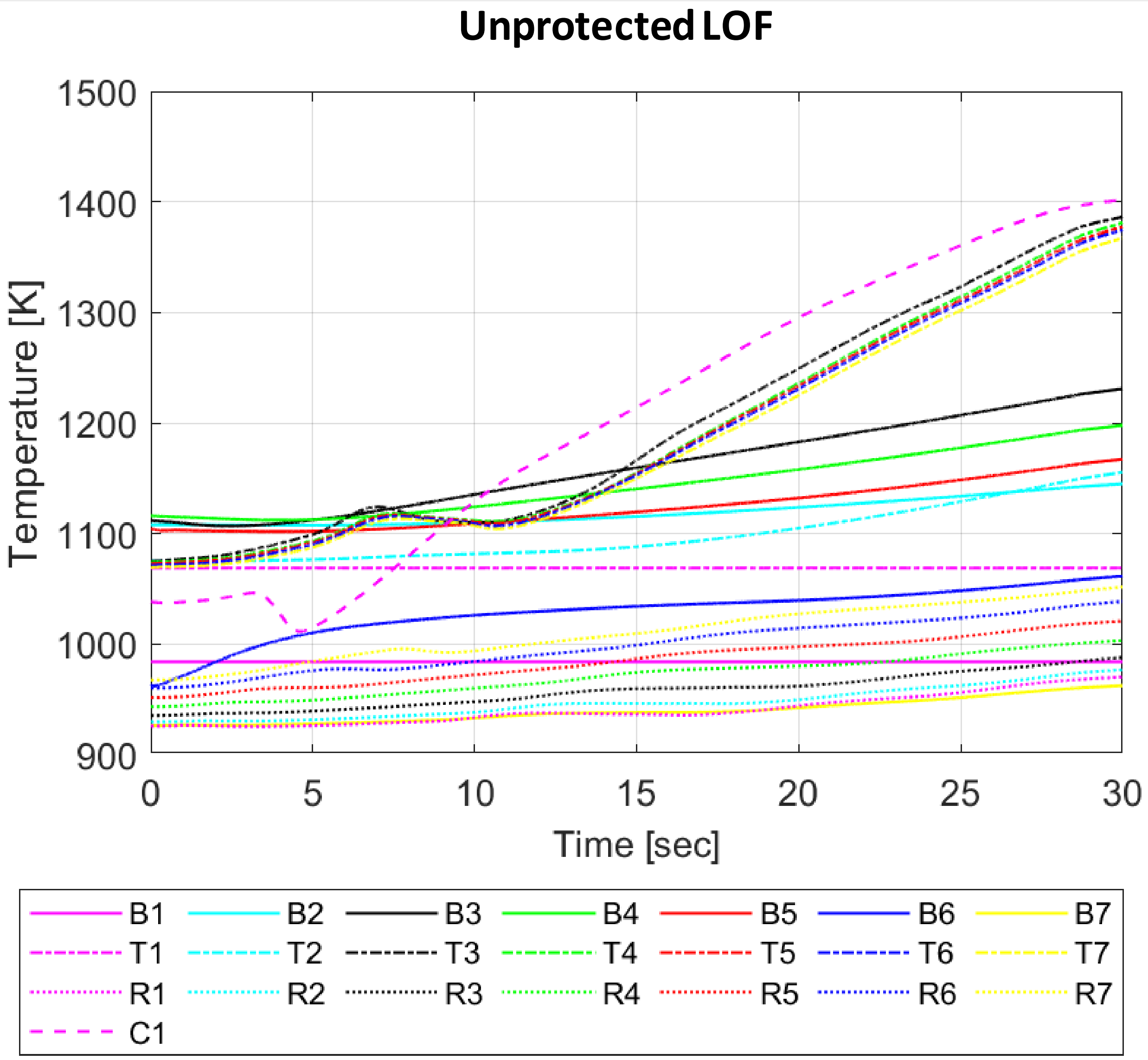

Other T2M activities:

- NDA with a commercial entity
- Publications on sensor placement and dopant segregation
- System fielded at INL and MITR (TRL 6)
- Plans: market the total package – fiber, interrogator, and control software

Single Crystal Distributed Sensing

Conclusions

- Distributed sensing is coming to numerous industries
- Single-crystal Optical fiber technology can extend into nuclear harsh-environments
- Raman DTS is a good distributed platform for SC-fiber
- Temperature mapping needed for LFMSR transient response
- Amazing new levels of visibility and automation are here!

Measure where it counts!

VISIT US AT: www.NETL.DOE.gov

@NETL_DOE

@NETL_DOE

@NationalEnergyTechnologyLaboratory

CONTACT:
Dr. Michael Buric, RIC, FMT
Michael.Buric@netl.doe.gov

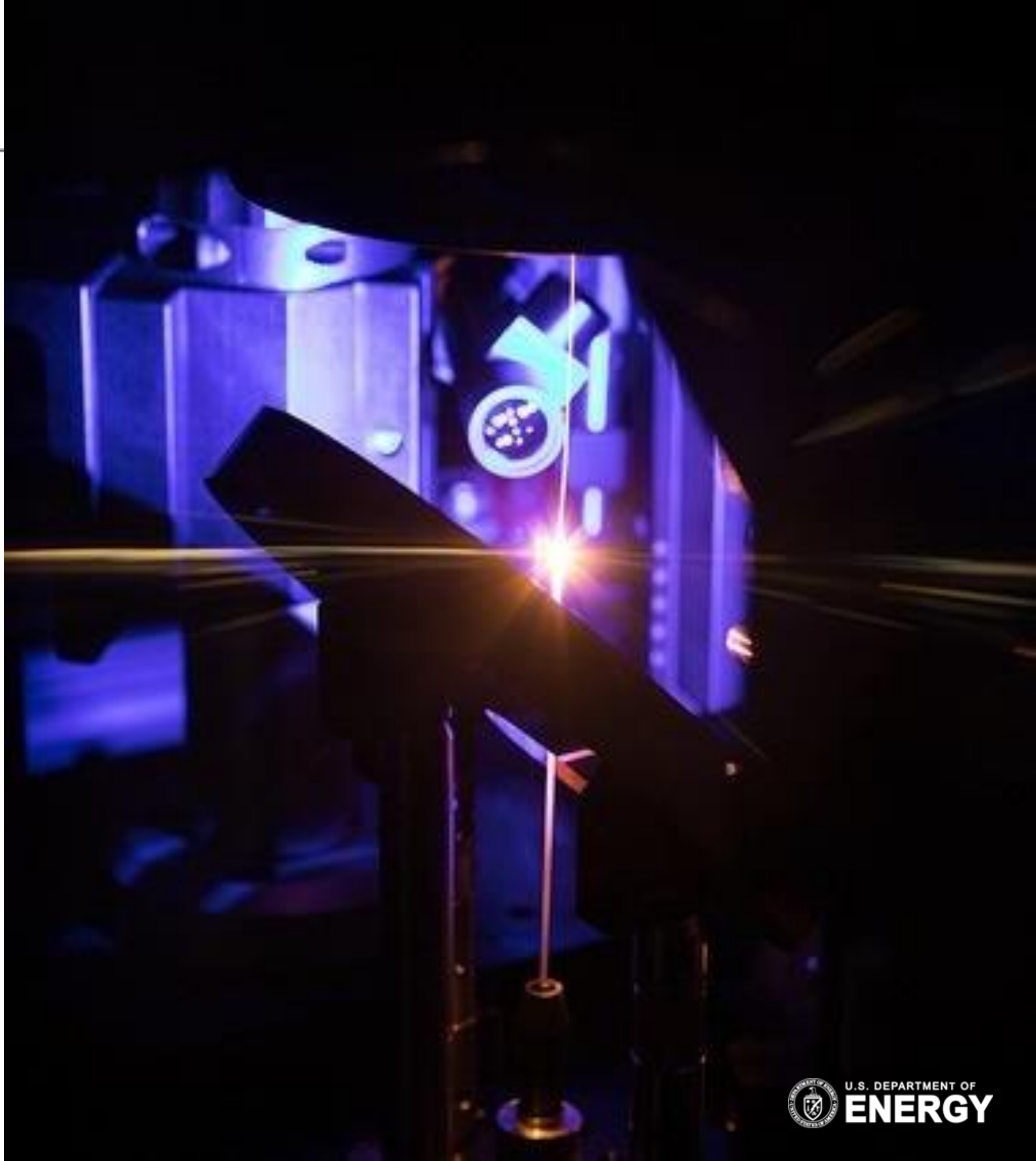

U.S. DEPARTMENT OF ENERGY

Advancement of Reduced Mode Sapphire Fiber (RMSF) Production Towards High Temperature Radiation Resilient Sensors

INL Sapphire Summit (via MS Teams)

S. Derek Rountree[1], O. John Ohanian[1], Andrew Boulanger[1], Dan Kominsky[1], Tom Blue[2], Joshua Jones[2], Kelly McCary[2], Tony Birri[2], Brandon Wilson[2,3], Kevin Chen[4], Chu Wang[4]

[1] Luna , [2]The Ohio State University, [3]Oak Ridge National Laboratory (currently), [4]The University of Pittsburgh

Introduction to Fiber Optic Sensing

- Laser light is coupled into a fiber.
- Light propagates and is reflected by defects.
- The reflected and transmitted signals can be used for sensing.
  - Reflected
    - Optical Frequency Domain Reflectometry (OFDR)
    - Optical Time Domain Reflectometry (OTDR)
    - Reflection Spectroscopy
  - Transmitted – Spectroscopy
- Sensing is achieved due to changes in optical path length and/or variations in reflectivity as a function of wavelength

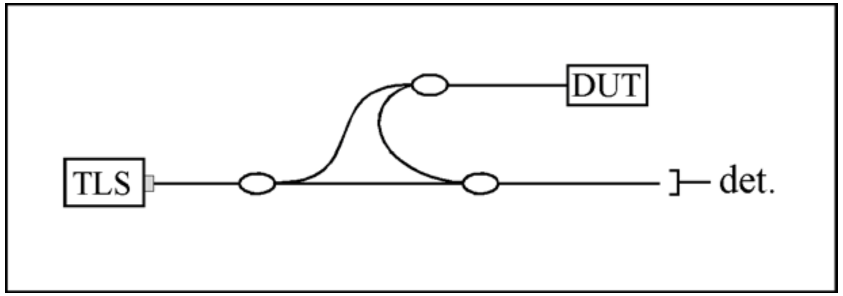

OFDR Sensing Optical Network

From: Luna Innovations Inc. OBR 4600 Users Guide

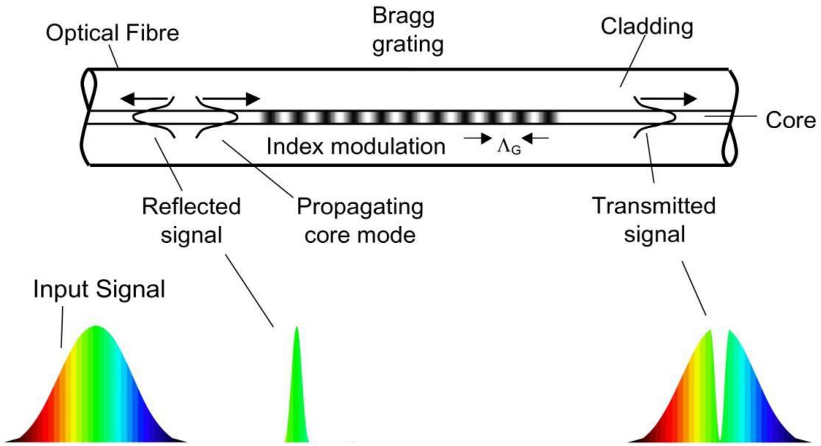

Bragg Grating Sensing Schematic

From: S. Mihailov, "Fiber Bragg Grating Sensors for Harsh Environments," doi:10.3390/s120201898

Single Mode Fiber Optics

- OFDR provides a measurement of the delay time to defects in a fiber or fiber network. Couple with the group velocity of light in a fiber, this provides distance to the defect.
- For high-precision low-noise measurements, all sensing light must travel along the same path.
  - One path for light to travel → "Single Mode"
  - Multiple paths for light to travel → "Multi-mode"
  - Mode support is wavelength dependent
- Traditionally, single mode fiber has been made out of doped silica glass.
  - Dopant regions created in a large pre-form
  - Draw tower pulls pre-form into a fiber
  - e.g. Corning SMF-28
    - Core Ø 8.2 μm, cladding Ø 125μm, coating Ø 242 μm

Image source: http://www.fiberopticshare.com/single-mode-fiber-vs-multimode-fiber-choose-2.html

Creation of an Internal Cladding in Sapphire Fiber

- The Ohio State University has developed a method for creating an intrinsic cladding in sapphire optical fiber
- By implanting ions into the periphery of a sapphire fiber, via the $^{6}Li(n,\alpha)^{3}H$ reaction, a refractive layer forms in the sapphire with a slightly lower index of refraction that acts as an internal cladding

$$^{6}_{3}Li + ^{1}_{0}n \rightarrow ^{4}_{2}He + ^{3}_{1}H + 4.8MeV$$

- The ions for implantation are created using Lithium-6 and the Ohio State Research Reactor reaction
- Using this method instead of an accelerator provides the benefit of creating large lengths of cladded sapphire fiber in a short amount of time.
- Cladding formed in this manner makes the fiber sufficiently few modes such that it can be used for OFDR distributed sensing.[1]
  - Continued development showed this was not the full story

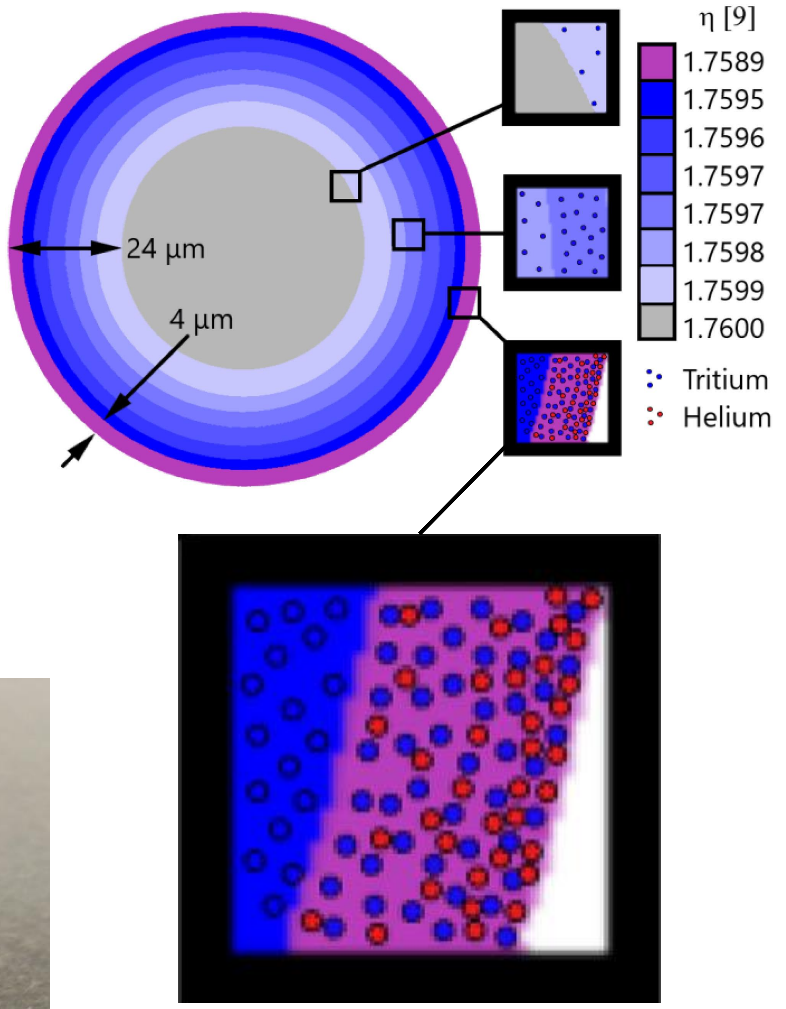

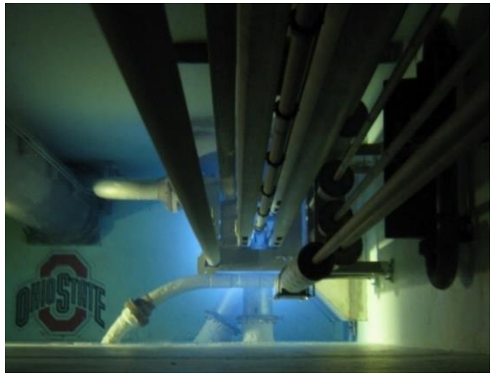

[1]B. Wilson, T. Blue, "Creation of an Internal Cladding in Sapphire Optical Fiber Using the 6Li(n,α)3H Reaction, DOI: 10.1109/JSEN.2017.2756448

RMSF Index Profile

- The graded cladding structure can be seen at approximately 40 µm radial distance from the fiber's core.
- The core-cladding index change is approximately 0.008.
- The structure near the fiber periphery is thought to be due to the non-cylindrical shape of the fiber.
- Additionally, the magnitude of the core-cladding index change may be affected by the non-cylindrical shape.

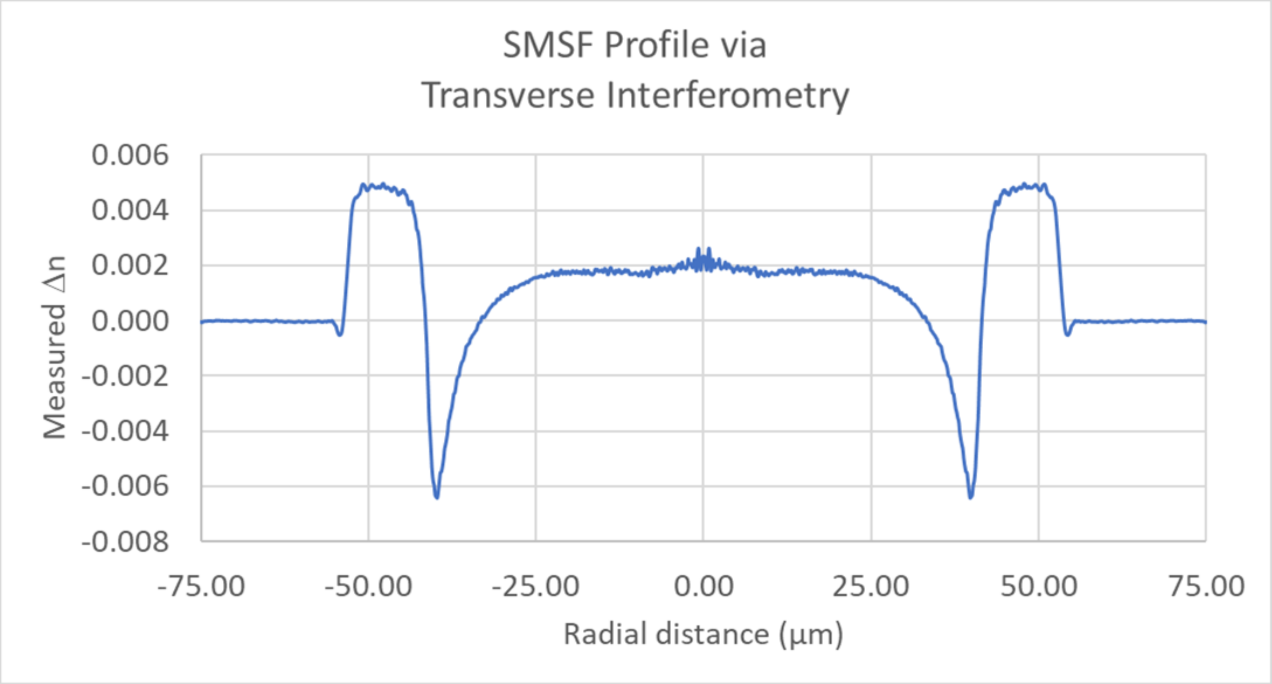

Repeatability Issues

- Based on preliminary successes at OSU, Luna and OSU partnered to further the technology and increase TRL and MRL.
  - DE-SC0018767 – “Extreme Temperature Distributed Sensing For Modular Energy Systems”
  - DE-SC0019834 – “Sapphire Single Mode Fiber Development Towards High Temperature Radiation Resilient Sensors”
  - Selected DE-FOA-0002555 Award # TBD – “Scaled Reduced Mode Sapphire Fiber Production Towards High Temperature Radiation Resilient Sensors”
  - Focus on manufacturing and cost reduction
- Reproduction of early results has not been straight forward.

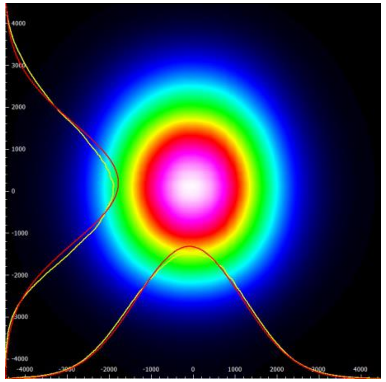

$\neq$

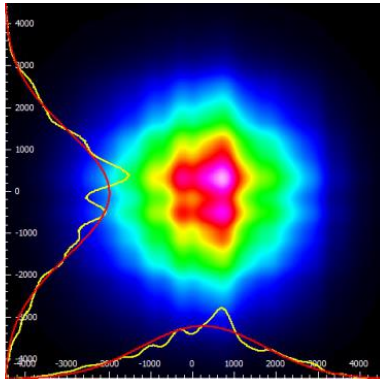

Breakthrough!

- Clad fibers are missing a mechanism to reject light from the cladding.[1]
- Splice condition affects how much light goes into the cladding vs core.[1]
  - Hexagonal surface creates uncertainty in alignment during splicing
  - Process is very sensitive to temperature and environmental conditions

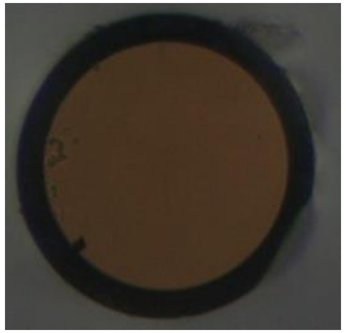

$\neq$

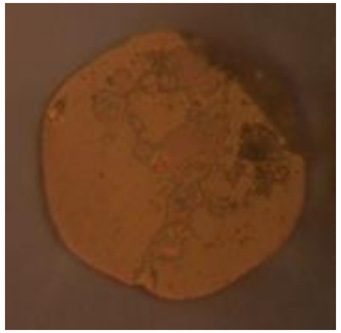

1) J. Jones, et al. “Light propagation considerations for internally clad sapphire optical fiber using the 6Li(n,α)3H reaction,” DOI: 10.1109/JLT.2021.3127863

Modality of the Clad Sapphire Core

- Adding index fluid shows core behavior.

		Wavelength	100 µm	75 µm
Sapphire Without Cladding	Air	675 nm	230,000	125,000
		1550 nm	43,000	23,762
	Index Fluid	675 nm	4,901	2,753
		1550 nm	929	392
Clad Sapphire Core	Modeled	675 nm	304	136
		1550 nm	58	26
	Measured	675 nm	1,593	678
		1550 nm	302	129

100 µm cladded RMSF

Cladding Modes Included | Cladding Modes Removed

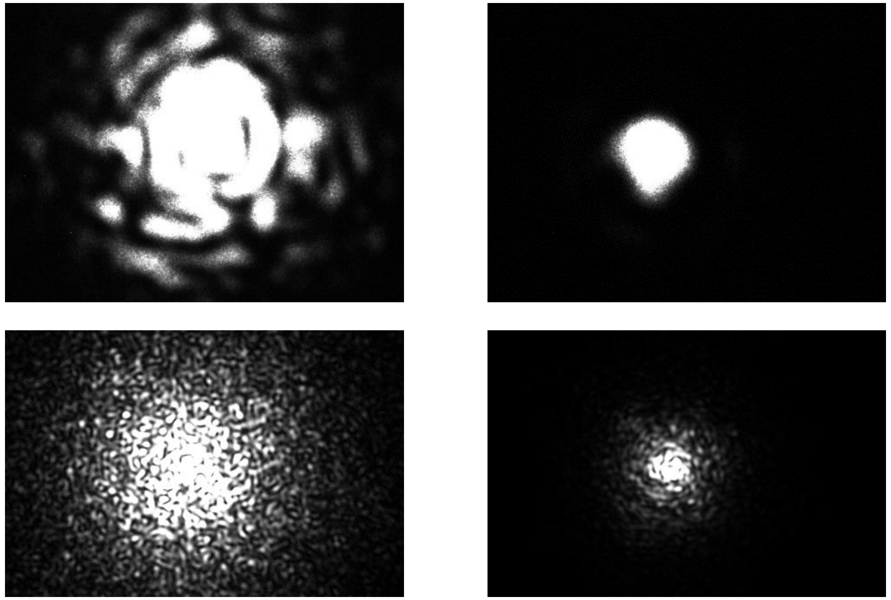

1) B. A. Wilson, S. Rana, H. Subbaraman, N. Kandadai and T. E. Blue, "Modeling of the Creation of an Internal Cladding in Sapphire Optical Fiber Using the 6 Li(n,α)3H Reaction," Journal of Lightwave Technology, vol. 36, no. 23, pp. 5381-5387, 1 December 2018.

LUNA | Performance Improvement

- When the fibers primarily sense with fundamental light, OFDR can be performed.
- Defects must be added to the highly crystalline sapphire structure (lacks random scatter points).
  - Fast neutron damage (not yet confirmed)
  - Non-neutron random damage (Enhanced Rayleigh, Oxidation, etc.)
  - Continuous Bragg gratings (LUNA proprietary specifications)
  - Fabry-Perot or other tuned response sensing structures
- Performance characterized beyond 1300°C

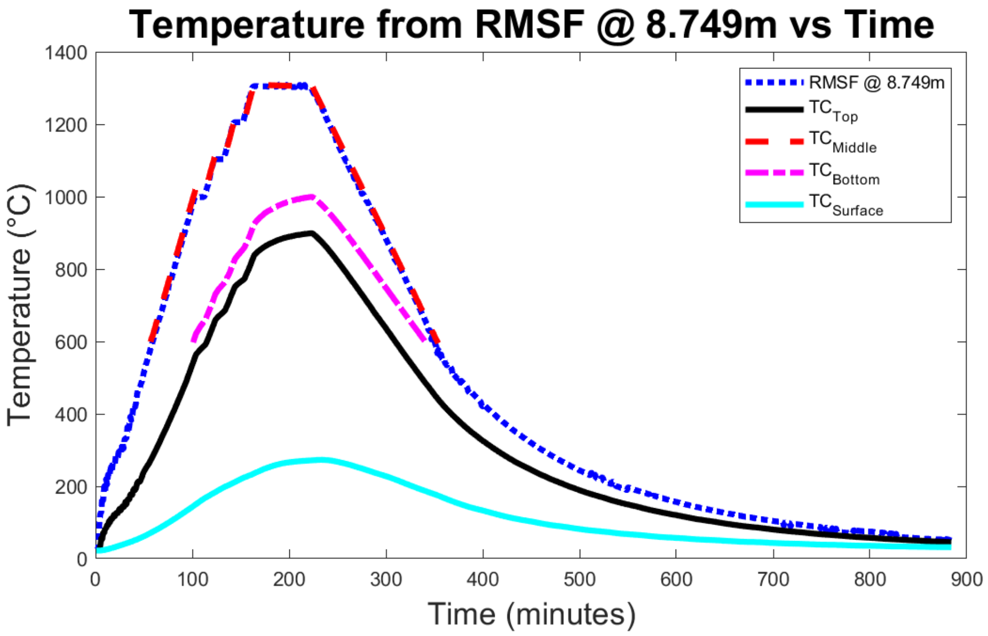

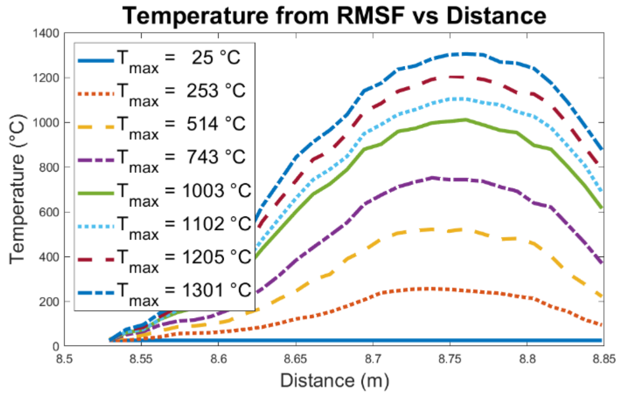

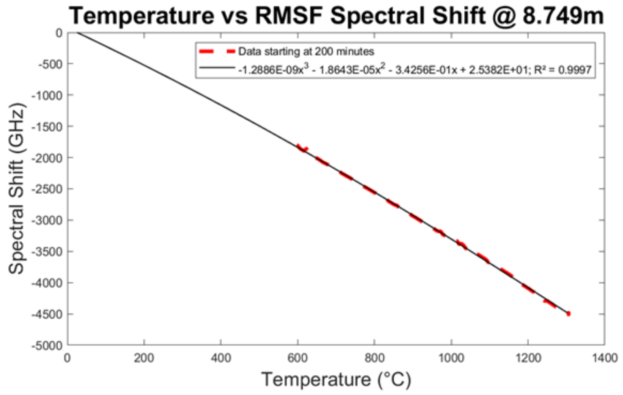

Bent Fiber Index Fluid Tests

No Index Fluid

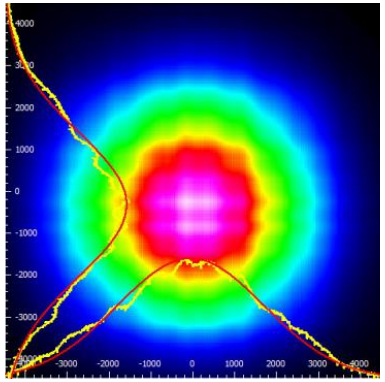

No Cladding Sapphire

Fluid Before Bend

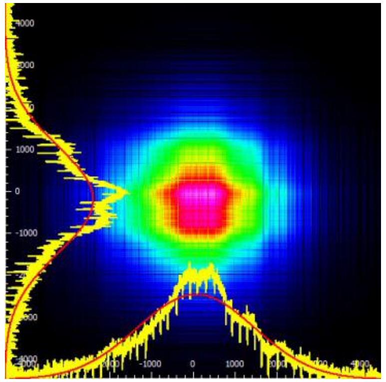

Fluid After Bend

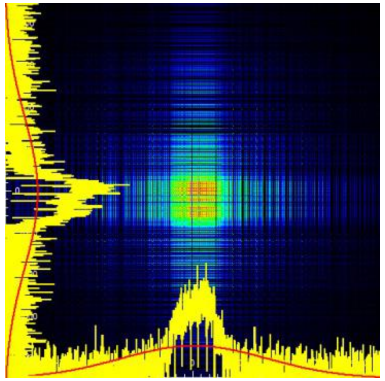

SMF-28

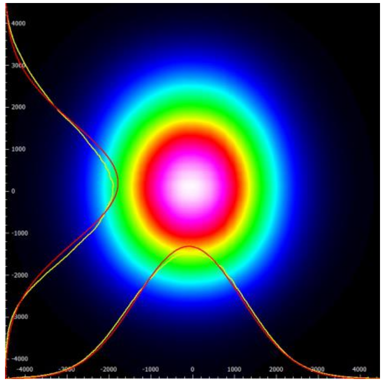

Pre-Irradiation

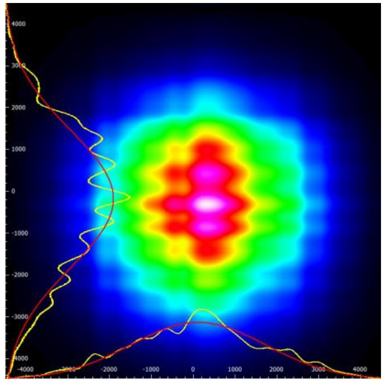

Post-Irradiation

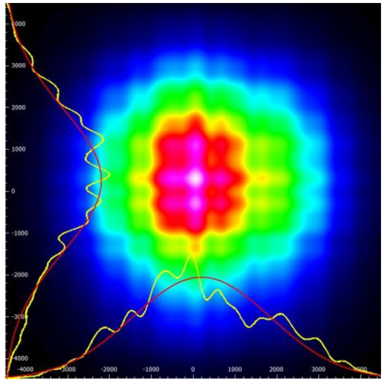

Post-Anneal →

← No Index Fluid

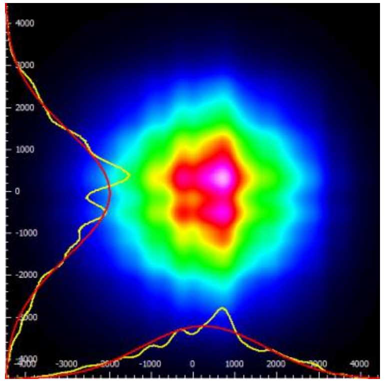

Fluid Before Bend

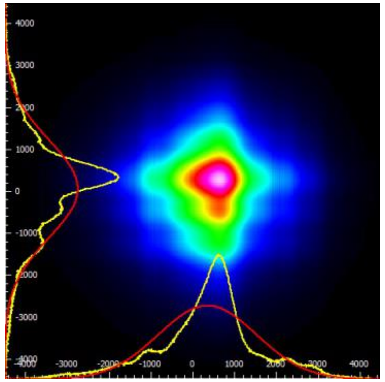

Fluid After Bend

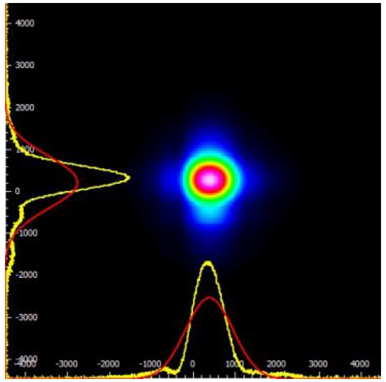

Permanent Mode Removal Methods

The Happy Accident

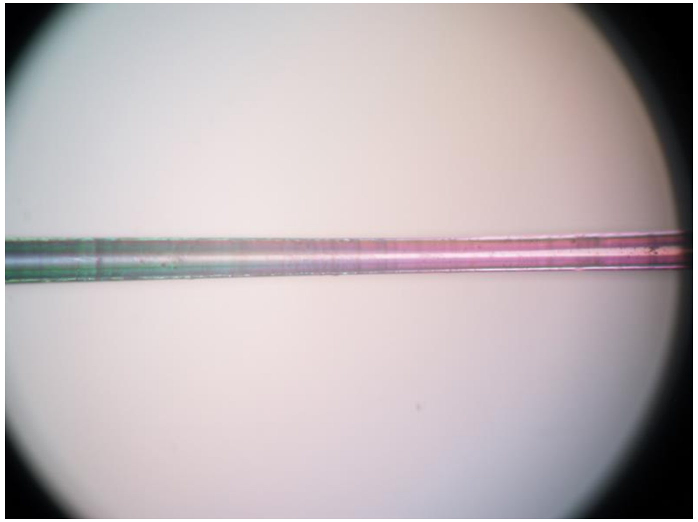

Aluminum oxyhydroxide surface defect

Intentional formation of Aluminum oxyhydroxide surface defect at <600°C

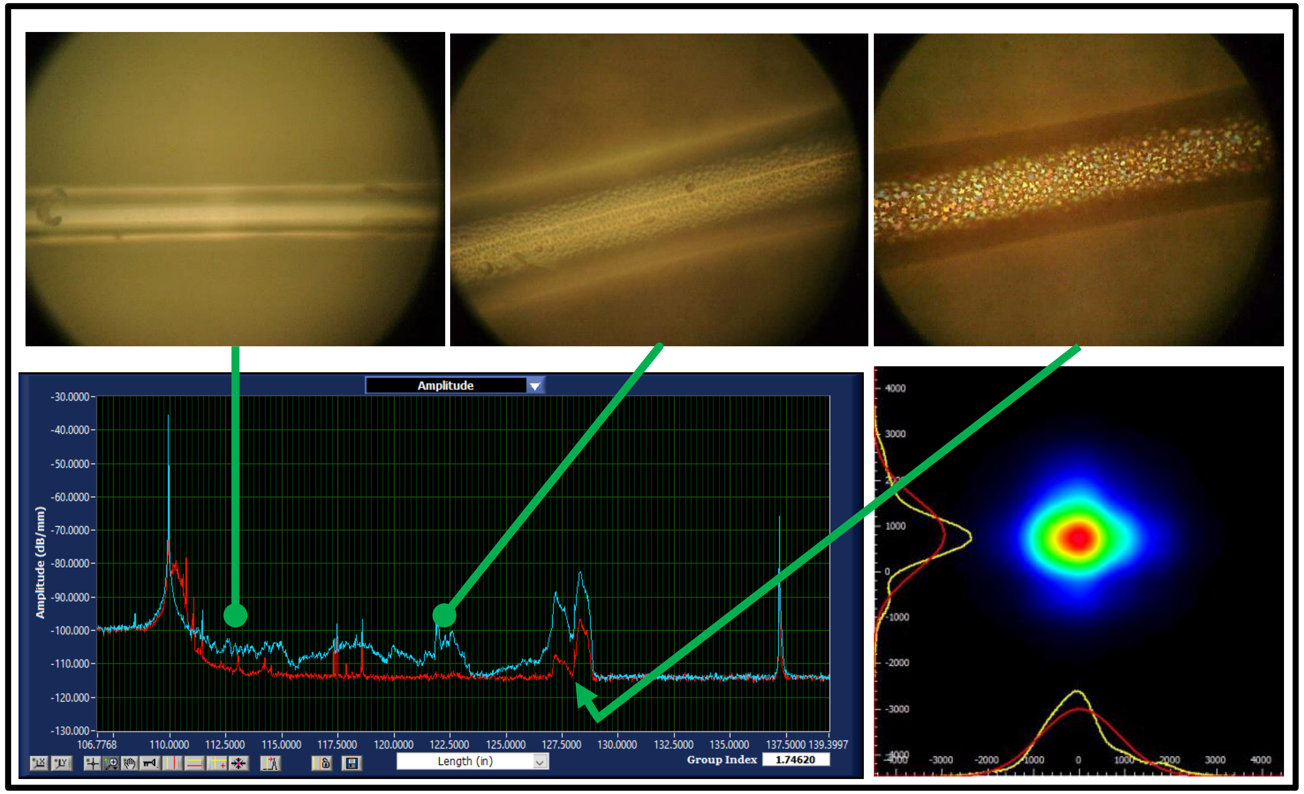

[1] https://patents.google.com/patent/WO2021211195A1/en?oq=WO2021211195A1

Thanks to the team members involved with this work

- Luna Innovations
  - S. Derek Rountree, O. John Ohanian, Andrew Boulanger, Dan Kominsky
- The Ohio State University
  - Tom Blue, **Joshua Jones, Kelly McCary, Tony Birri, Brandon Wilson**
- University of Pittsburgh
  - Kevin Chen, **Chu Wang**

LUNA | Conclusions and Next steps

- There are significant advancements occurring in the field of optical fiber sensing, making the technology more useful as an alternative to more traditional sensing methods (thermocouples and strain gauges).
- Items being addressed in 2022 and 2023 via DE-FOA-0002555 Award # TBD – “Scaled Reduced Mode Sapphire Fiber Production Towards High Temperature Radiation Resilient Sensors”
  - Removal of cladding modes
  - Appropriate splicing to Si-SMF
  - Connectorizing RMSF
  - Reduction of production cost
  - Production of significant quantities of RMSF (order 10 meters)

This material is based upon work supported by the Department of Energy, Office of Science, Office of Energy Efficiency and Renewable Energy under Award Numbers DE-SC0018767, DE-SC0019834.

Questions / Action Items

Sapphire Summit
Idaho National Lab
May 31, 2022
9:45 am – 10:00 am

SINGLE CRYSTAL SAPPHIRE FIBER SENSING
Technology & Outlook

Gary Pickrell, Anbo Wang, Daniel Homa
Virginia Tech
Center for Photonics Technology
Blacksburg, VA 24061
pickrell@vt.edu, awang@vt.edu, dan24@vt.edu

Overview

- Center for Photonics Technology
- Optical Fiber Waveguide Sensing
- Acoustic Fiber Based Sensing
- Future Outlook

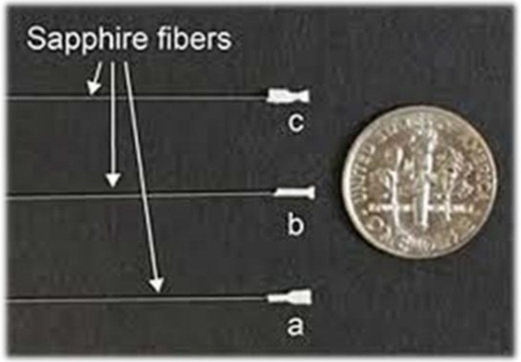

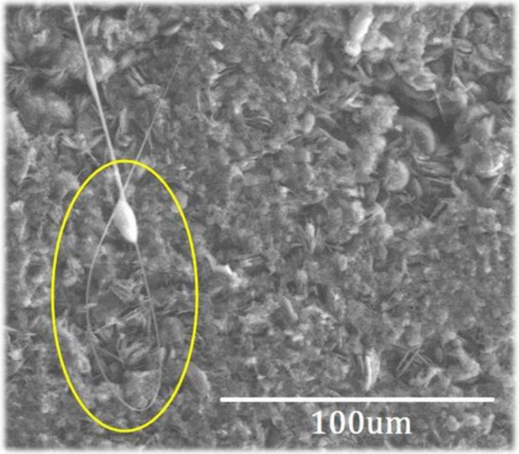

SENTEK INSTRUMENT CPT CENTER FOR PHOTONICS TECHNOLOGY VirginiaTech Invent the Future

Center for Photonics Technology

- Focused on innovation in fiber optics, fiber optic sensors, and harsh environment sensors
  - Dedicated to development and commercialization of next generation sensing technologies
  - 40 faculty, staff and students
- Wide array of facilities and specialized equipment
  - Commercial scale fiber optic draw tower
  - Laser heated pedestal growth system (LHPG)
  - Fully automated glass working lathes
  - Femto-second laser micro-machining system
- “Systems approach” to the development of fully-integrated complete sensing systems
- Extensive track record for the deployment and field testing of next generation harsh environment sensing systems

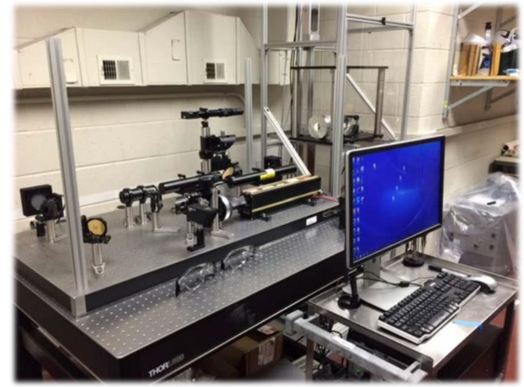

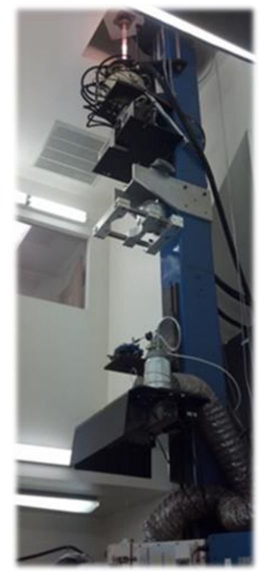

SENTEK INSTRUMENT

CPT
CENTER FOR PHOTONICS TECHNOLOGY

VirginiaTech
Invent the Future

SELECTED SAPPHIRE RELATED OPTICAL FIBER SENSOR TECHNOLOGY

Single Point Sensors

Pressure, Temperature, Strain

- Temperature sensors
  - Fabry-Perot cavity directly fabricated on the sapphire fiber tip
  - Demonstrated performance up to 1600ºC
- Pressure sensors
  - Monolithic sapphire Fabry-Pérot (FP) cavity
  - Adhesive free; reactive ion etching used in conjunction with direct wafer bonding
  - Demonstrated performance up to 1.34 MPa
- Strain Sensors
  - Extrinsic Fabry-Pérot interferometric strain sensors based on the white light interferometric spectrum demodulation technique.
  - Demonstrated resolution of 0.2 microstrain

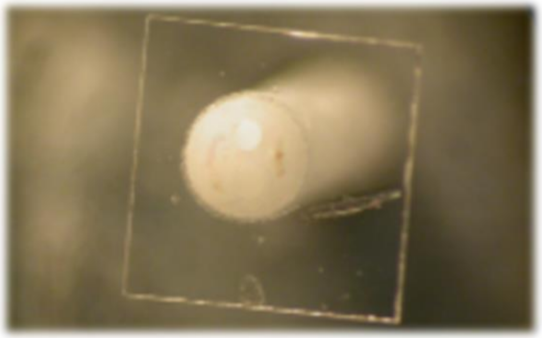

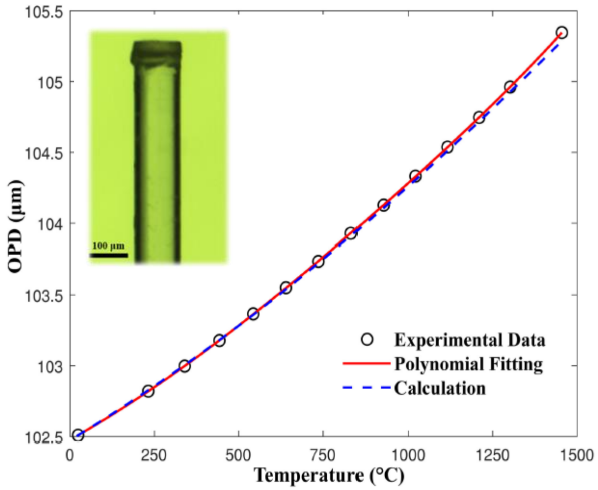

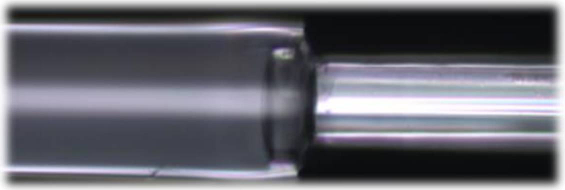

Yang, Shuo, Ziang Feng, Xiaoting Jia, Gary Pickrell, Wing Ng, Anbo Wang, and Yizheng Zhu. "All-sapphire miniature optical fiber tip sensor for high temperature measurement." Journal of Lightwave Technology 38, no. 7 (2019): 1988-1997.

Distributed Temperature Sensing

Raman Backscatter

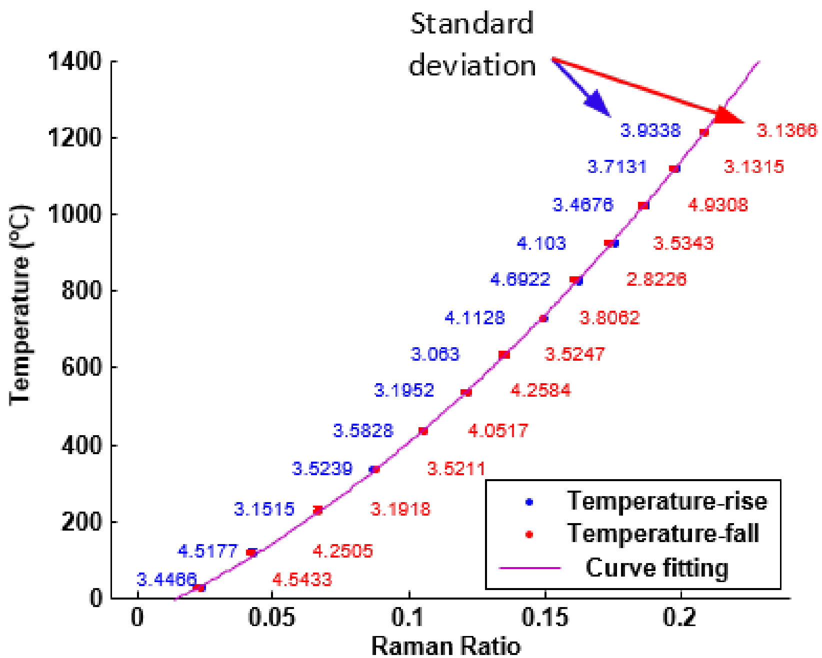

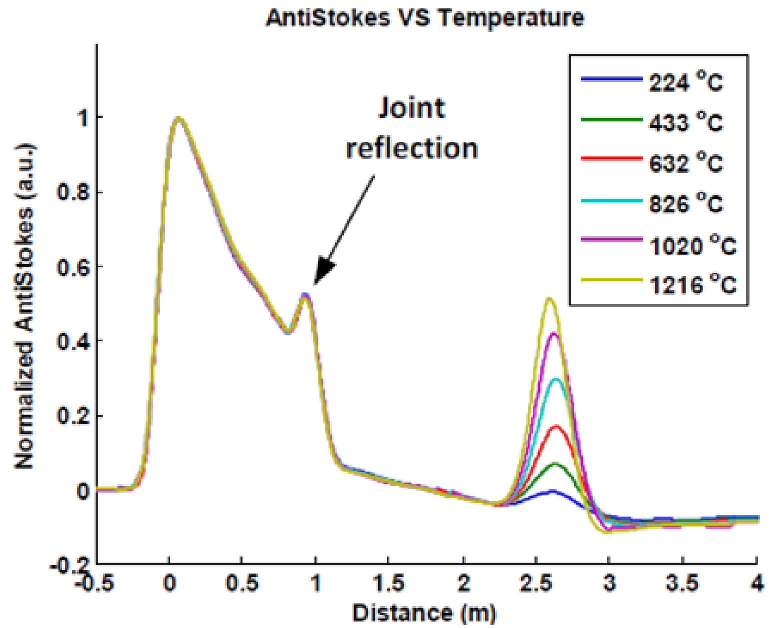

Liu, Bo, Zhihao Yu, Cary Hill, Yujie Cheng, Daniel Homa, Gary Pickrell, and Anbo Wang. Sapphire-fiber-based distributed high-temperature sensing system, Optics letters 41, no. 18 (2016): 4405-4408.

Reduced Mode Sapphire Fiber

FABRICATION AND MODAL CHARACTERIZATION

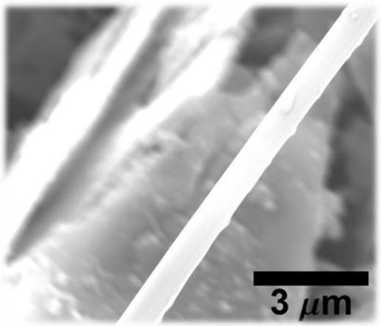

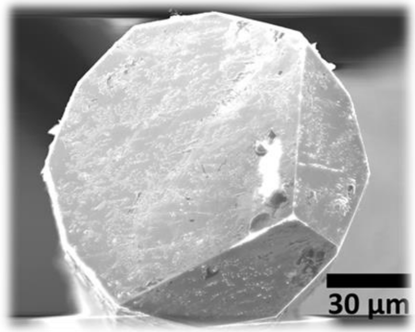

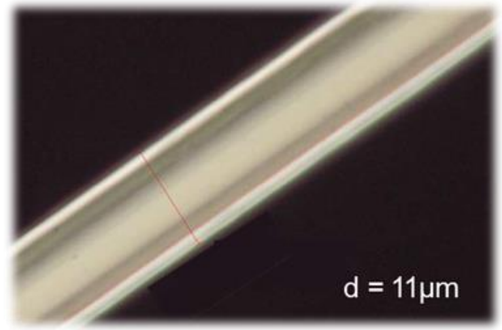

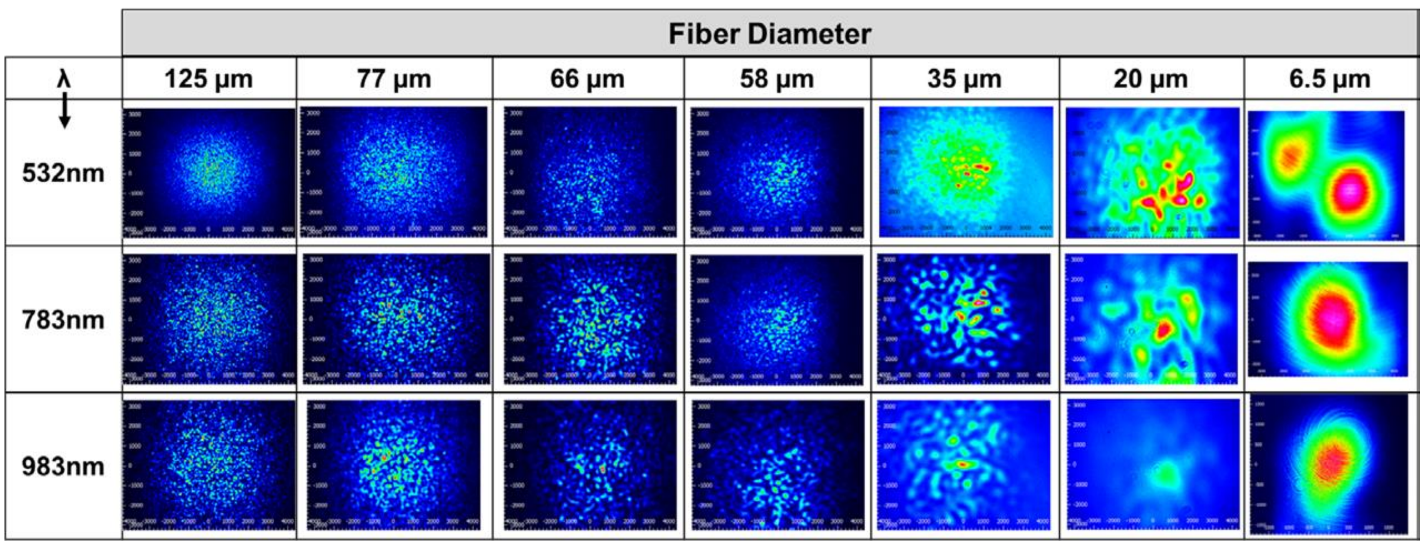

Fiber Bragg Gratings

Low Modal Volume Single Crystal Sapphire Fiber: Fabrication

Step 1: Point-by-Point FBG Fabrication

Step 2: Hot-Wet Acid Etching

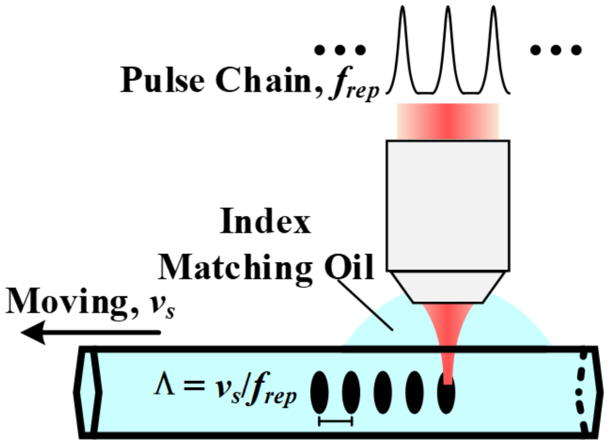

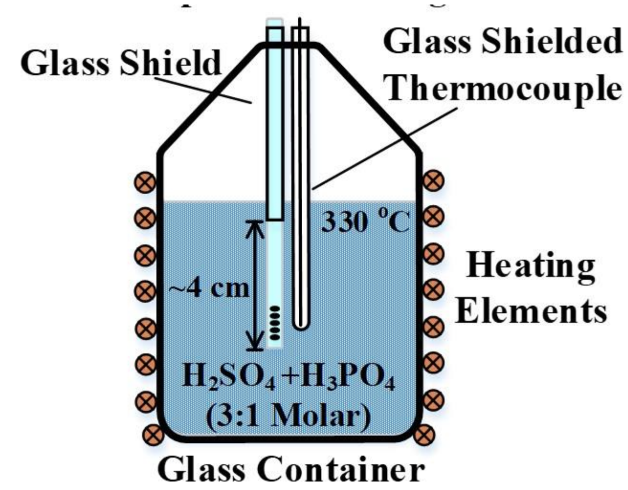

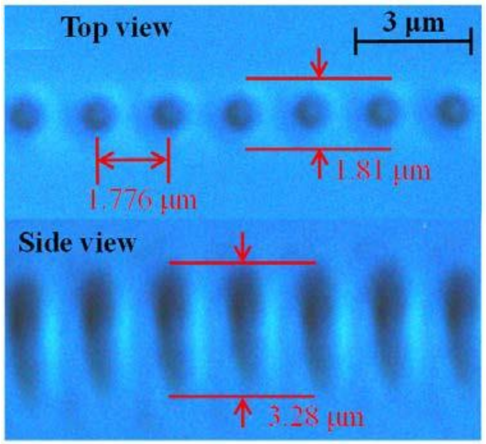

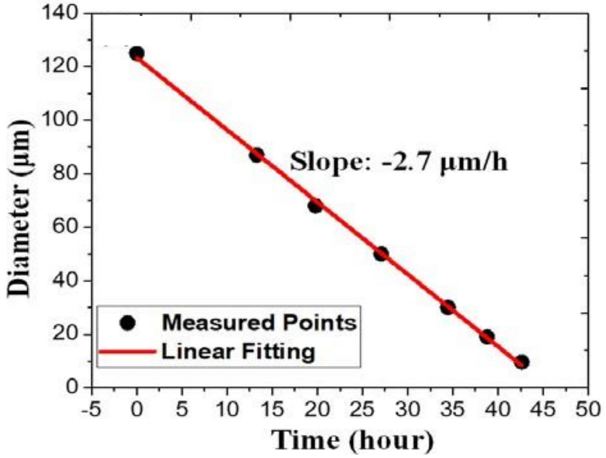

Fiber Bragg Gratings

Low Modal Volume Single Crystal Sapphire Fiber: Performance

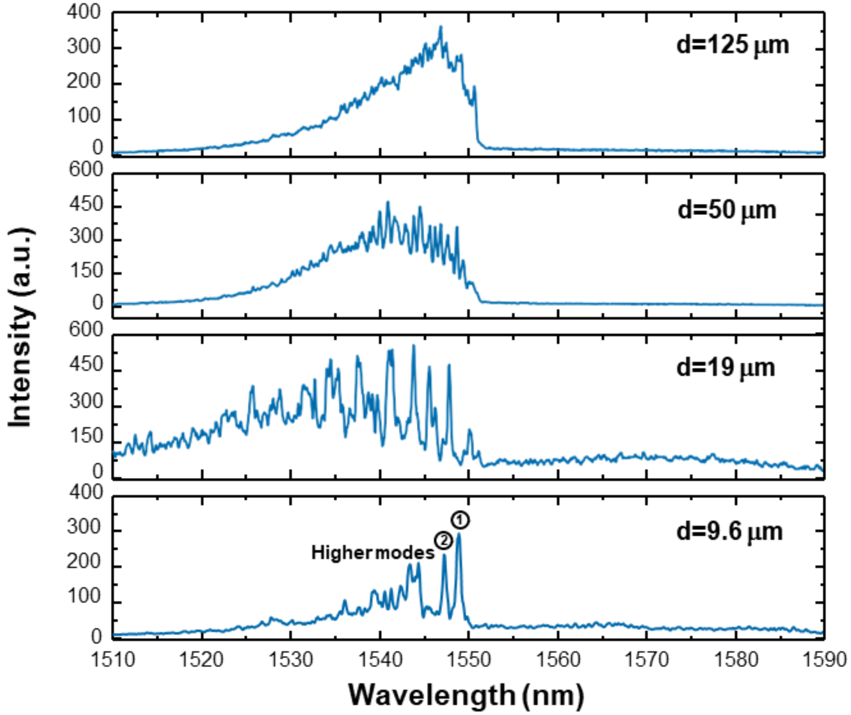

Reduced modal volume improves FBG peak fidelity

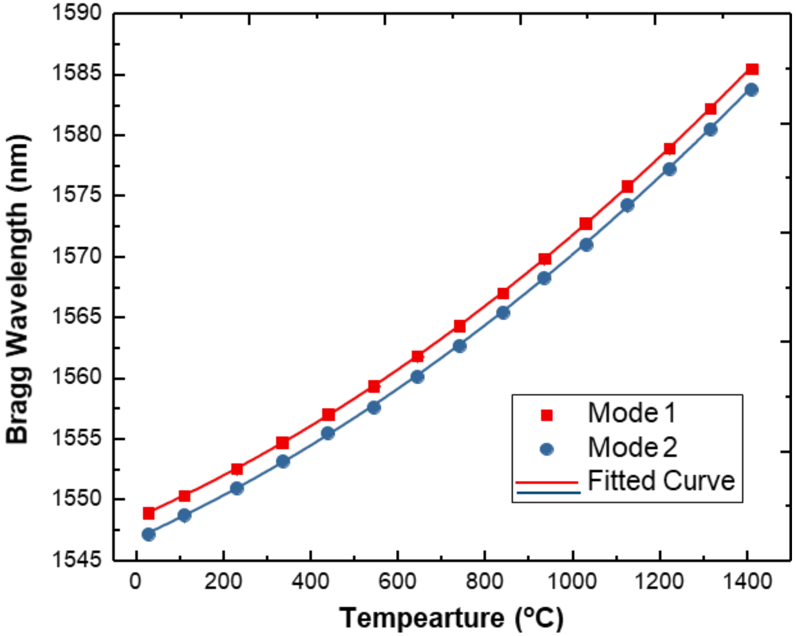

Demonstrated to temperature of 1400°C ; ~26.5 pm/°C

Yang, Shuo, Daniel Homa, Gary Pickrell, and Anbo Wang. Fiber Bragg grating fabricated in micro-single-crystal sapphire fiber, Optics letters 43, no. 1 (2018): 62-65.

Technology Maturation

FIELD TRIAL DEPLOYMENTS AND EASE OF USE

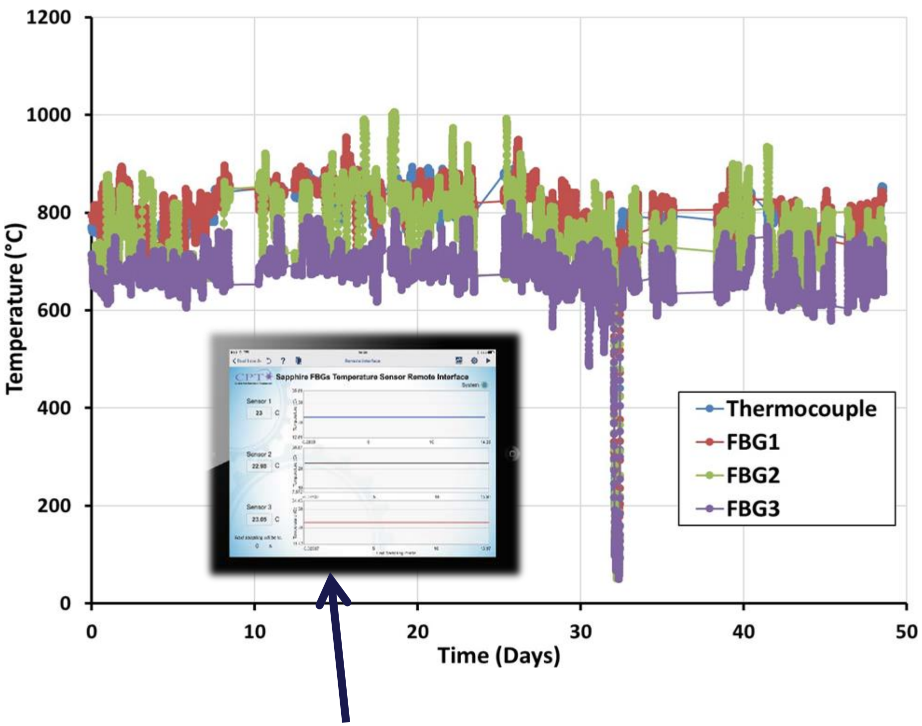

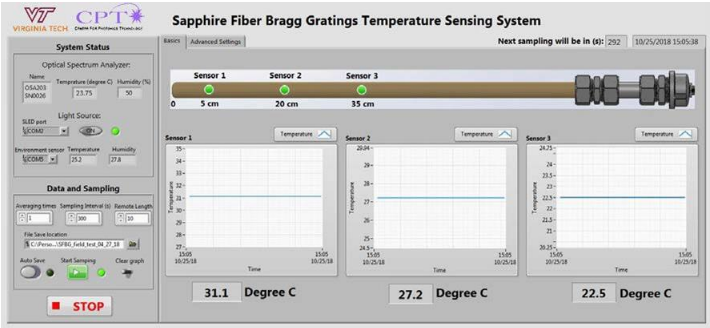

Real time monitoring on mobile device (iPad)

Yang, Shuo, Daniel Homa, Gary Pickrell, and Anbo Wang. Fiber Bragg grating fabricated in micro-single-crystal sapphire fiber, Optics letters 43, no. 1 (2018): 62-65.

ACOUSTIC FIBER SENSING

Acoustic Fiber Sensing

TECHNOLOGY OVERVIEW

- Sensing via fiber Bragg gratings (AFBGs) on a single mode acoustic fiber waveguide (AFW)
- Equally spaced “nodes” are inscribed in the AFW
- Time-division spectral interrogation scheme can be employed for fully-distributed sensing on a single fiber.
- AFBG central frequency position shifts proportionally to external perturbations (temperature, strain, pressure and corrosion)
- **Can be implemented on a wide array of materials**

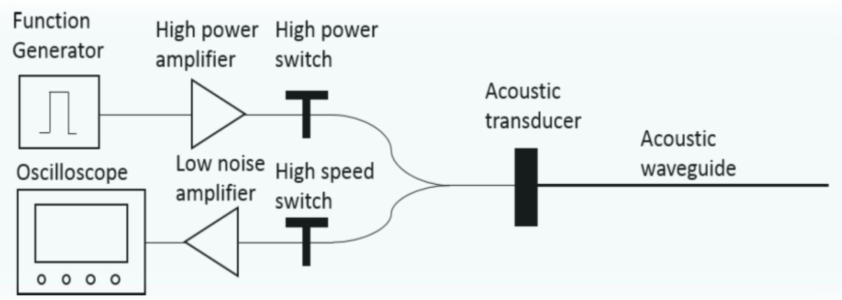

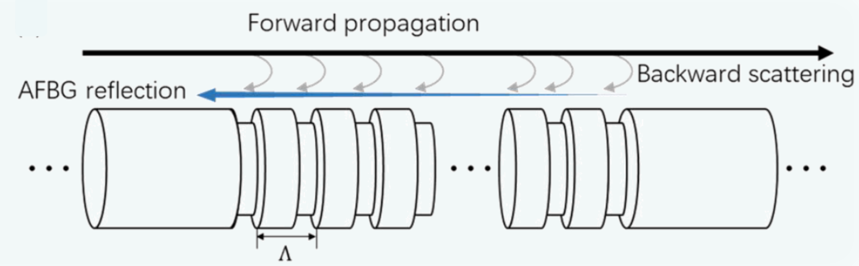

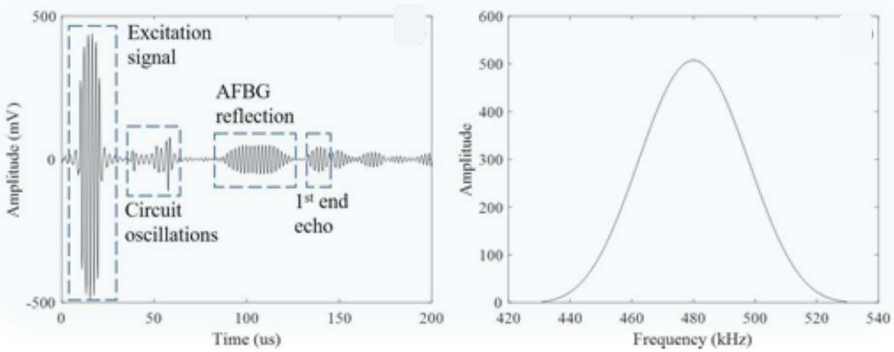

Acoustic Fiber Bragg Gratings

Femto-Second Laser Inscription

- Inscribed via femtosecond laser micromachining system
  - Scan laser focus around the waveguide to create “notches”
  - Translate linear stage at a distance that corresponds to AFBG period

- High frequency (~3.4 MHz) SCS AFBG sensor
  - Inscribed via a femtosecond laser
  - 250 µm SCS fiber
  - 20 nodes: period of 1.57 mm
  - Depth/width: 12 µm/60 µm

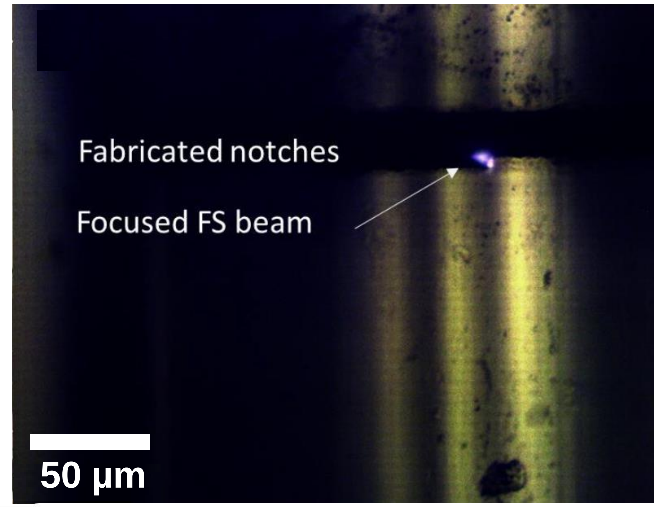

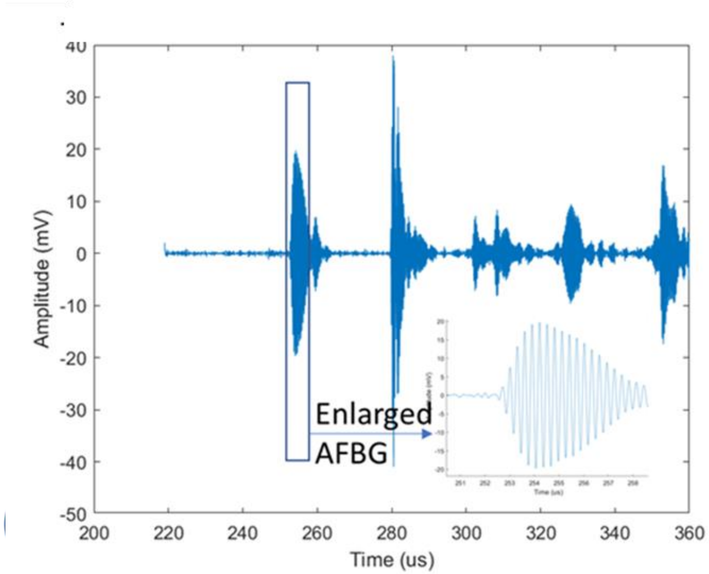

AFBG Temperature Sensing

TEMPERATURE RESPONSE AND LONG TERM STABILITY

- Full system integration and calibration up 1100ºC
- Long Term Stability Testing: >240 hrs @ 1100ºC

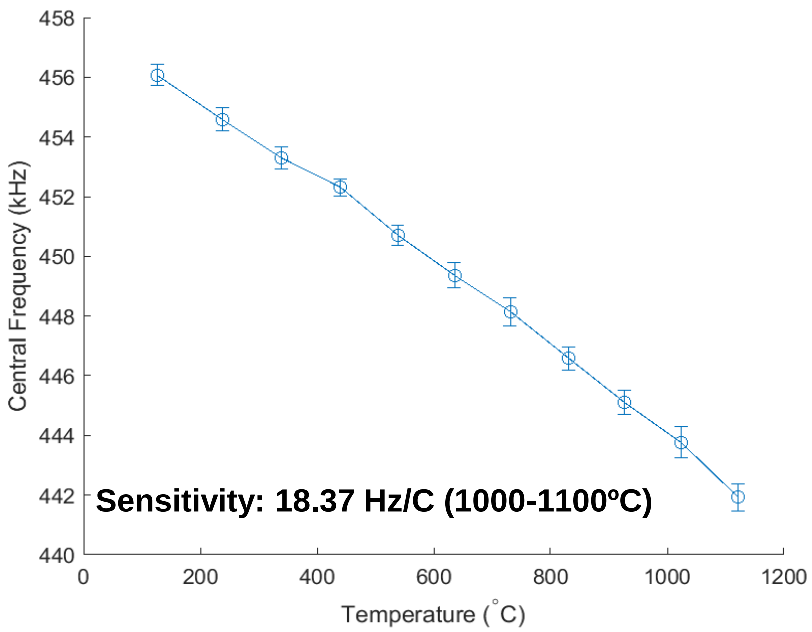

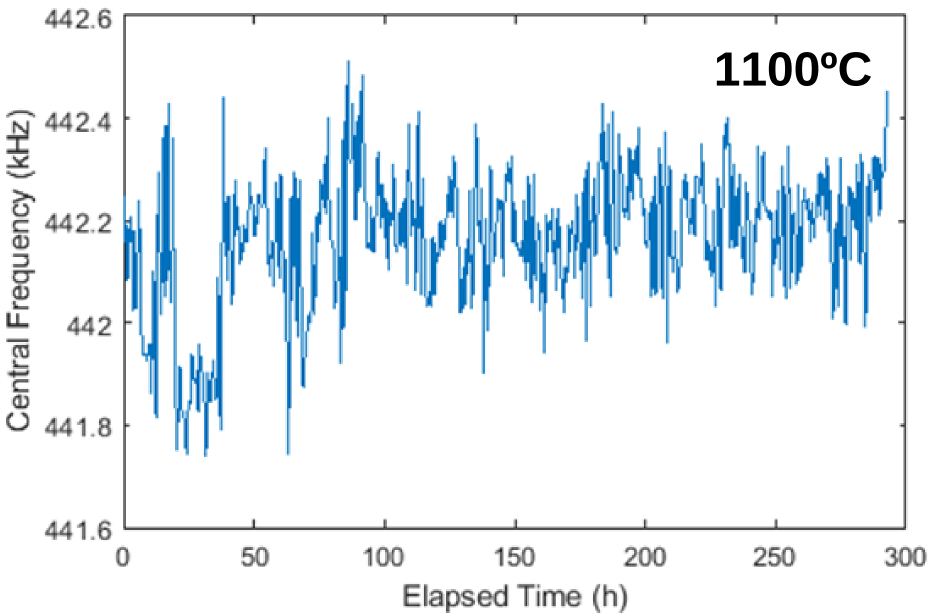

Technology Maturation

SUCCESSFUL DEPLOYMENTS AND EASE OF USE

- User friendly interface
  - Labview environment
  - Sensor diagnostics
  - Monitoring mode
- “Deployable” complete system
  - Interrogator components available from National Instruments
- Next generation custom components
  - Utilize higher quality commercially available electrical components
  - Enhance coupling between transducer and acoustic waveguide
  - Application-specific packaging

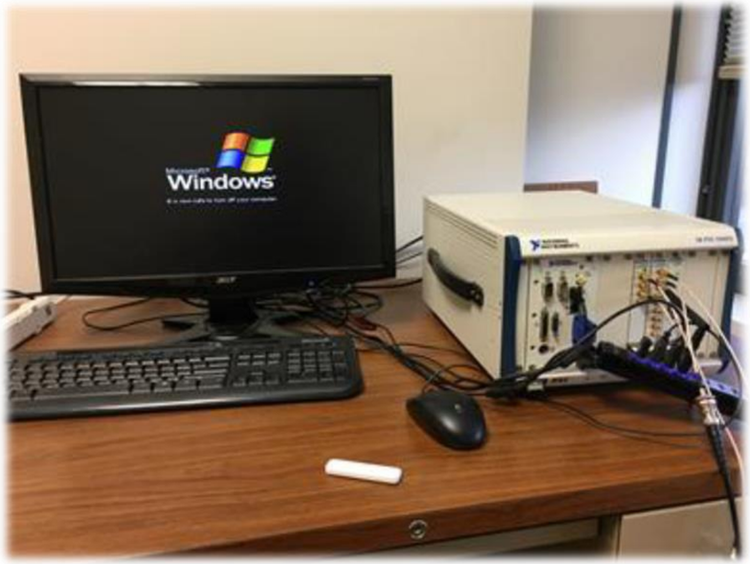

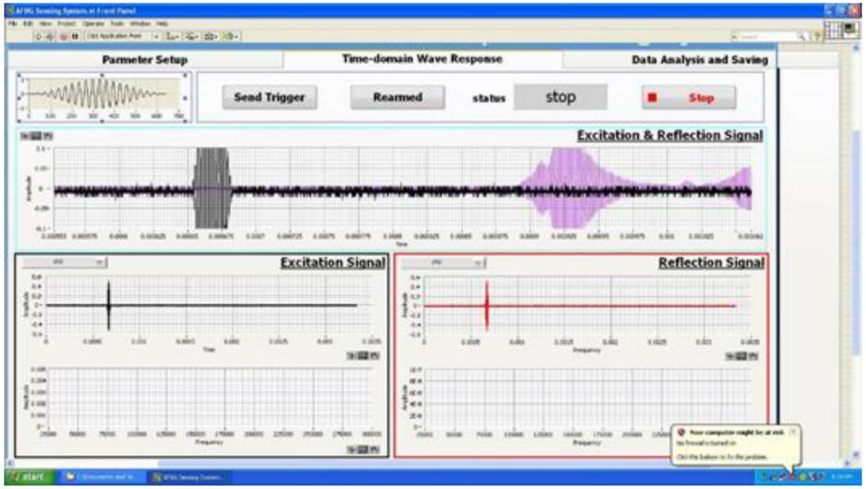

Performance in Nuclear Environment

GAMMA RADIATION EXPOSURE: AFBG & OFBG SENSORS

- Irradiation performed at Oak Ridge National Laboratory
  - High-intensity gamma ray field (~3-4x10^4 rad/hr) using a J.L. Shepherd irradiator which contains 60Co (1173 keV and 1332 keV gamma rays) cylindrical sealed sources.
- “Single crystal sapphire OFBG and AFBG sensors
- Continuous sensor interrogation for over 40 days
  - Non-interrupted, “hands-off” operation

SENTEK INSTRUMENT CPT CENTER FOR PHOTONICS TECHNOLOGY VirginiaTech Invent the Future

Performance in Nuclear Environment

Gamma Radiation Exposure: OFBG & AFBG Sensors

OFBG

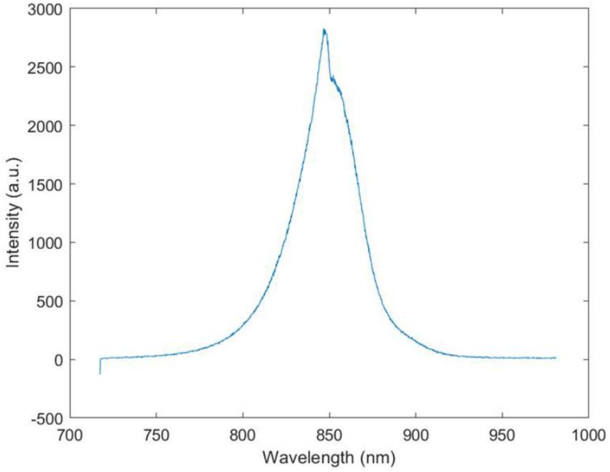

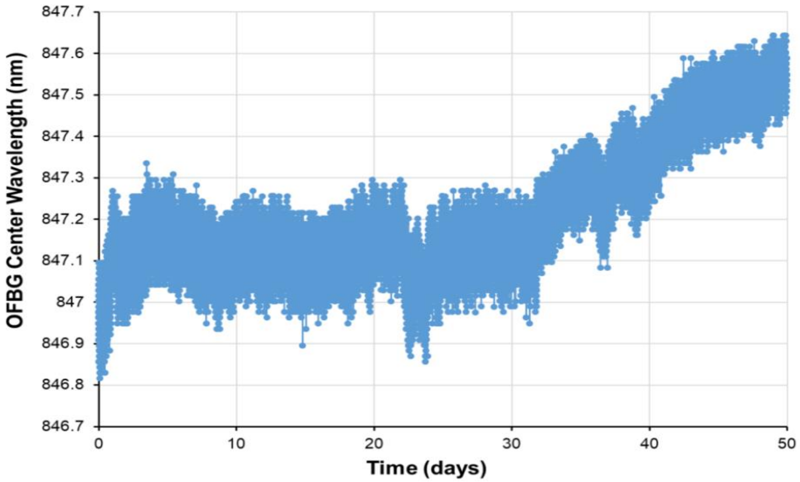

AFBG

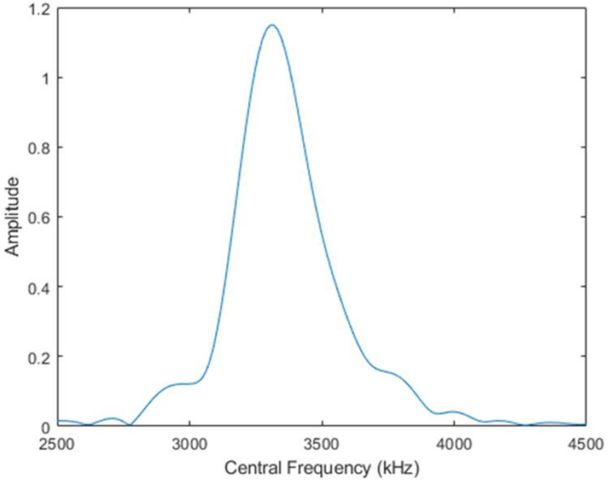

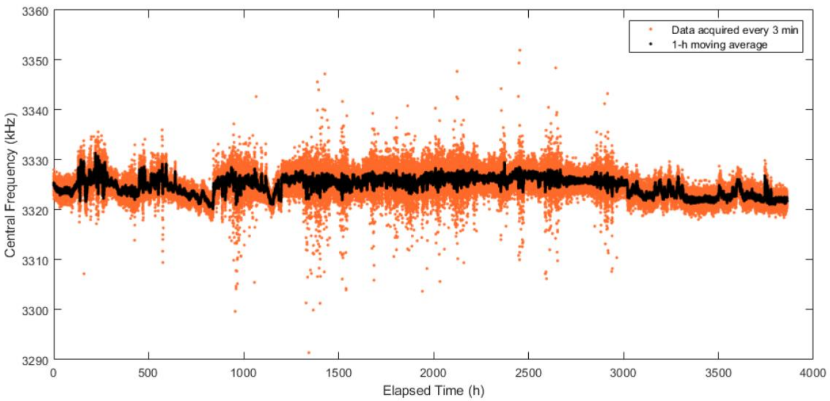

CENTER FOR PHOTONICS TECHNOLOGY

Invent the Future

Overview and Outlook

- Optical Fiber Sensors
  - Wide array of single point sensors (pressure, temperature, strain)
  - Distributed temperature sensing via Raman backscatter
  - Multiplexed measurements via FBGs
- Acoustic Fiber Sensors
  - Fabricated AFBGs in single crystal sapphire fiber
  - Developed fully integrated temperature sensing system
  - Demonstrated performance up to 1200ºC
- Demonstrated performance of AFBG and OFBG based sensing systems in high gamma radiation environments
- Technology Development/Outlook
  - Optimize and refine sensor configurations and interrogation systems
  - Collaboration with experts to fully evaluate sensor performance in selected nuclear radiation environments
  - Collaboration with experts to identify best fit applications
    - Develop fully integrated monitoring system
    - Deployment and field trial testing

Acknowledgements

Department of Energy

National Energy Technology Laboratory

Project Manager: Jessica Mullen

Sydni Credle

Susan Maley*

**Now with Electric Power Research Institute*

Department of Energy

Idaho National Laboratory:

Joshua Daw

Craig Primer

Patrick Calderoni

Prysmian Group

Industrial Support: Brian Risch

Oak Ridge National Laboratory

National Lab Collaborators:

Alexander Braatz

Denise Lee

THANK YOU FOR YOUR TIME

LHPG for Growth of Functional Ceramic Oxides and Machine Vision Methods for Process Monitoring and Control

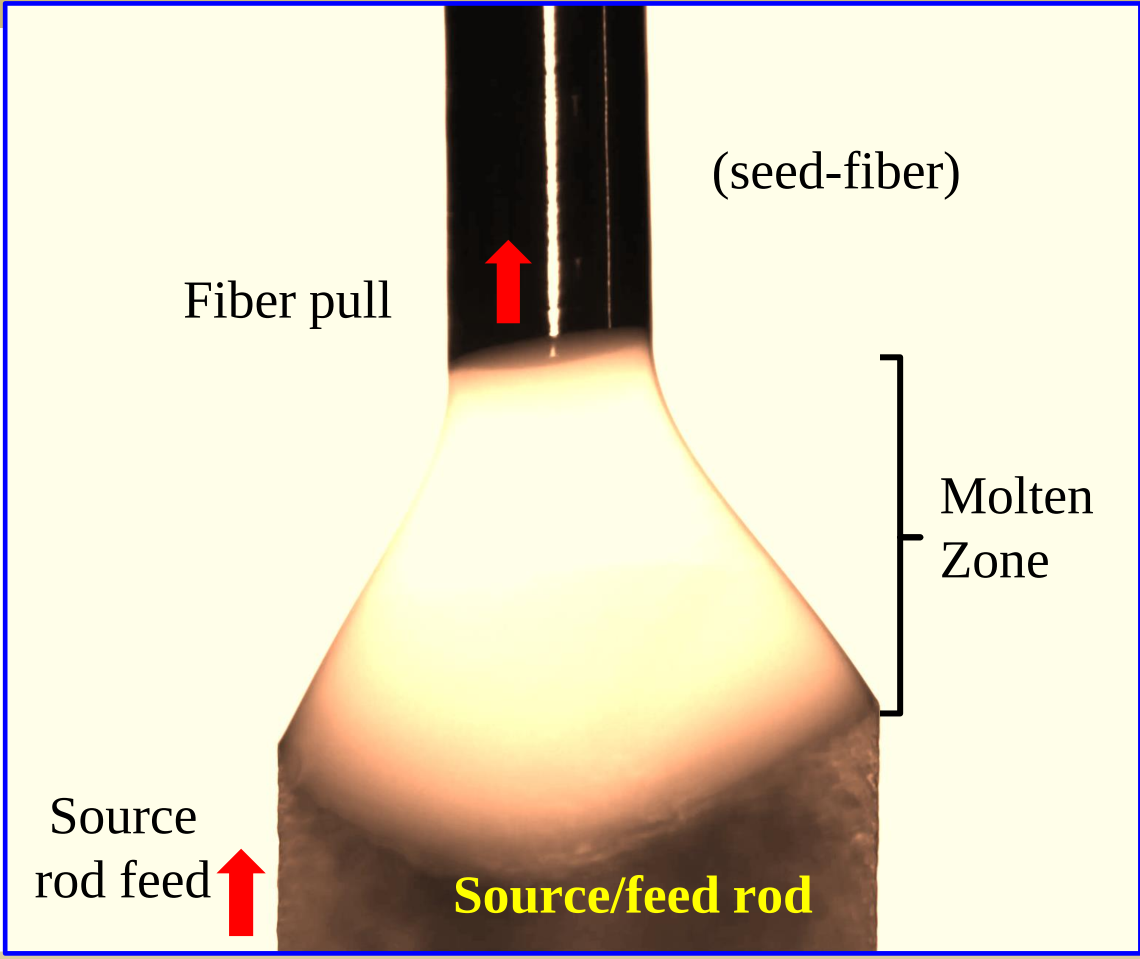

Presenter: Prof. Paul Ohodnicki

Authors: Dolendra Karki[a], Edward Hoffman[a], Shengye Dong[a], Victoria Schmotzer[a], Suraj Mullurkara, B. Liu[a]

Dept. of Mechanical Engineering and Materials Science,

[a]University of Pittsburgh, 3700 O'Hara St, Pittsburgh, PA, USA

Applications of fibers of various refractory oxides

B. Liu, P. R. Ohodnicki,
"Fabrication and Application of Single Crystal Fiber: Review and Prospective"; July 2021; Advanced Materials Technologies
https://doi.org/10.1002/admt.202100125

- **Sapphire (Al_2O_3)**

❖ High temperature sensors

FBG, FPI , Raman scattering based (Range up to 1400°C)

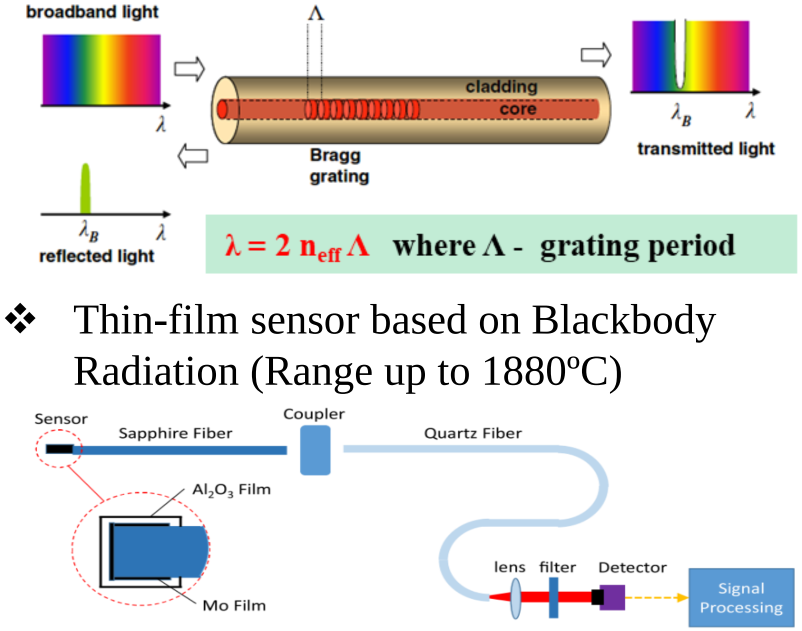

❖ Thin-film sensor based on Blackbody Radiation (Range up to 1880°C)

Grobnic et al, IEEE (2004), Yang et al, Opt Lett (2017), Wilson, IEEE Sensor (2018)

- **YAG ($Y_3Al_5O_{12}$) fibers**

❖ Radiation Sensing

❖ Transmission response to incident radiation; Loss due to radiation is recoverable

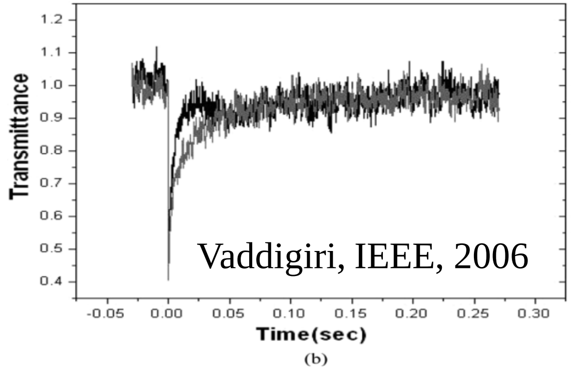

❖ Fiber-lasers materials

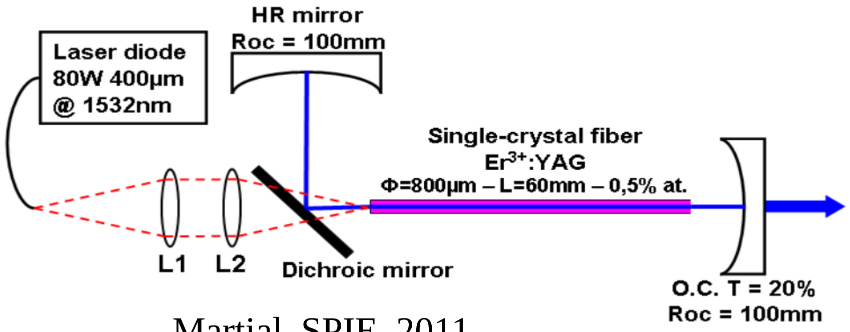

Martial, SPIE, 2011

- **SC fibers of electronic materials**
  - Lithium niobate LN (LiNbO3)
  - Barium titanium oxide, BTO (BaTiO3)

- **SC fibers of magnetic materials**
  - Yttrium Iron garnet, YIG ($Y_3Fe_5O_{12}$)

LHPG growth dynamics

- **Steady state growth factors of single crystal fibers of constant diameter**
- conservation of mass,

$$\pi d^2 v_{fiber} = \pi d^2 v_{source\ rod} \Rightarrow \frac{V_f}{V_S} = \left(\frac{d_s}{d_f}\right)^2 = \left(\frac{1000}{330}\right)^2 \approx 9:1$$

- conservation of energy,

$$Q_s = Q_f + Q_m = A\rho_s \Delta H_f \frac{dx}{dt} + AK_\ell \left(\frac{dT}{dx}\right)_l = AK_s \left(\frac{\delta T}{\delta x}\right)_s = \text{const.},$$

Q_s- heat flux in the crystal away from the growth interface,
Q_m- heat flux from the melt toward the interface,
Q_f - latent heat of crystallization, *A*- area of interface, ρ_s-density of solid,
ΔH_f -latent heat, K_l and *Ks* - thermal conductivity of the liquid and solid
(dT/dx)~ and (dT/dx): - temperature gradient in the solid and liquid respectively

- conservation of shape,

$$\phi = \phi_0$$

Where ϕ_0 material constant, (Sapphire-12^0, YAG- 8^0, $LiNbO_3$- 4^0)
l $-$ *molten zone length = 3 * fiber diameter = diameter of feed rod*

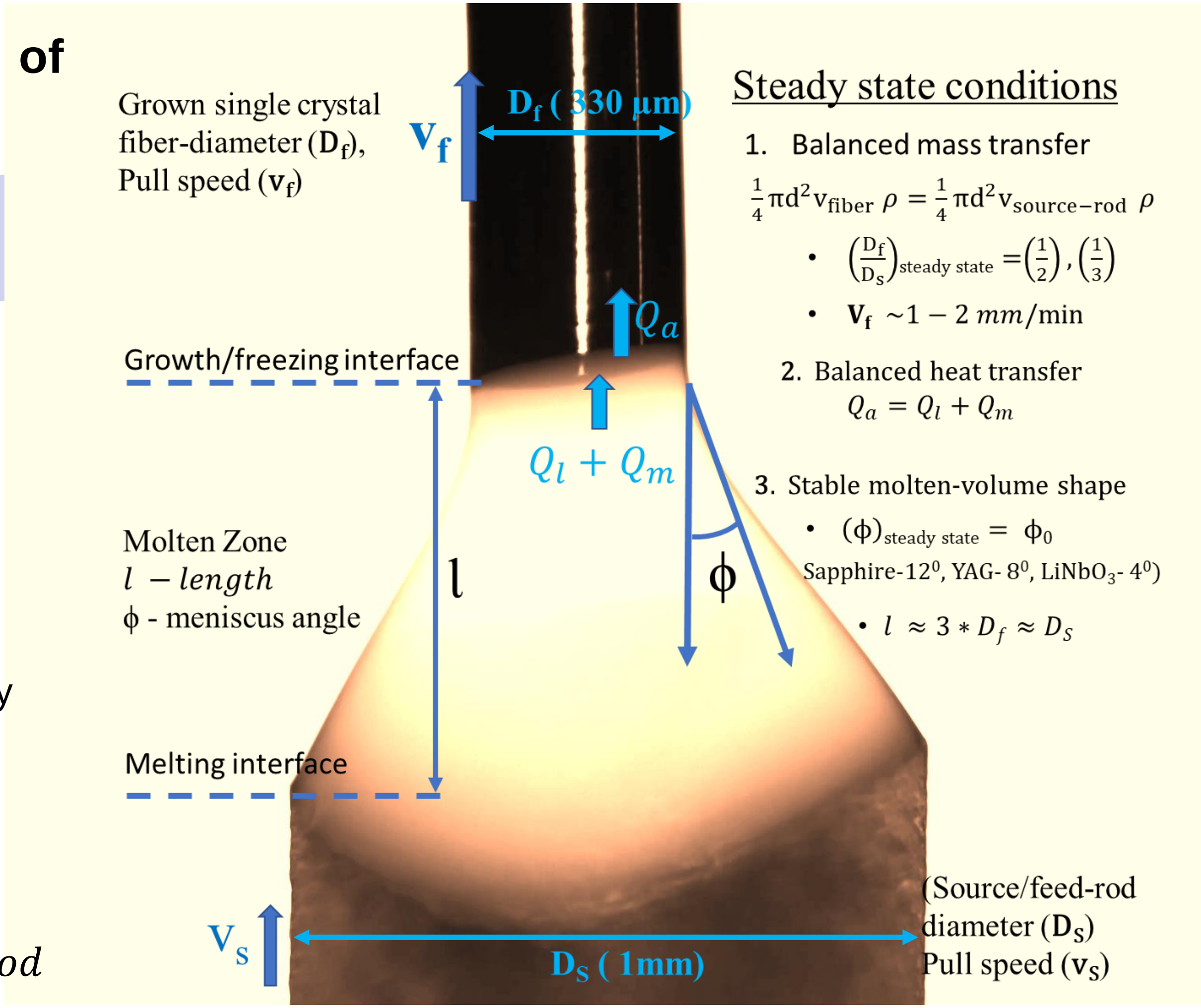

LHPG system design: conventional vs simplified design at U. Pitt.

Conventional design

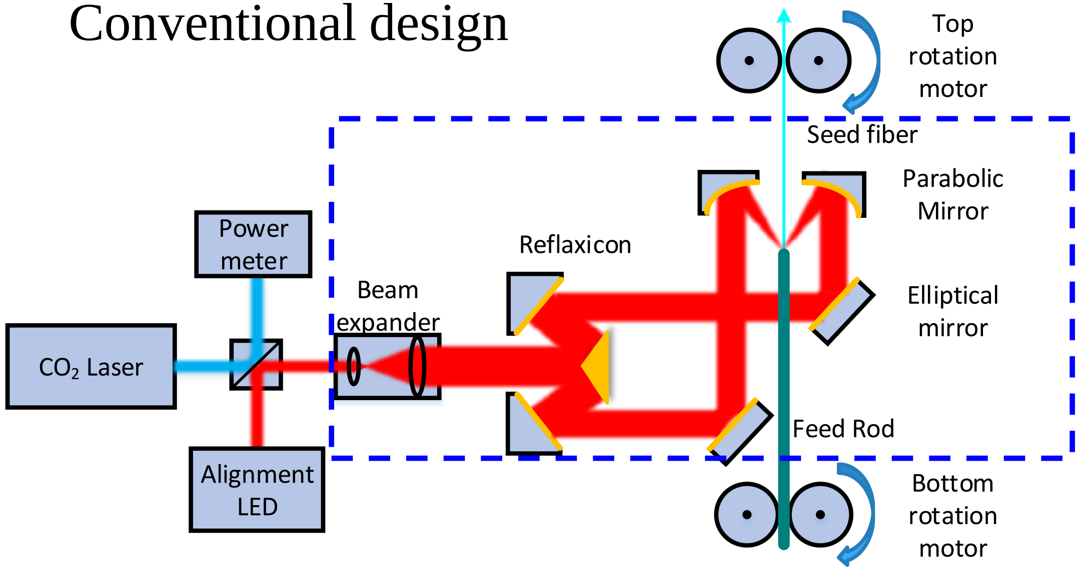

Simplified design (Univ. of Pittsburgh)

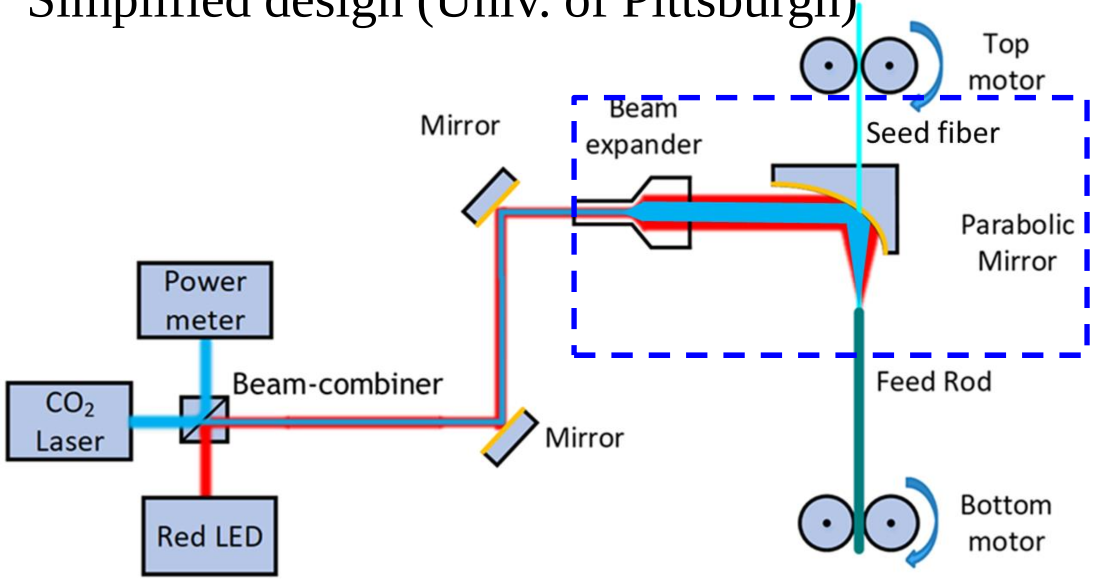

Old design

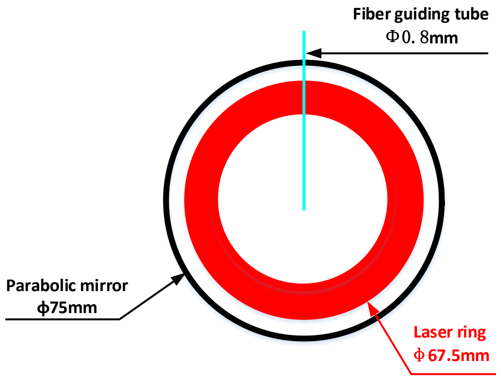

	Conventional design	Upitt. simplified design
Focusing optics	Axicons + turning mirror + paraboloidal mirror	Beam expander + 90 degree off-axis mirror
built	Customization	Off-the-shelf
Alignment DOF	27	18
Beam profile	Ring/Donut shape (axially symmetric)	Gaussian/flat top (axially asymmetric)

Simplified design

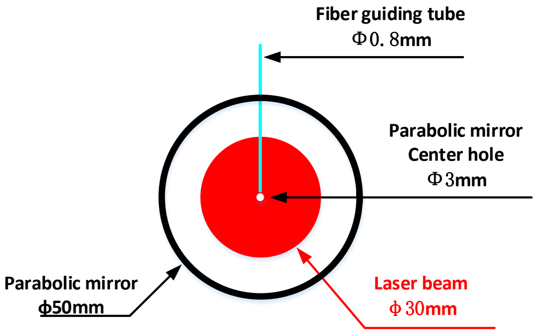

ZEMAX simulation of candidate LHPG set-ups

Conventional set -up

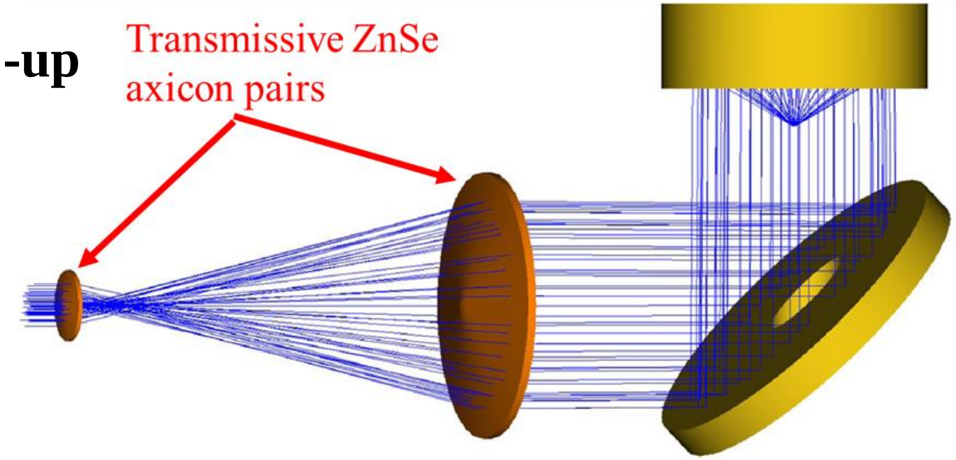

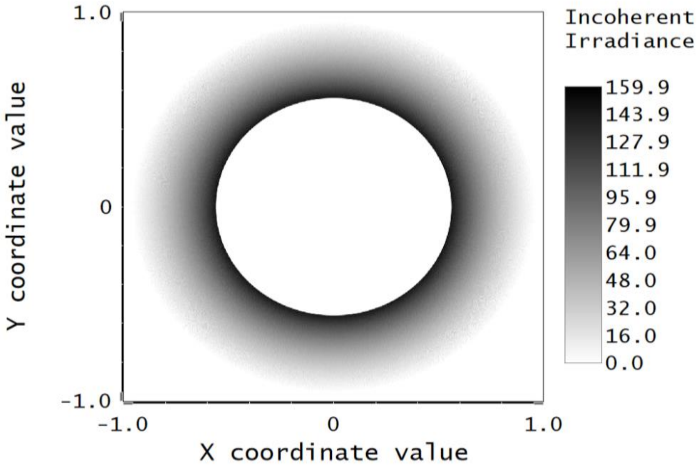

UPitt-LHPG set up

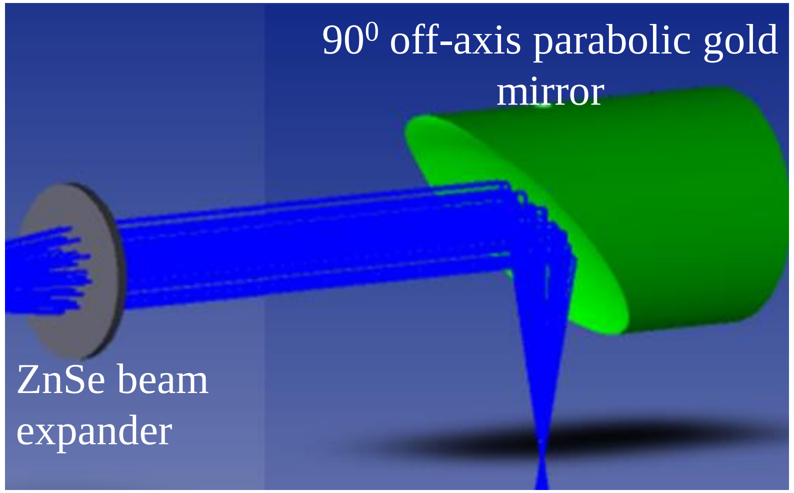

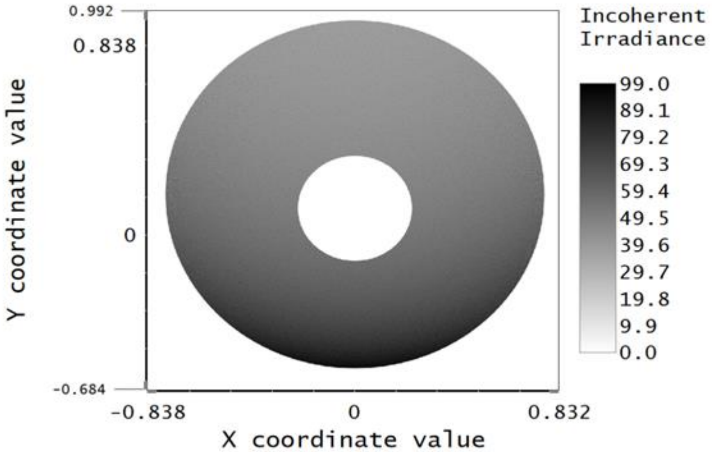

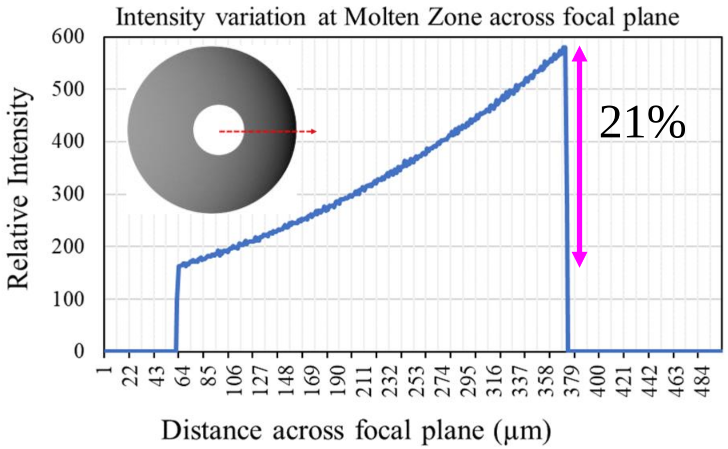

LHPG challenges

Machine vision approach of process control during single crystal fiber growth via laser heated pedestal growth method, D Karki, E Hoffman, D Shengye, VT Schmotzer, B Liu, PR Ohodnicki, Fiber Optic Sensors and Applications XVIII 12105, 57-66 (2022).

Main factors inducing diameter fluctuations

Control schemes

Floating zone meniscus held by surface tension effect prone to instability due to perturbations :

- Laser power fluctuations (±4-5% in medium cost CO_2 lasers) → Power meter feedback loop (power meter, Laser, Volt/current input/output controller device)
- Fiber-pedestal and laser beam misalignment → Guide tubes, Camera inspection from top and sideways
- Perturbations in fiber-pull and pedestal speeds → Machine vision cameras, fiber diameter feedback loop to vary the pull & feed speed
- Air current induced and other vibrations → air-tight enclosed chamber, Helium gas fill, vibration damping optical bench etc.

CO_2-laser power stabilization via PID feedback loop

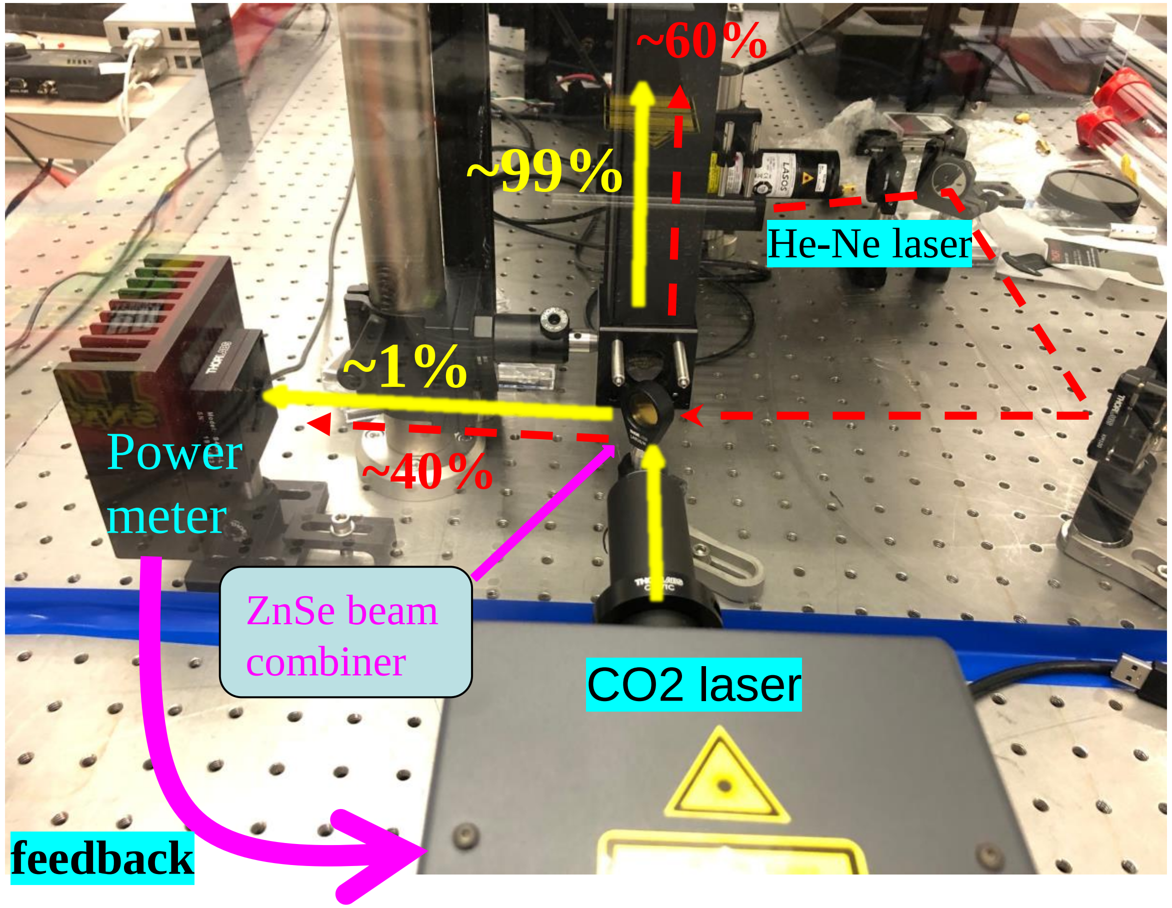

Laser power increases ~ linearly with PWM duty cycle

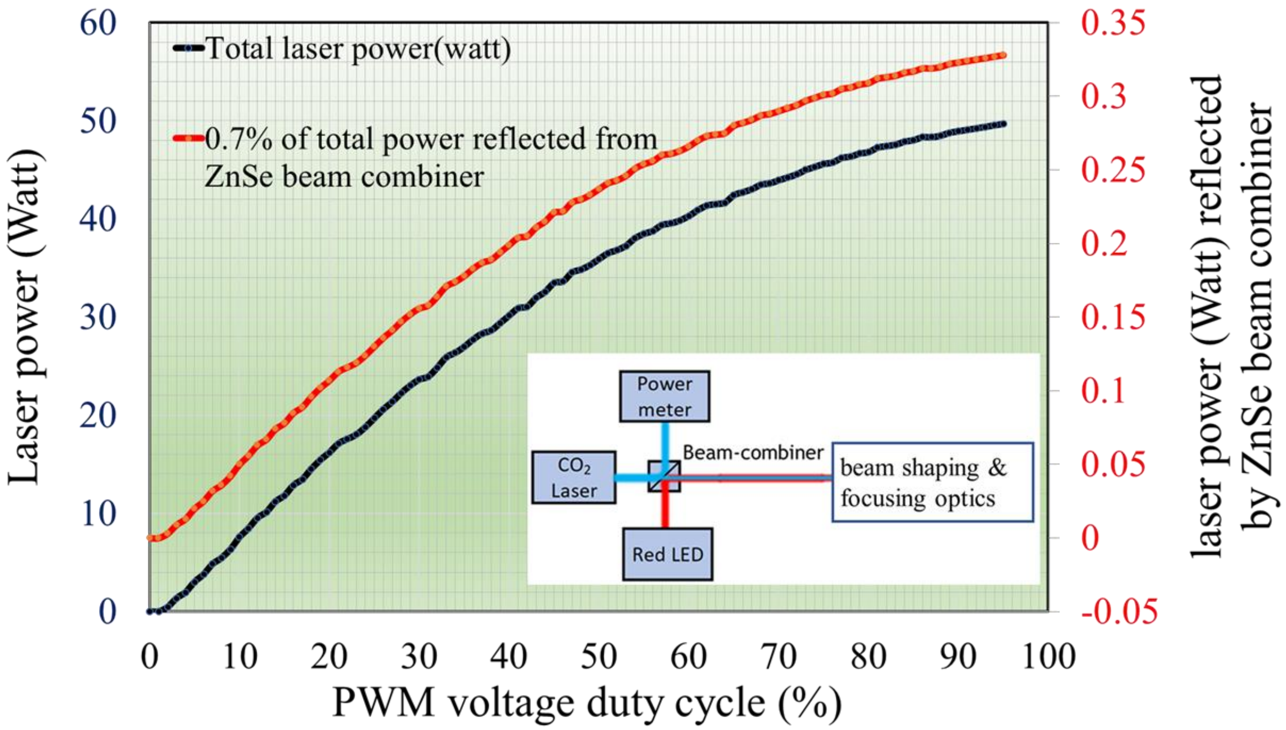

CO_2-laser power stabilization via PID feedback loop

Original Laser power

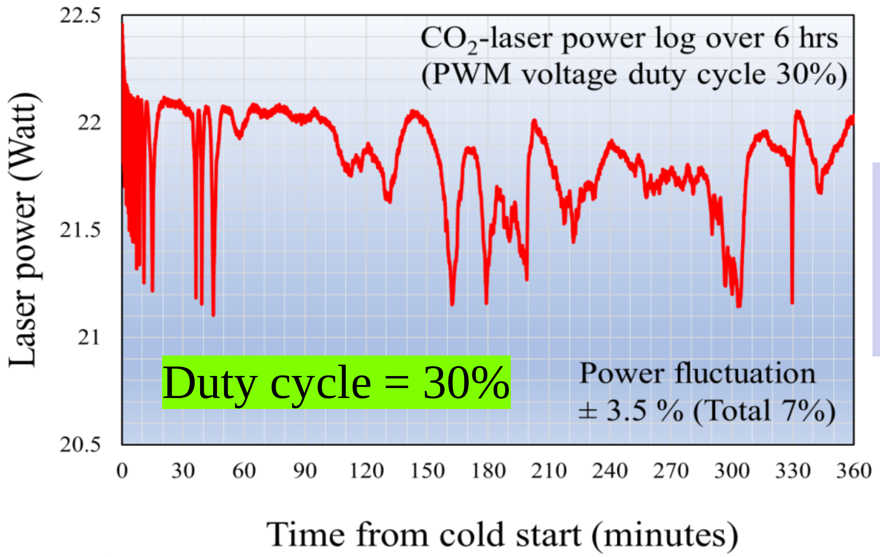

Laser power variation ± (3.5-4)% (total 7-8%)

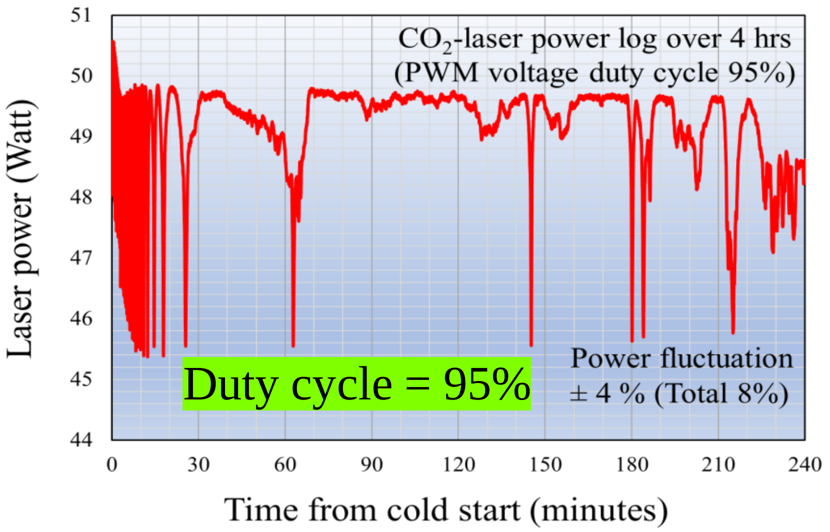

Laser power after PID feedback loop activated

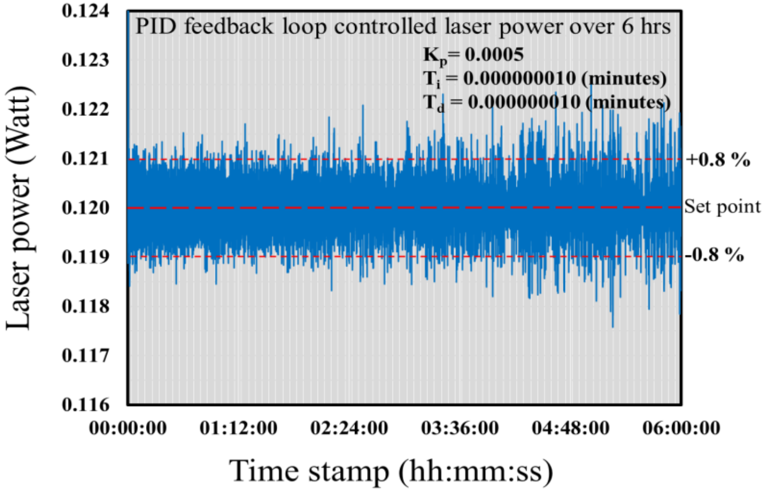

Laser power variation ± (0.5-0.8) %

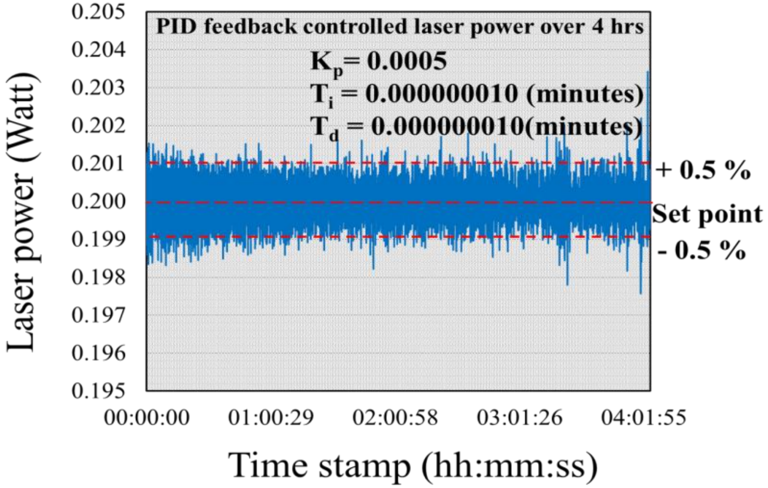

Machine vision approach of process control in LHPG

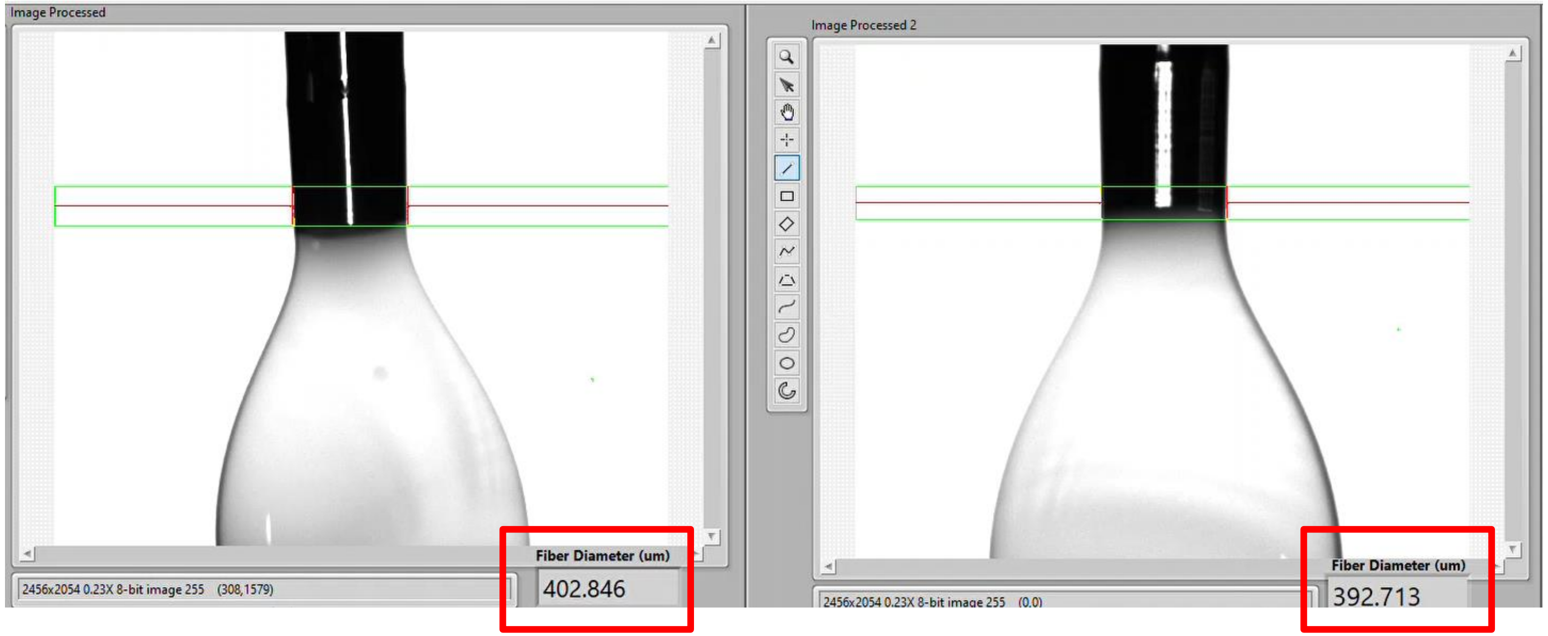

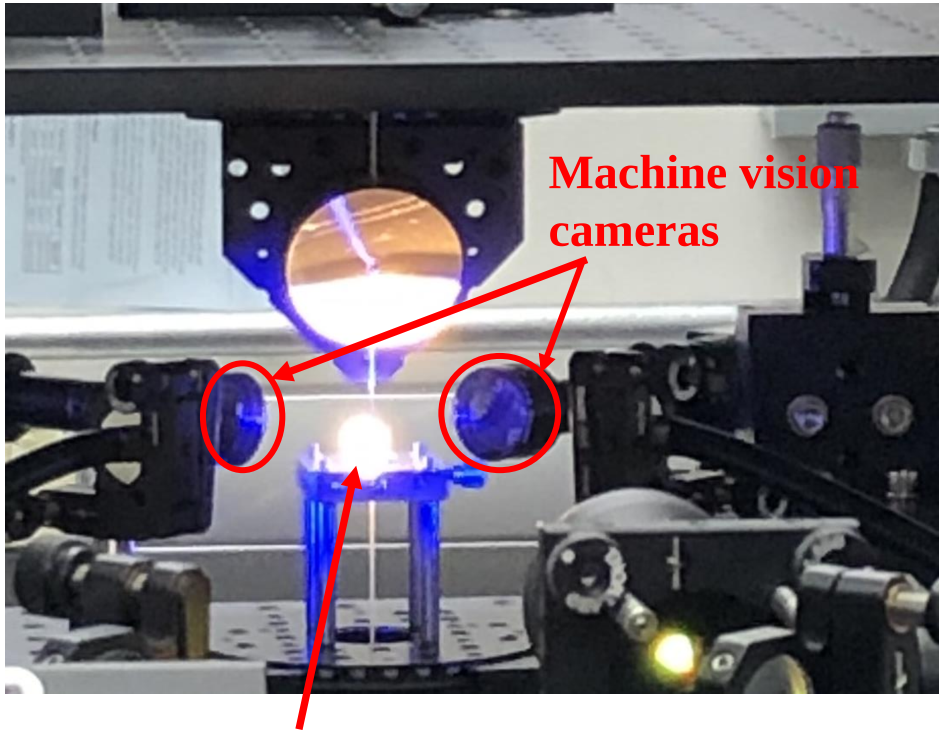

LabVIEW machine vision

In-situ

- Diameter tracking and measurement
- In-situ molten zone contour tracking and volume estimation
- Molten zone height/length tracking and measurement

Machine vision approach of molten zone volume monitoring

$$x(y) = \frac{y^3}{6C^2} + \frac{\lambda y^2}{2C} + C_0 y + C_1 C$$

$$y_i = a_i x^3 + b_i x^2 + c_i x + d_i\,, \quad i = \begin{Bmatrix} 1\ (top) \\ 2\ \ (bottom) \end{Bmatrix}$$

where x is the molten zone edge position on horizontal axis, y is the height of the point of interest on the edge of the molten zone, C the capillary constant, λ, C_0 and C_1 constants (related to feed rod diameter, molten zone surface area, and the floating liquid zone height)

$$A = \pi(y_{top} - y_{bottom})^2,\ V = \int_{h1}^{h2} A\,dx$$

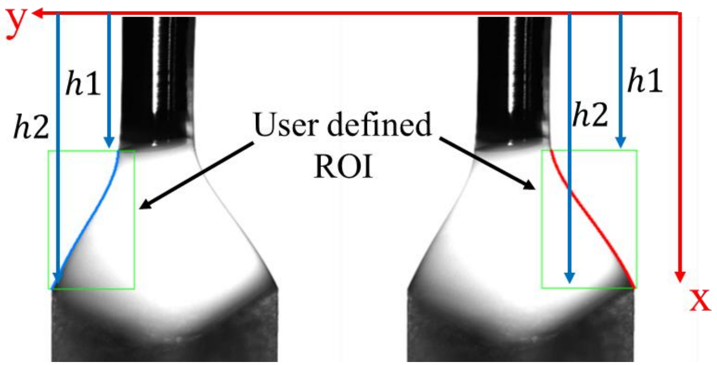

Fiber diameter ~ 330 µm
Feed/source rod diameter = 1mm

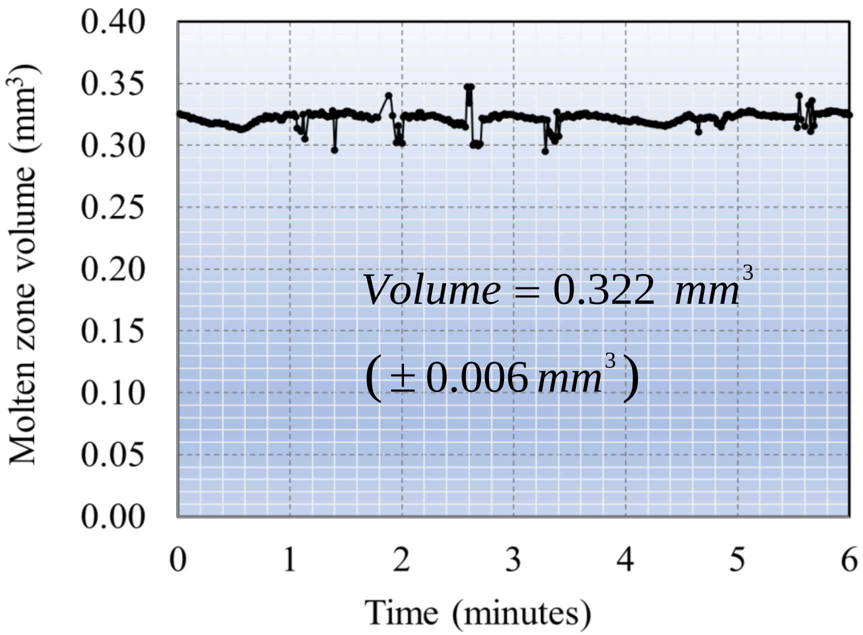

Machine vision approach of molten zone volume monitoring

$\pm 56.55\ \mu m$

$$y_{i=1,2} = e_i x + f_i$$

$$H_{i=1,2} = \frac{\int_{left}^{right} y_i \, dx}{x_{right} - x_{left}}$$

$$l = H_2 - H_1$$

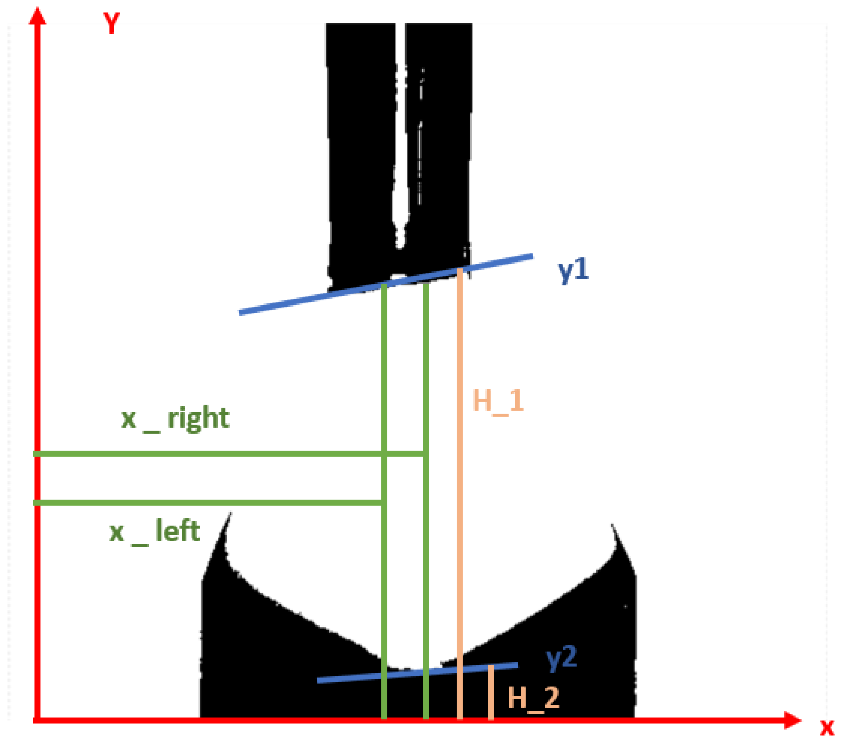

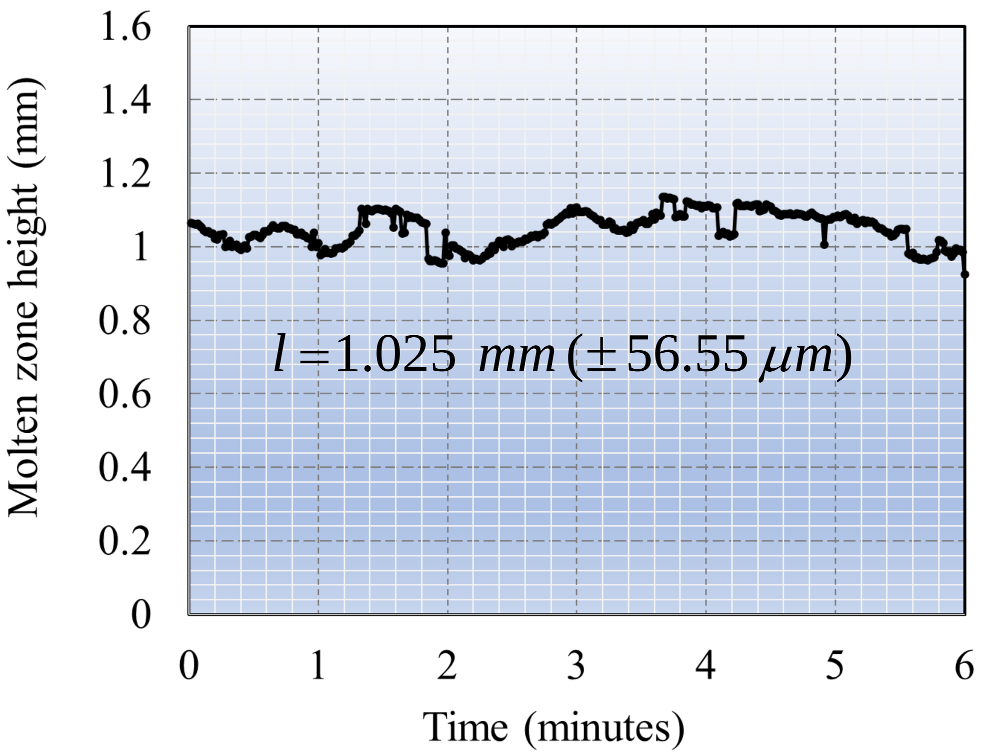

LHPG growth parameters and optimizations

Closed loop PID control (fiber diameter control)

- *Calculates error value* = setpoint (SP) - measured process variable (PV)
- applies a correction to the controller output based on proportional (P), integral (I), and derivative terms (D)

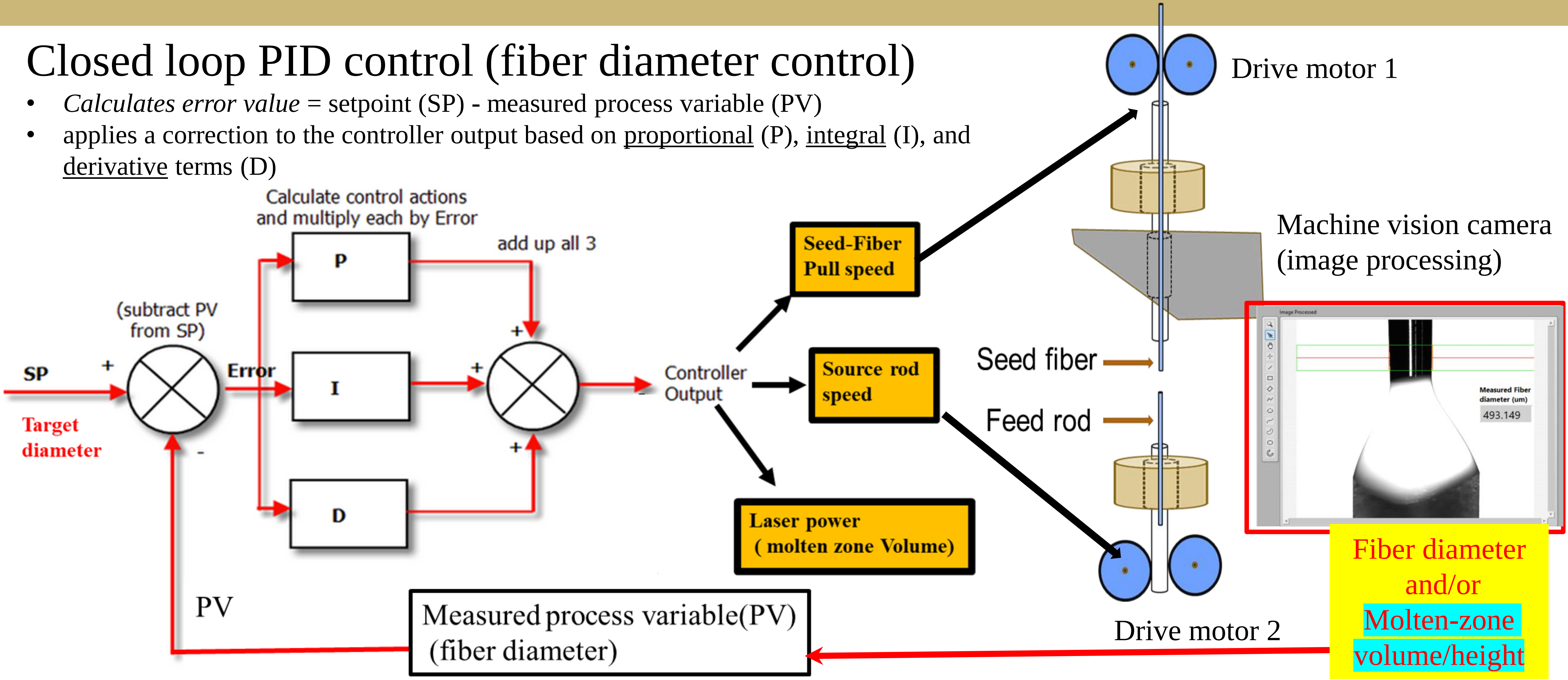

Conclusive remarks on progress towards LHPG process control

- ZEMAX simulation revealed the uniform intensity distribution in conventional set-up and non-uniform intensity distribution in Univ. of Pitt.-LHPG set-up
    - CO_2 laser power controlled within ± (0.5- 0.8)% down from ±(3-4)% as received in commercial lasers
        - Machine-vision approach implemented to quantify the molten-zone volume and height
- **Future work**

Employ molten-zone volume and height as manipulated/control variable towards growth of SC fiber with constant fiber-diameter and low loss

LHPG of Functional Oxides: Congruent and Incongruent Melting

Incongruently melting

Congruently melting

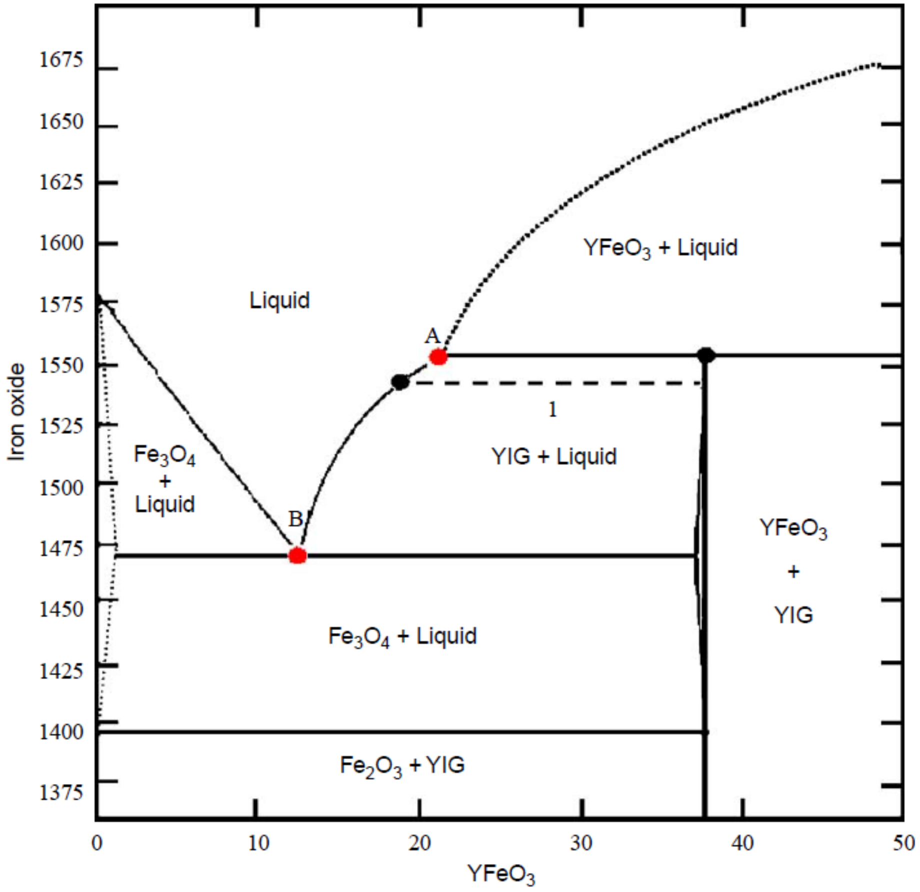

Fig. 1. Phase diagram of Fe_2O_3–$YFeO_3$ in air [14].

Mao et al (2005)

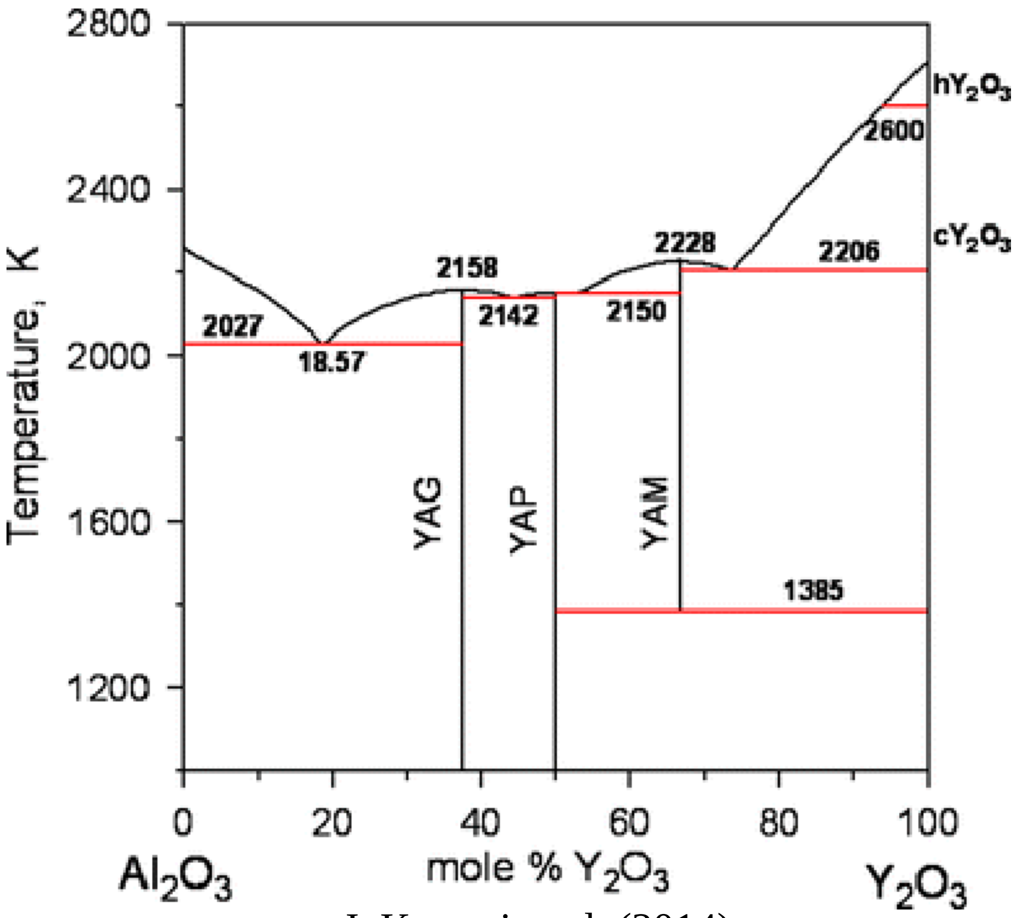

J. Kazemi et al. (2014)

LHPG of Functional Oxides: Congruent and Incongruent Melting

Incongruently melting

Typical NIR transmission spectrum of Ce:YIG/Bi:YIG

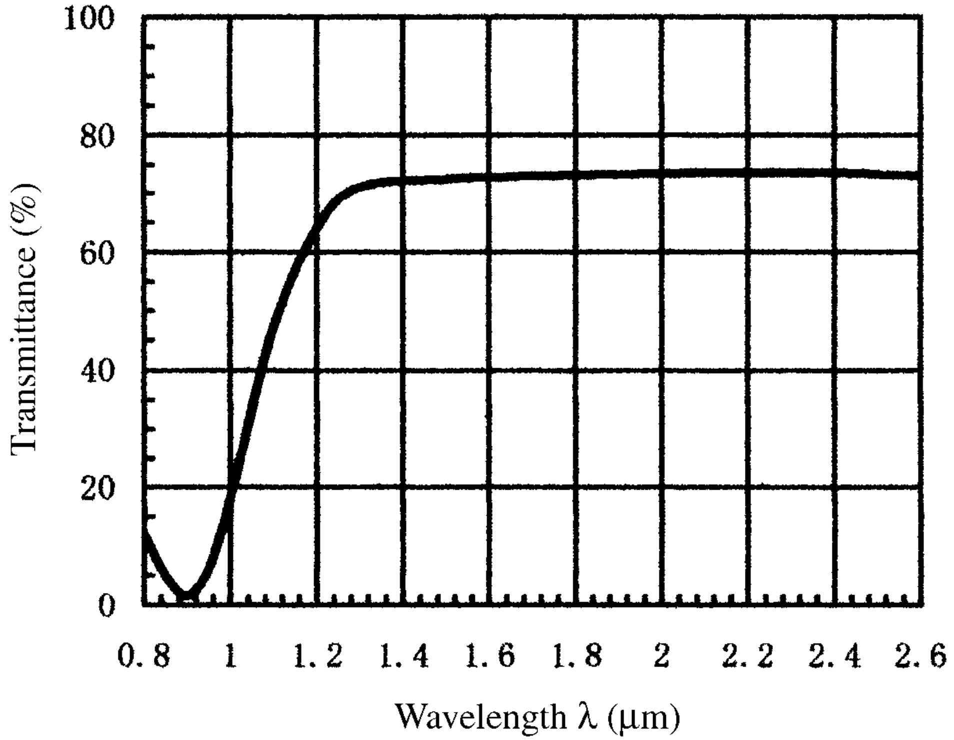

M. Huang et al. *Appl Phys* (2002)

- BiYIG transparent in NIR to IR >1um wavelengths

Where as Sapphire / YAG is transparent in visible wavelengths

- BIYIG incongruently melting (m.p. 1555^{0}C) vs YAG / Sapphire congruently
- YIG molten zone (YFeO3 + YIG)

Congruently melting

NIR transmission spectrum of Sapphire / YAG

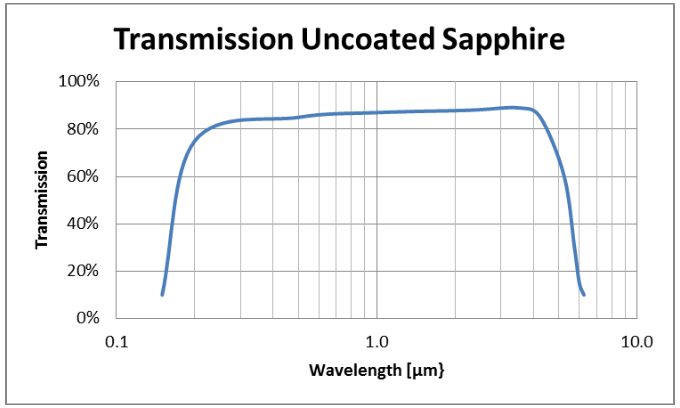

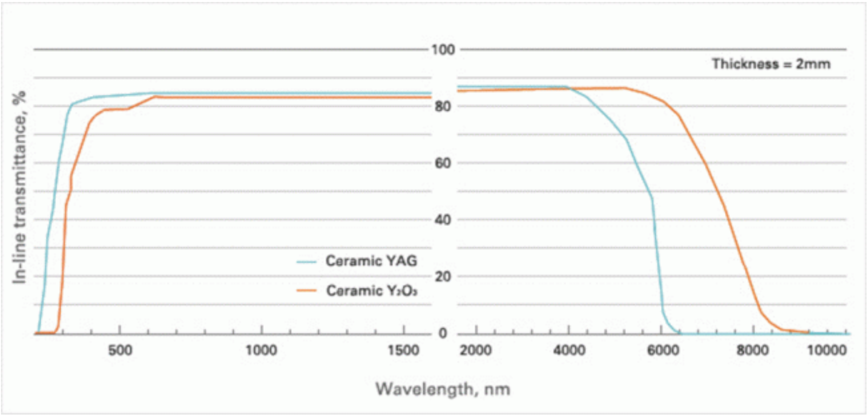

Ceramic Powder Processing for Feedstock Materials of YIG Oxides

Powder processing for YIG feed-stock preparation

$$2Y_3Fe_5O_{12} \longrightarrow 3Y_2O_3 + 5Fe_2O_3$$

3:5 ratio

- ❑ Ball mill – 24 hrs, 300 rpm, ZrO_2 balls, mill jar, Comapction-200MPa
- ❑ Sintering 1450^0C 12 hrs

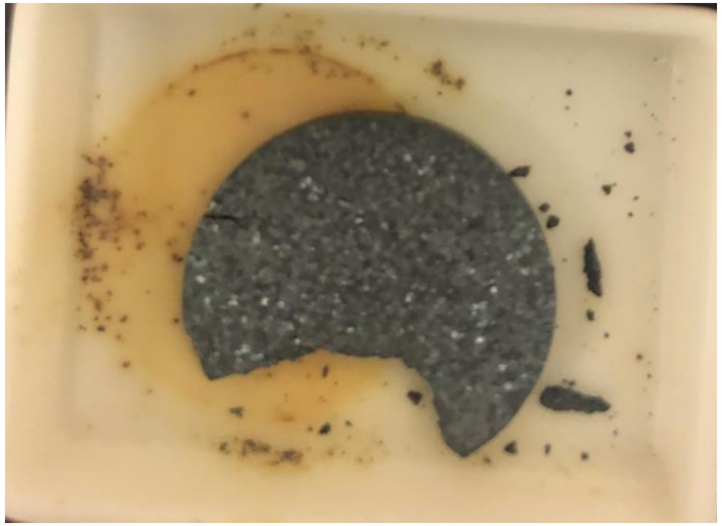

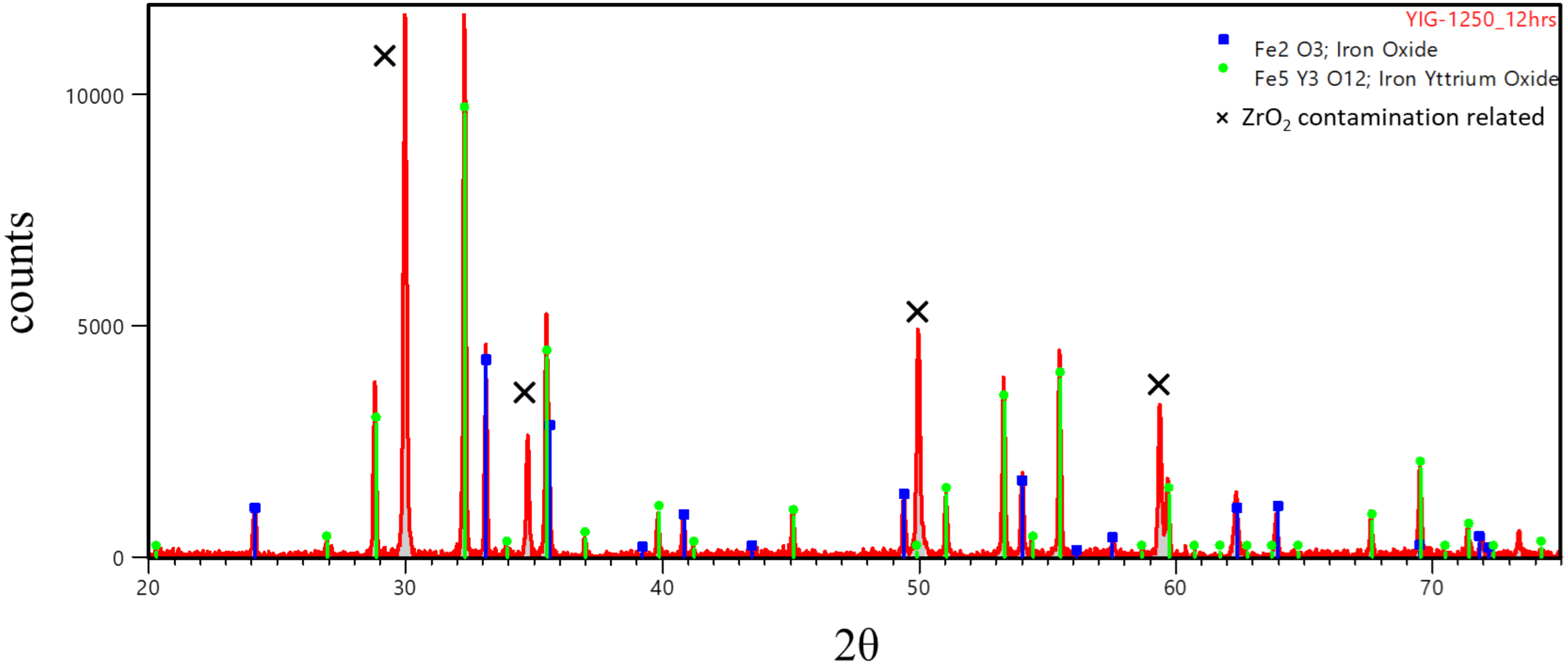

Ceramic Powder Feedstock Characterizations of Phase / Composition

SEM/EDS characterization of sintered YIG pellets

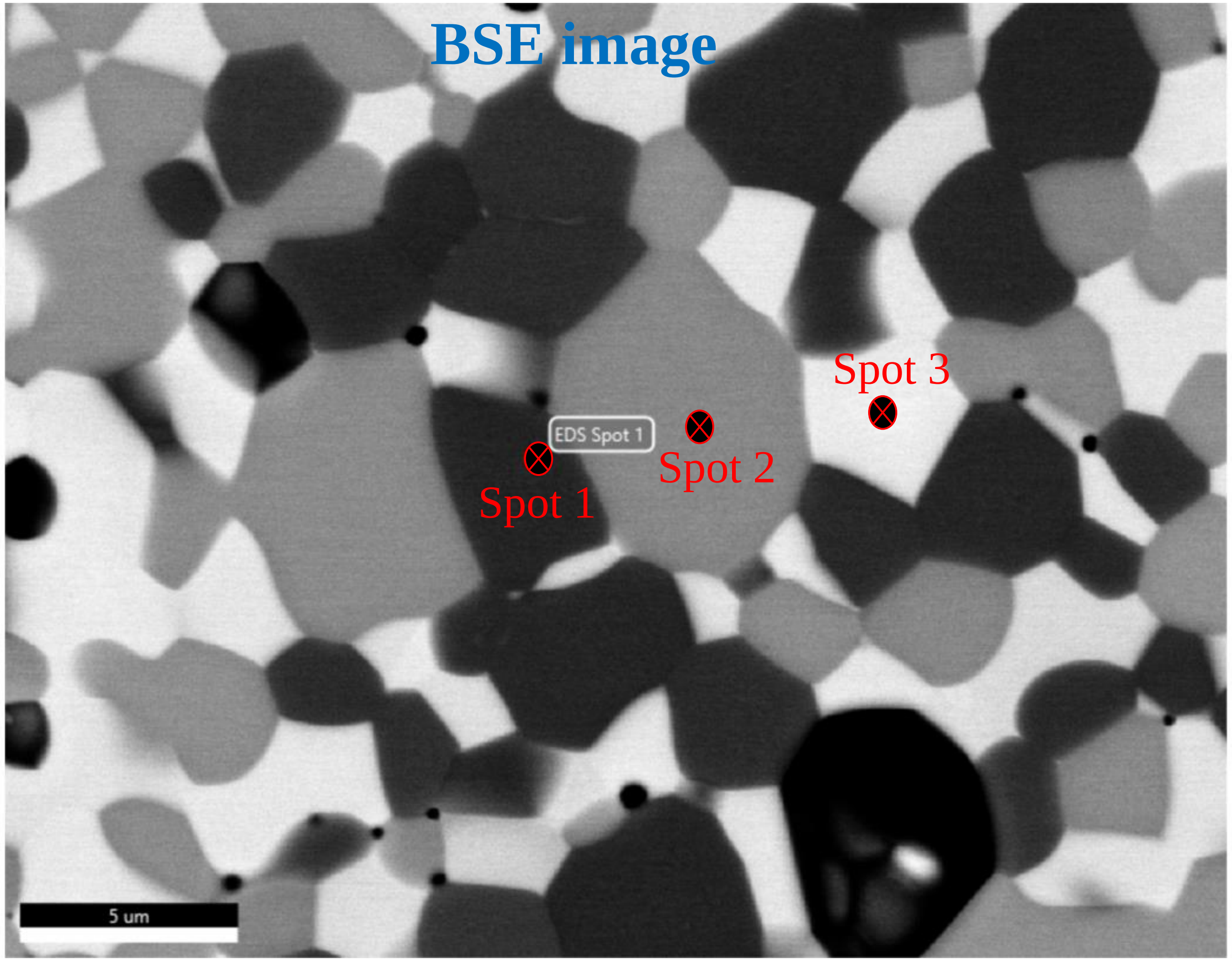

Spot 1

Element	Weight %	MDL	Atomic %
O K	38.44	0.12	68.85
Fe K	59.34	0.45	30.45
Zr L	2.22	0.24	0.70

→ Fe_2O_3

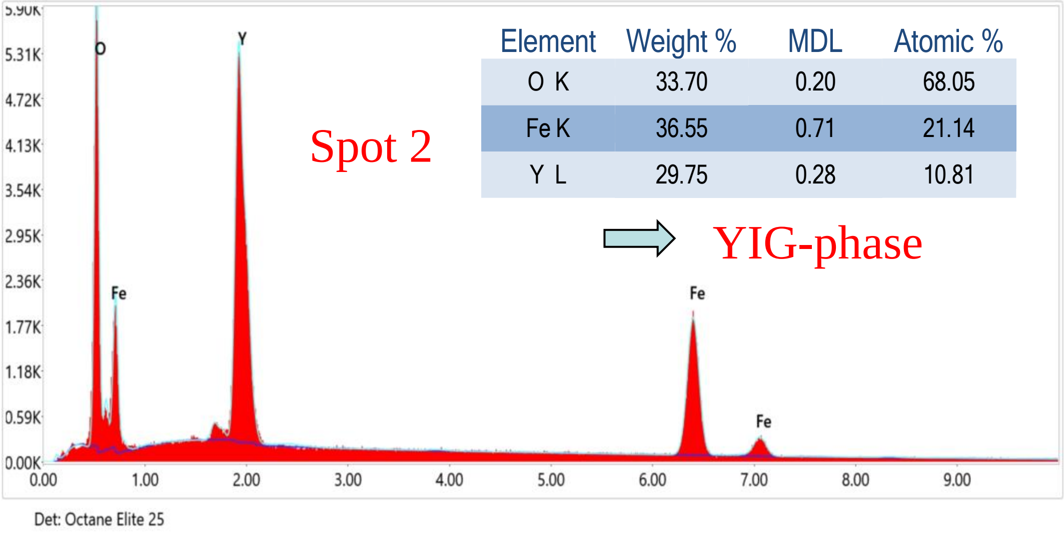

Spot 2

Element	Weight %	MDL	Atomic %
O K	33.70	0.20	68.05
Fe K	36.55	0.71	21.14
Y L	29.75	0.28	10.81

→ YIG-phase

Spot 3

Element	Weight %	MDL	Atomic %
O K	34.50	0.28	73.99
Fe K	4.88	0.55	3.00
Y L	21.07	0.25	8.13
Zr L	39.54	0.60	14.87

→ ZrO_2 contamination

Ceramic Powder Feedstock Characterizations of Phase / Composition

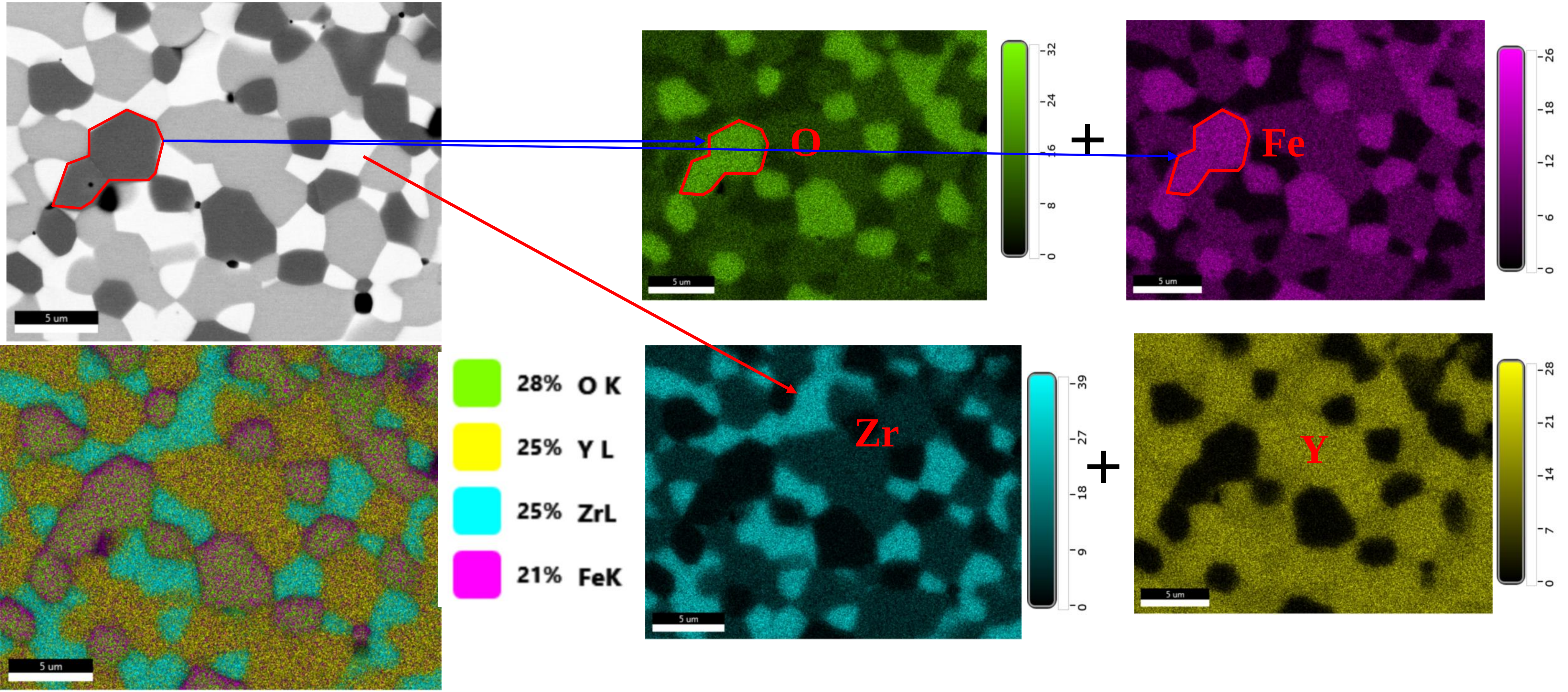

Ceramic Powder Feedstock Characterizations of Phase / Composition

VSM measurements (M vs H loop)

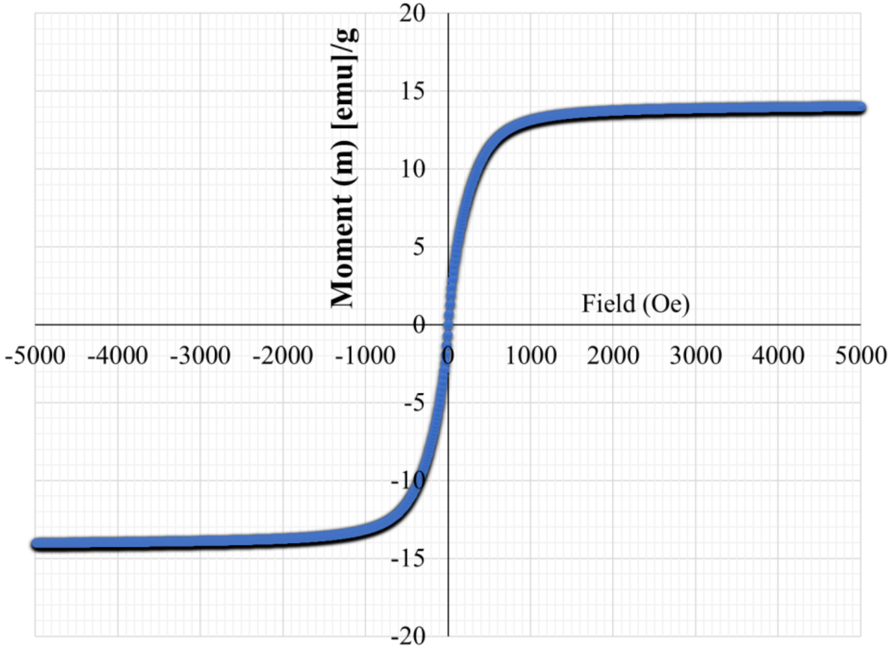

YIG Hysteresis, sintering 1500 C, 12 hrs

VSM measurements (M vs T)

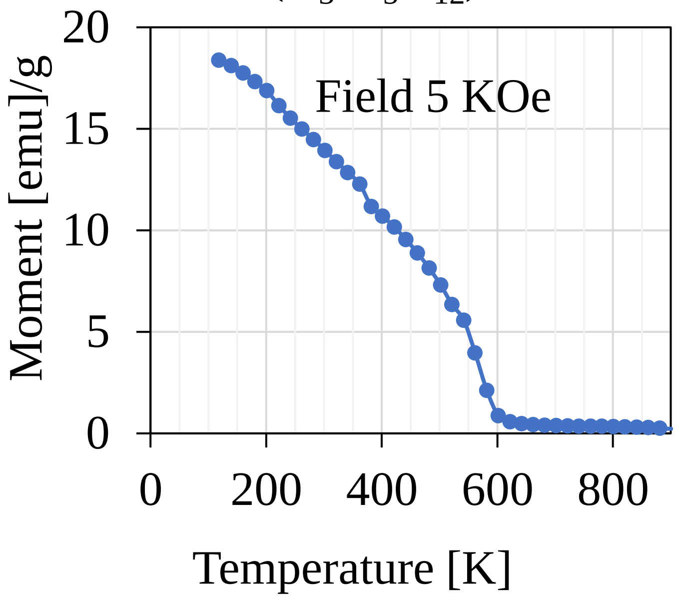

Curie Temperature ~600 K
(literature 580K)

Saturation magnetic moment 14.026 emu/g
(within the range reported in literatures)

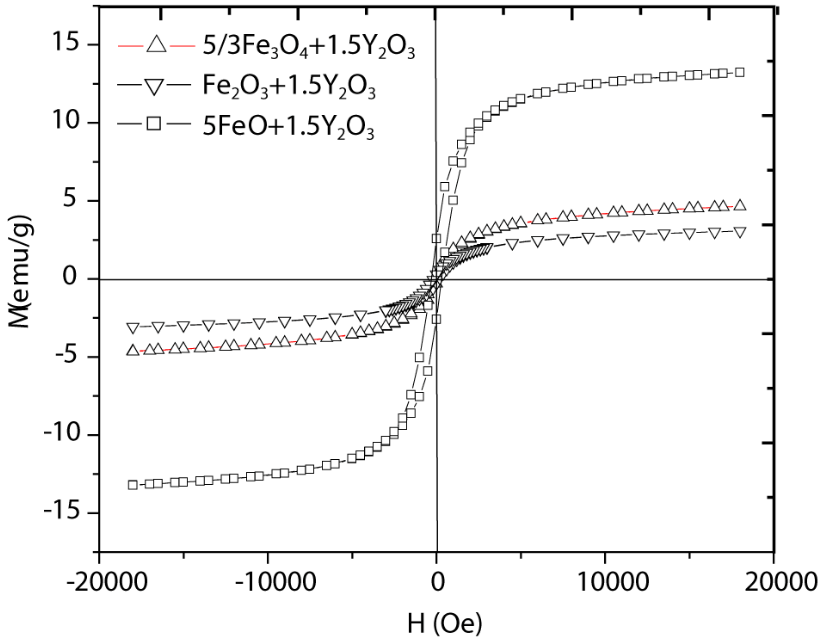

Cortés-Escobedo et al (2013)

YIG fiber growth via LHPG

Stable laser power controlled via PID feedback loop

~ 1.5 mm length grown
- Rectangular feed rod (1mm by 0.5 mm cross-section)

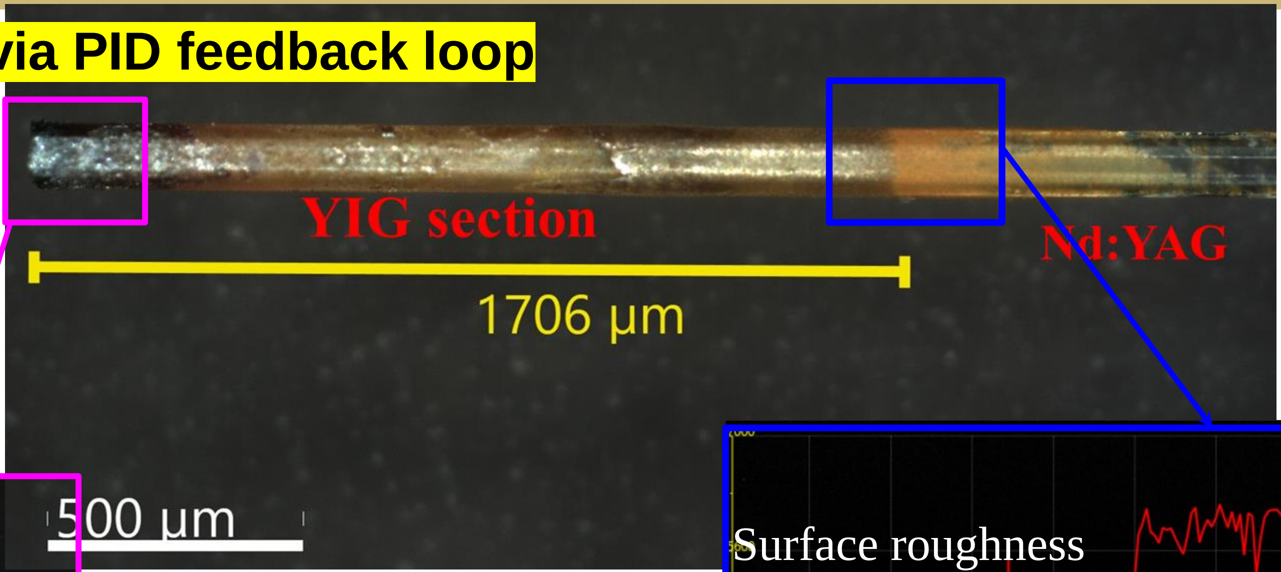

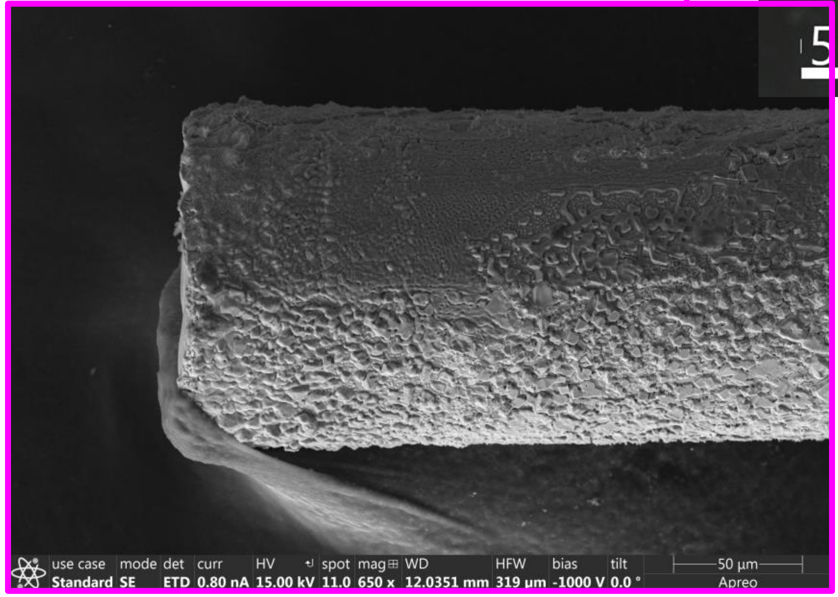

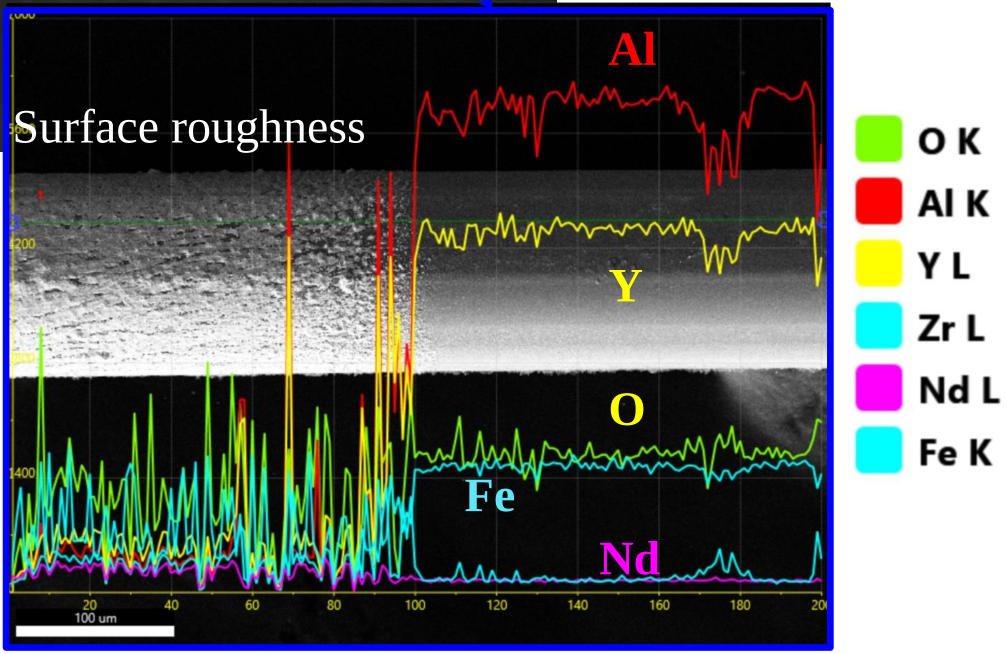

Concluding remarks on LHPG efforts of functional oxides fibers

- ❑ Synthesized feedstock source materials for LHPG
- ❑ Material characterization confirmed the desired phase
- ❑ Short length fibers of congruently and incongruently melting oxides successfully grown via LHPG
- ❑ Needs further characterization/optimization for optical quality improvement

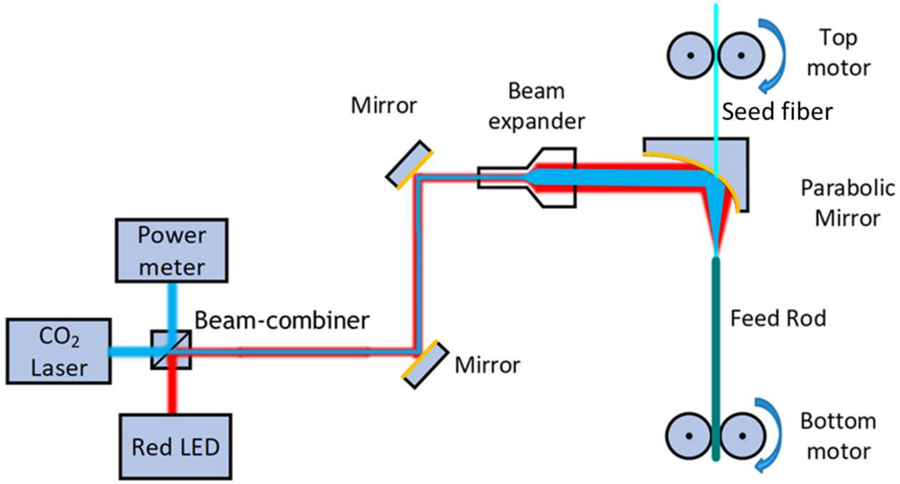

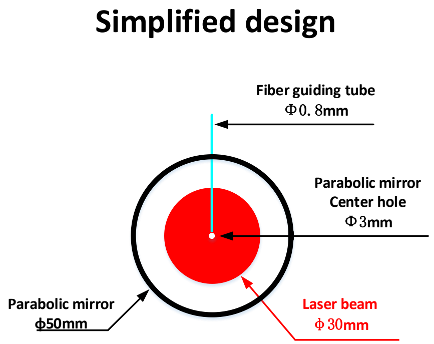

Continuation of the work

- ❑ Further optimization for optical quality fiber growth
- ❑ EBSD, EPMA characterization
- ❑ Understanding of thermodynamics and kinetics of crystal growth